UNIVERSIDADE FEDERAL DE MINAS GERAIS
Instituto de Ciências Biológicas
Programa de Pós-Graduação em Bioquímica e Imunologia

Christina Aparecida Martins

MOLECULAR ANALYSIS OF THE HUMAN ANTIBODY REPERTOIRE ELICITED AFTER VACCINATION AGAINST YELLOW FEVER VIRUS

Belo Horizonte
2024

Christina Aparecida Martins

MOLECULAR ANALYSIS OF THE HUMAN ANTIBODY REPERTOIRE ELICITED AFTER VACCINATION AGAINST YELLOW FEVER VIRUS

Tese apresentada ao Programa de Pós-Graduação em Bioquímica e Imunologia da Universidade Federal de Minas Gerais como requisito parcial para obtenção do título de Doutora em Bioquímica e Imunologia.

Orientadora: Profa. Dra. Liza Figueiredo Felicori Vilela

Coorientador: Dr. Gregory Ippolito

Belo Horizonte
2024

043 Martins, Christina Aparecida.
Molecular analysis of the human antibody repertoire elicited after vaccination against Yellow Fever Vírus [manuscrito] / Christina Aparecida Martins. – 2024.
127 f. : il. ; 29,5 cm.

Orientadora: Profa. Dra. Liza Figueiredo Felicori Vilela. Coorientador: Dr. Gregory Ippolito.
Tese (doutorado) – Universidade Federal de Minas Gerais, Instituto de Ciências Biológicas. Programa de Pós-Graduação em Bioquímica e Imunologia.

1. Bioquímica e imunologia. 2. Vacina contra Febre Amarela. 3. Proteção Cruzada. 4. Flavivirus. 5. Anticorpos. I. Vilela, Liza Figueiredo Felicori. II. Ippolito, Gregory. III. Universidade Federal de Minas Gerais. Instituto de Ciências Biológicas. IV. Título.

CDU: 577.1

Ficha catalografica elaborada pela bibliotecária Fabiane C M Reis - CRB 6 2680

Universidade Federal de Minas Gerais
Curso de Pós-Graduação em Bioquímica e Imunologia ICB/UFMG
Av. Antônio Carlos, 6627 – Pampulha
31270-901 – Belo Horizonte – MG
e-mail: pg-biq@icb.ufmg.br (31)3409-2615

ATA DA DEFESA DA TESE DE DOUTORADO DE CHRISTINA APARECIDA MARTINS. Aos vinte e cinco dias do mês de outubro de 2024 às 13:00 horas, reuniu-se no na sala F2-254 do Instituto de Ciências Biológicas da Universidade Federal de Minas Gerais e de forma "online" utilizando a plataforma "Zoom", a Comissão Examinadora da tese de Doutorado, indicada *ad referendum* do Colegiado do Curso, para julgar, em exame final, o trabalho intitulado "Molecular Analysis of the Human Antibody Repertoire Elicited After Vaccination Against Yellow Fever Virus", requisito final para a obtenção do grau de Doutor em Ciências: Bioquímica. Abrindo a sessão, a Presidente da Comissão, Profª. Liza Figueiredo Felicori Vilela, da Universidade Federal de Minas Gerais, após dar a conhecer aos presentes o teor das Normas Regulamentares do Trabalho Final, passou a palavra à candidata para apresentação de seu trabalho. Seguiu-se a arguição pelos examinadores, com a respectiva defesa da candidata. Logo após a Comissão se reuniu, sem a presença da candidata e do público, para julgamento e expedição do resultado final. Foram atribuídas as seguintes indicações: Dr. Jonathan McDaniel (Pfizer), aprovada; Dra. Vivian Vasconcelos Costa (Universidade Federal de Minas Gerais), aprovada; Dr. André Macedo Vale (Universidade Federal do Rio de Janeiro), aprovada; Dr. Helton da Costa Santiago (Universidade Federal de Minas Gerais), aprovada; Dr. Gregory Ippolito - Coorientador (Texas Biomedical Research Institute (Texas Biomed), San Antonio), aprovada; Dra. Liza Figueiredo Felicori Vilela - Orientadora (Universidade Federal de Minas Gerais), aprovada. Pelas indicações a candidata foi considerada:

(x) APROVADA
( ) REPROVADA

O resultado final foi comunicado publicamente à candidata pela Presidente da Comissão. Nada mais havendo a tratar, a Presidente da Comissão encerrou a reunião e lavrou a presente Ata que será assinada por todos os membros participantes da Comissão Examinadora. Belo Horizonte, 25 de outubro de 2024.

Dr. Jonathan McDaniel (Pfizer)

gov.br Documento assinado digitalmente
VIVIAN VASCONCELOS COSTA LITWINSKI
Data: 29/10/2024 13:46:57-0300
Verifique em https://validar.iti.gov.br

Dra. Vivian Vasconcelos Costa (UFMG)

Dr. André Macedo Vale (UFRJ)

Dr. Helton da Costa Santiago (UFMG)

Dr. Gregory Ippolito - Coorientador (Texas Biomed, San Antonio)

Dra. Liza Figueiredo Felicori Vilela - Orientadora (UFMG)

Com todo meu amor, dedico este trabalho à minha estimada madrinha Aparecida Teixeira Silva. Saudades Eternas.

AGRADECIMENTOS

Em primeiro lugar, gostaria de agradecer a Deus por todas as oportunidades, inclusive por esta conquista, que seria impossível de realizar sem o incentivo e apoio de grandes pessoas, às quais sou eternamente grata. Aos meus pais, Nelson e Cida, eu agradeço pelo carinho e conselhos que me fizeram a pessoa que sou. À minha orientadora de pesquisa, Dra. Liza Felicori, e ao meu coorientador, Dr. Gregory Ippolito, que admiro como pessoas e cientistas brilhantes. Obrigada por confiar em mim um projeto de pesquisa tão importante quanto este e pela orientação durante esses anos. Não tenho dúvidas de que o conhecimento, a experiência, a paciência e o incentivo compartilhados comigo foram essenciais para o meu desenvolvimento como pessoa e como cientista. Gostaria também de agradecer à minha irmã Jakeline, ao meu cunhado Agnaldo e à minha adorável sobrinha Elisa por me manterem firme e sã ao longo desses anos de doutorado. Também não posso esquecer-me de agradecer aos meus queridos amigos Mirian, Lais, Bruno, Luciana, Sandra, Simone, Adriano, e Lilian por todo apoio e amizade. Agradeço especialmente a vários outros pesquisadores do Brasil e dos Estados Unidos, que colaboraram neste trabalho e me treinaram no laboratório durante meu doutorado, incluindo a Dra. Milene Barbosa Carvalho da UFSJ, Dra. Carlena Navas – UFMG, membros da Fiocruz - RJ: Adriana de Souza Azevedo Soares, Brenda de Moura Dias, Nathalia dos Santos Alves, Sheila Maria Barbosa de Lima, Waleska Dias Schwarcz, Ana Paula Dinis Ano Bom, Camilla Bayma Fernandes, Renata Carvalho Pereira e Andrea Marques Vieira da Silva e membros da UT Austin: Jason Lavinder, George Georgiou, Will Voss, Allison Seeger, Edward Satterwhite, Dalton Towers, Jeffrey Marchioni e Juyeon Park. Gostaria de agradecer a todos os membros do laboratório SYNBIOM e BIGG pela ajuda, dicas, truques e tempo de discussão. Continuarei grata aos meus amigos Doug, Dalton, Sean, Eric, Alessandra, Makiko, Jeffrey, Will, Juyeon e Ladan pela amizade e por fazerem do laboratório um lugar incrível. Muito obrigada ao Dr. Mauro Teixeira, Dra. Vivian Vasconcellos e Lisia pela colaboração neste trabalho, bem como ao Departamento de Bioquímica e Imunologia – UFMG pelo apoio a esta pesquisa. Por fim, obrigado às agências financiadoras, NIH, Capes, CNPq e Fapemig e aos membros do meu comitê de tese pela ajuda e aconselhamento.

ACKNOWLEDGEMENTS

First and foremost, I would like to thank God for all the opportunities, including this achievement, in which I would not be able to persuit without the encouragement and support from great people, who I am forever grateful. My parents Nelson and Cida, I thank for the love and advice that made the person I am. To my research advisor, Dr. Liza Felicori and my co-advisor, Dr. Gregory Ippolito, whose I admire as person and brilliant scientists. Thank you for trusting me with such important research Project and for your mentorship. I have no doubt that the shared knowledge, experience, patience, and compassion have been essential for my development as a person and as a scientist. I would also like to thank my sister Jakeline, my brother-in-law, Agnaldo, and my lovely niece, Elisa for keeping me sane over these years of PhD. I also cannot forget to mention my dearest friends Mirian, Lais, Sandra, Simone, Adriano, and Lilian for all support and friendship. Thanks especially to several other research scientists from Brazil and United States, who collaborated in this work and trained me in the laboratory during my PhD, including Dr. Milene Barbosa Carvalho from UFSJ, Fiocruz - RJ members: Adriana de Souza Azevedo Soares, Brenda de Moura Dias, Nathalia dos Santos Alves, Sheila Maria Barbosa de Lima, Waleska Dias Schwarcz, Ana Paula Dinis Ano Bom, Camilla Bayma Fernandes, Renata Carvalho Pereira and Andrea Marques Vieira da Silva and UT Austin members: Jason Lavinder, George Georgiou, Will Voss, Allison Seeger, Edward Satterwhite, Dalton Towers, Jeffrey Marchioni and Juyeon Park. I would like to thank all the SYNBIOM and BIGG laboratory members for your help, tips, tricks, and time. I will remain thankful to Doug, Dalton, Sean, Eric, Alessandra, Makiko, Jeffrey, Will, Juyeon and Ladan for the friendship and for making the laboratory an incredibly place. Many thanks to Dr. Mauro Teixeira, Dr. Vivian Vasconcellos, and Lisia for the collaboration in this work, as well as to the Department of Biochemistry and Immunology – UFMG for the support of this research. Finally, thank you to my funding sources, NIH, Capes, CNPq and Fapemig and to the members of my thesis committee for your help and advice.

RESUMO

A vacina contra o vírus da febre amarela (YFV) (17DD, 17D, 17D-213) é uma vacina de vírus atenuado que constitui a principal medida contra a doença da febre amarela. Apesar da sua eficácia, disponibilidade e boa cobertura vacinal, o YFV continua a ser uma ameaça persistente devido aos surtos recorrentes em regiões endêmicas. Já se sabe que infecções prévias ou repetidas vacinações induzem uma imunidade humoral que pode afetar tanto os resultados da vacina como o curso de futuras exposições a vírus antigenicamente relacionados, como o dengue (DENV) e o zika (ZIKV). No presente estudo, o repertório de anticorpos de indivíduos revacinados contra YFV foi analisado para melhor compreender o impacto da cocirculação de DENV e ZIKV em uma área endêmica, nos resultados da vacina contra YFV e na existência de anticorpos com reatividade cruzada para os três vírus. Nesse sentido, este estudo foi dividido em dois capítulos, nos quais o primeiro deles apresenta uma análise da dinâmica molecular do repertório de anticorpos após a revacinação de quatro doadores contra YFV. Combinando métodos de análise sorológica e de sequenciamento de receptores de célula B (BCR-seq), foi verificado que a dose de reforço contra a YFV induz uma resposta discreta em termos de anticorpos, a qual apresenta rápido decaimento ao longo do tempo. Essa cinética de anticorpos foi correlacionada com uma rápida expansão de linhagens pré-existentes e novas, com grande predomínio de IgA. Também foram identificadas no repertório de vacinados contra YFV, linhagens expandidas com alto *score* de identidade a nível de aminoácidos que compõe o CDRH3, com o de anticorpos anti-DENV e anti-ZIKV já caracterizados. O segundo capítulo do estudo mostra a composição do repertório de sorológico e sua relação com células B expandidas após 6 meses da revacinação dos indivíduos contra YFV. Usando uma abordagem proteômica (Ig-seq) combinada com dados de sequenciamento BCR (BCR-seq) dos transcritos de anticorpos, verificou-se que uma fração considerável do repertório é constituída de anticorpos reativos a DENV2 e ZIKV. Além disso, foi identificado uma média de ~35 % destas linhagens de anticorpos pré-existindo no repertório antes da vacinação contra YFV. Comparando essas linhagens de anticorpos identificadas a nível transcriptômico e proteômico, foram detectadas diferenças significativas nas taxas de hipermutação somática (SHM), uso gênico e tamanho do CDRH3. Portanto, os resultados apresentados mostram em conjunto, evidências de que a cocirculação dos doadores aos flavivírus podem influenciar na complexidade, a qualidade e persistência das respostas de anticorpos da vacina contra o vírus da febre amarela.

Palavras-chave: Flavivirus; Repertório de anticorpos; Vacina contra YFV; Imunidade cruzada.

ABSTRACT

Yellow fever virus (YFV) vaccine (17DD, 17D, 17D-213) is a live-attenuated vaccine that constitutes the main countermeasure against the yellow fever disease. Despite its efficacy, availability, and good vaccination coverage, YFV remains a persistent threat due to recurrent outbreaks in endemic regions. It is already known that previous infections or vaccinations elicit humoral immunity that may affect both vaccine outcomes and the course of future exposures to antigenically related viruses, such as dengue (DENV) and zika (ZIKV). In the present study, the antibody repertoire of subjects revaccinated against YFV was analyzed to better understand the impact of the co-circulation of DENV and ZIKV in an endemic area, on YFV vaccine outcomes and the existence of cross-reactive antibodies to the three viruses. To address this goal, this study is divided into two chapters. The first chapter presents an analysis of the molecular dynamics of the antibody repertoire after YFV revaccination of four donors. Combining serological analysis and B cell receptor sequencing (BCR-seq) methods, we found that YFV booster induces a modest antibody response followed by rapid temporal decay revaccinated individuals. Antibody kinetics in these individuals can be correlated with a rapid expansion of pre-existing lineages as well as newly generated lineages that are mostly dominated by IgA. We also identified expanded lineages containing high CDRH3 amino acid sequence identity to DENV and/or ZIKV characterized antibodies, suggesting the influence of the flavivirus co-circulation in the vaccine outcomes. The second chapter of the study describes the composition of the IgG serological antibody repertoire and its relationship to B-cell clonal expansions after 6 months in the subjects revaccinated against YFV. Using a proteomic approach (Ig-seq) combined with BCR sequencing data (BCR-seq) of the antibody transcripts, we show that secreted antibody molecules reactive to DENV2 and ZIKV comprise a substantial fraction of the serological repertoire, with an average of ~35% of these antibody lineages pre-existing from the YFV vaccination. We compared these antibody lineages which were identified at transcriptomic and proteomic level and we observed significative diferences in the somatic hypermutation rates (SHM), gene usage and CDRH3 lenght. Taken together, we found evidence that flavivirus co-circulation and pre-existing humoral immunity may influence the complexity, quality and persistence of the YFV vaccine antibody responses.

Keywords: Flavivirus; Antibody Repertoire; YFV Vaccine; Cross-Immunity.

SUMÁRIO

1. INTRODUCTION 10
2. LITERATURE BACKGROUND 11
2.1 The Human Antibody Repertoire 11
2.2 Antibody repertoire sequencing as an important tool to dissect the humoral immunity 13
2.3 The Yellow Fever vaccine (17DD, 17D, 17D-213) 15
2.4 Epidemiology and pathogenicity of the yellow fever disease in Brazil 18
2.5 Biological aspects of the YFV virus 21
2.5.1 Origin and replication 21
2.5.2 Structural organization 23
2.6 Implications of flavivirus antibody cross-reactivity 27
3. SIGNIFICANCE 32
4. OBJECTIVES 33
4.1 Main Objective: 33
4.2 Specific Objectives: 33
CHAPTER 1 34
5. INTRODUCTION 35
6. MATERIALS AND METHODS 37
7. RESULTS 44
8. DISCUSSION 58
9. CONCLUSION 63
CHAPTER 2 64
10. INTRODUCTION 65
11. MATERIAL AND METHODS 67
12. RESULTS 78
13. DISCUSSION 90
14. CONCLUSION 94
REFERENCES 95
SUPPLEMENTAL INFORMATION 125

1. INTRODUCTION

The Yellow Fever Virus (YFV) is an important human pathogen that is transmitted by infected mosquitoes of the genera *Aedes* and *Haemagogus*[1]. It is endemic in tropical regions of Sub-Saharan Africa and South America and belongs to the genus Flavivirus that comprises more than thirty antigenically related viruses, including Dengue (DENV) and Zika (ZIKV)[2-3]. Infections caused by YFV may vary from asymptomatic to severe illness, which represents high risk of morbidity and mortality due to ocurrence of haemorrhagic manifestations and hepatorenal syndromes[4-5]. To date, there is no specific treatment for YFV disease and vector control is challenging. The recent YFV outbreaks happened in Brazil (2016-2019) have increased the mortality 1.5 times in comparison to past epidemies that ocurred in the country, revealing that YFV remains a persistent threat despite the availability of an effective vaccine and good vaccination coverage[6-7].

The YFV vaccine (17DD, 17D, 17D-213) is a live-attenuated vaccine recognized as one of the best vaccines ever developed. The main reasons for this fact are the longlife immunity and safety induced by one single dose[8-9]. Recently, it was observed the development of a more robust protective immunity, in terms of neutralizing antibodies and components of cellular immunity, when using just a fractional dose (one-fifth of the standard dose) of 17DD-YF vaccine[10]. This evidence highlights the effectiviness and feasibility of YFV vaccine administration, especially in endemic areas with low vaccination coverage due to stock shortages.

All flaviviruses share a very similar structural arrangement, mechanisms of maturation and assembly[11-12]. This implies in a close antigenic relationship between the different flaviviruses that favors the occurrence of cross-reactive responses mediated by antibodies[13]. Studies have reported that immunity to one flavivirus can affect the YFV vaccine outcomes[14-15] and this is mostly due to these antibodies. Therefore, the present study hypothesize that populations living in endemic regions with co-circulation of related flaviviruses, such as DENV, ZIKV, and YFV, tend to present cross-reactive antibodies in their repertoire that can affect the YFV vaccine outcomes. A better understanding of the factors that influence the flavivirus cross-immunity and vaccine efficacy gives insights for future therapeutics and improved vaccine design. Furthermore, it can contributes for prevention and better management of the outbreaks.

2. LITERATURE BACKGROUND

2.1 The Human Antibody Repertoire

In vertebrates, the immune system can be systematically divided into innate and adaptive. Upon exposure to an antigen, different cells and molecules of both immunities orchestratelly work to generate a rapid and long lasting response. In the adaptive system, B lymphocytes have a fundamental role to produce immunological memory against past encountered antigens. These cells express receptors on their surface (B cell receptors - BCRs) which are unique and capable of specifically recognize and bind to the antigen, initiating its clearance[16]. This process starts after the interaction between BCR and antigen, which results in the activation of these unique B lymphocytes to proliferation (clonal expansion) and diferentiation into antibody secreating cells (plasmablasts and plasma cells)[16-17].

BCRs and antibodies share the same structure, though antibodies are secreated and BCRs are membrane-bound[18] (Figure 1). In general, they are comprised of two heavy chains (IgH) and two light chains (IgL). Each IgL contain one variable (VL) and one constant (CL) region, while IgH is comprised of one variable (VH) domain and three constant domains (CH1-3)[19-20]. In addition, the antibody can be structurally divided into two portions: fragment crystallizable (Fc) and fragment antigen binding (Fab). The Fc portion contains the CH domains and it is responsible for the effector functions of the antibodies. On the other hand, the Fab is the portion that interacts with the antigen[20]. This interaction specifically happens most of the time in six specific regions (three from the VH and three from VL) named complementarity-determining regions 1-3 (CDR1-3). In the antibody three-dimentional structure, these regions form three loops with great sequence variability that allows each unique molecule to react to a different antigen. Among these CDRs, the CDR3 on the heavy chain (CDRH3) is the most variable and, in some cases, is the largest. For this reason, it is believed that CDRH3 contributes most for antigen-antibody interaction[21].

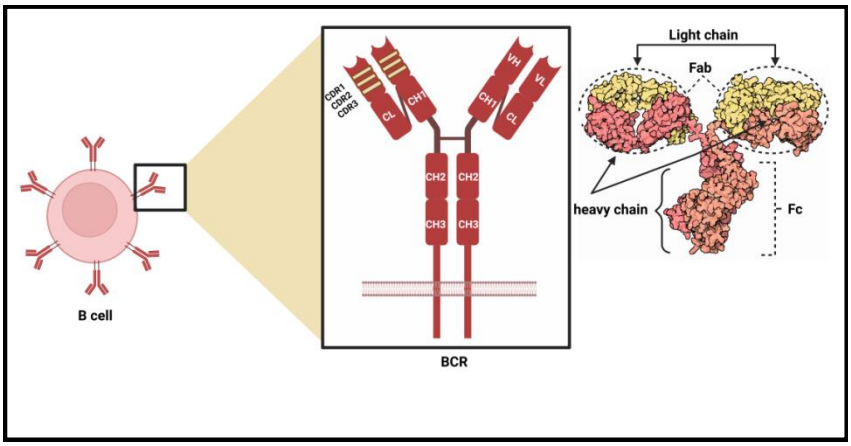

Figure 1. Overview of the BCR/antibody structures. The middle-right image shows that BCRs and secreted antibodies are structurally similar, being comprised of two light (CL) and two heavy (CH) chains. Each chain contains the variable (VL and VH) and constant (CL and CH) domains. The variable domains contain three CDRs which form the antigen binding site. The right image is a 3D structure of an IgG antibody highlighting the fragment crystallizable (Fc) and fragment antigen binding (Fab) regions in the heavy and light chains respectively. Created by the author using Biorender®.

A wide range of BCRs and antibodies with both affinity and specificity is required to recognize millions of different foreing antigens[22]. In humans, the diversity of the BCRs is currently estimated in 10^{15} unique sequences and the entire set of these sequences and the secreted antibodies is called repertoire[23-25]. Having a diverse and large antibody repertoire increases the chance of antigen encountering and consequently the proper establish of the immune response[18]. This diversity is a result of many and distinct molecular mechanisms taken during both early B cell development and at the moment when B cells are experiencing antigen stimuli. One example is the rearrangement of the variable (V), diversity (D) and joining (J) gene segments (V(D)J recombination) on the long arm (q) of the 14 chromossome for IgH, and in the V and J genes (VJ recombination) on the short arm (p) of the chromossome 2 (Igκ) or 22 (Igλ) for IgL. Thus, at the end of this process, only one segment from 44 segments of V, 25 of D and 6 of J is selected to originate an exon that will be translated into a functional BCR[26-28]. Another important mechanism consists of somatic hypermutation (SHM) of the germline DNA and refers to random deletion or insertion of nucleotides that codify the constant and variable regions of IgH and IgL in response to antigen stimuli. These mutations result in different antibody isotypes (class-switch recombination) with higher affinity to antigen[29]. Thus, the final outcome of these processes is the generation of an enriched antibody repertoire against to that target antigen.

2.2 Antibody repertoire sequencing as an important tool to dissect the humoral immunity

Many aspects can determine the antibody repertoire of an individual, including the genetics[30], age[31], and prior exposure to antigens[32]. Moreover, different classes of antigens, such as bacteria, viruses, vaccines, autoimmune diseases, among others, can induce the immune system to produce specific antibody repertoires. By studying these antibody repertoires, it is possible to extract valuable understanding about the humoral immunity, especially the protective characteristics of the antibody responses, as well as the molecular basis of the pathogenic immunity[33]. Antibody repertoire research-based has improved the current knowledge on autoimmune diseases by describing important features of B cells that are associated with pathogenic mechanisms[34-36]. Moreover, many antibodies which were isolated from either vaccinees or convalescent plasma repertoires have shown promised use as treatment and diagnostic tools for different diseases[37-39]. Yet, analysis of antibody repertoires has permitted to better design vaccines towards the development of a more efficient immune response[40].

Over the past few decades, diverse approaches have been created to study both cellular and serological antibody repertoires[41-44]. Among those, the high-throughput next-generation sequencing (NGS) technology has expanded the scale of the antibody repertoire analysis to millions of sequences, enabling the deep characterization of the entire repertoires, antigen-specific B cell populations and their functional antibodies[45]. Depending on the purpose of the study, total B cells, sorted plasmablasts, plasma cells, memory B cells and tissue-infiltrating B cells can be used as source of information of the repertoire nature and composition. In some cases of more precise understanding is needed, these B cells subsets can be further sorted by fluorescence-activated single cell sorting (FACS) and the rearranged antibody DNA from these defined cells can be amplified and sequenced[46].

The resulting sequences can be compared to germline antibody gene to identify differential characteristics of the B cell development in health and disease. Furthermore, antibody repertoire sequencing can identify clonal families important for the immune response and predict their specificities and epitopes without expressing the antibodies. Moreover, it is possible to estimate the diversity and expansion degree of repertoires upon stimuli. Although it is not possible to

sequence the entire B cell repertoire, representative samples are able to provide comprehensive insights on repertoire size, frequencies of VDJ segment gene usage, CDR3 amino acid sequences and length, as well as frequencies of somatic hypermutation rates (SHM), among other characteristics[40].

Advances on bioinformatic tools enabled the integration of VH antibody NGS data sequencing (BCR-seq) to serum antibody repertoire data (Ig-seq) obtained by high-resolution liquid chromatography tandem mass spectrometry[42]. This approach has shown the relationship between BCR repertoire and secreated antibodies that are specific to antigens, providing a link of sequencing data and functional activity of the antibodies (Figure 2). Importantly, this technique has solved the enigma of distinguish total repertoire from antigen-specific antibody repertoires which are responsive to specific conditions, such as infections and vaccinations[42].

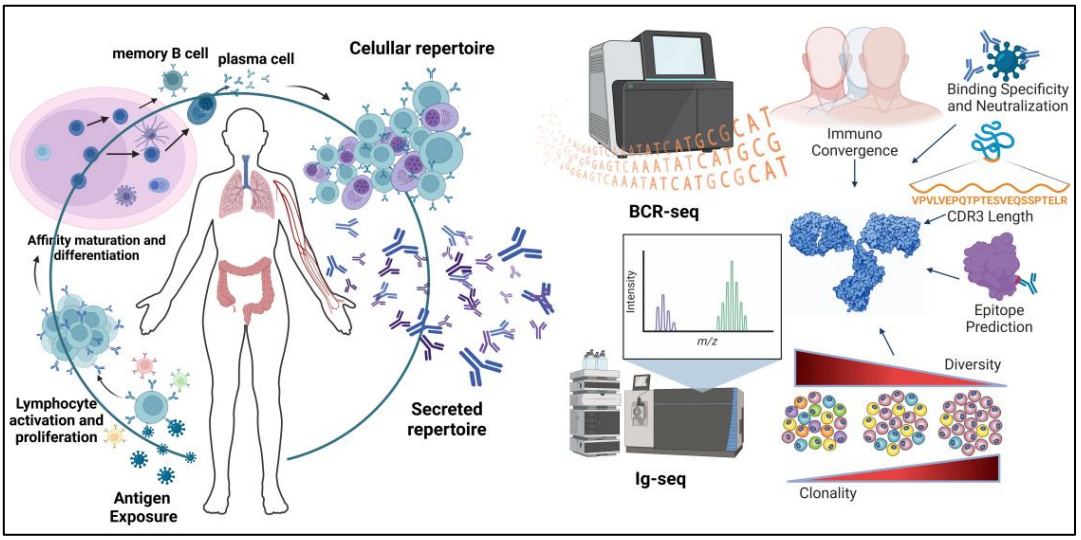

Figure 2. Unveiling the human antibody repertoire through Ig-seq and BCR-seq. Upon antigen exposure, B cells are activated and undergo proliferation, affinity maturation and differentiation stages, resulting in plasmablasts, plasma cells, and memory B cells that can settle in the blood, respiratory mucosa or gut mucosa. These cells comprise the cellular repertoire and can be used to study the antibody responses after infection and/or vaccination through BCR-seq. Likewise, secreted antibodies constitute the serologic repertoire and can be investigated through Ig-seq pipeline. Both analysis can be combined to better inform about the specificity, diversity, convergent responses between individuals, epitope prediction, CDR3 length, clonality and etc. Created by the author using Biorender®.

Studies on antibody repertoire characterization are exponentially growing. Many of them are focoused on monitoring changes after vaccination[47-49] and infections[50-51]. These studies have helped to understand the dynamics of the

antibody responses, including the role of the germinal center (GC) activity and affinity maturation on vaccine efficacy[48]. In addition, most abundant antibodies obtained in these studies could be extracted and cloned into vectors for recombinant expression and functional characterization. Alternatively, this extracted information has contributed for creation of antibody sequences' databases, such as iReceptor[52], VDJServer[53], PLAbDab[54], ImmuneDB[55], that are useful for new studies on protective responses to the certain antigens. This is possible because these databases gather detailed information of structure, function and specificity of characterized antibodies.

In vaccinology, antibody repertoire sequencing studies have also contributed for determination of dose schedules[47, 56-57]. Since in some cases the timing between vaccination and boosting affects the vaccine immunogenicity, it is important to determine the dynamics of GC reactions and affinity maturation to set the ideal vaccination schedule[56]. By observing the B cell expansion and SHM loads of these cells in the repertoire, it is possible to gain insights into dose interval and antibody affinity maturation and then, prevent unnecessary vaccinations[46]. Additionaly, these studies have elucidated the breadth of the antibody response, long-term protection, effects of vaccine formulations (including antigens and adjuvants) on the repertoire shape and convergent antibody responses between individuals. One example is a well succeeded study that applied the antibody repertoire analysis at single-cell level to describe the dynamics of the YFV-17D vaccine, providing key understanding about its efficacy[48]. Taken together, this knowledge can help improving the flavivirus vaccine design and finding targets for future therapeutics.

2.3 The Yellow Fever vaccine (17DD, 17D, 17D-213)

The YFV vaccine is a live attenuated vaccine derived from the strain 17D and developed in the 1930s[58-59]. Over the years, this vaccine has been recognized as one of the best vaccines ever developed. The main reasons for this fact are the high safety, efficacy and long–term immunity that can last to more than 35 years after one single immunization[60]. The molecular basis of this long-term immunity has not been completely elucidated yet, but it is speculated that part of this long lasting effect is due to transient viremia caused by vacine virus replication that can last for decades, increasing the vaccine immunogenicity[61-62]. It has been shown

that viremia caused by the YFV vaccine peaks at around 5 to 7 days following vaccination[63] (Figure 3). Furthermore, the effectiveness of this vaccine is attributed to neutralizing antibodies that are mostly induced against structural envelope protein (E)[64].

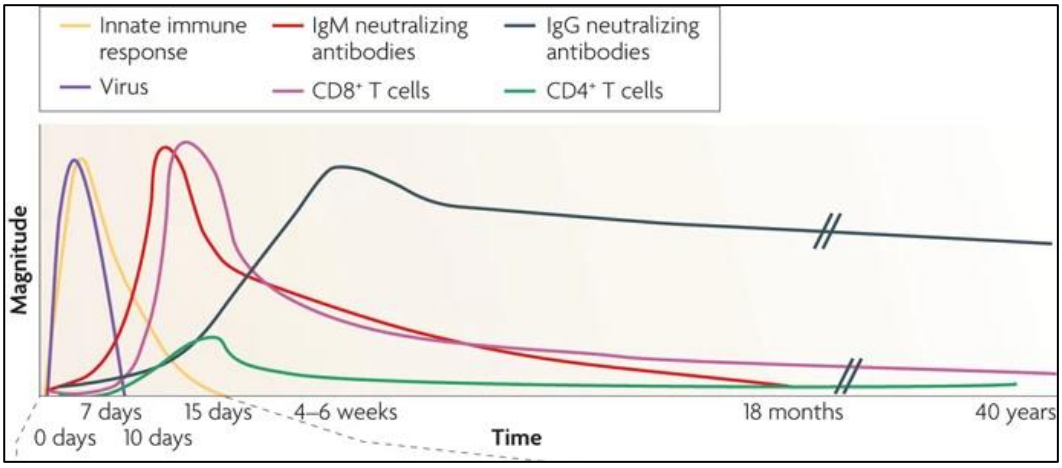

Figure 3. Immune responses following vaccination against YFV[63]. Transient viral replication occurs within the first week after immunization. IgM and IgG neutralizing antibodies rapidly appear, peaking at 2 and 4 weeks respectively. IgM antibodies can persist up to 1.5 years while IgG can be detected in the vaccinees sera up to 40 years. Adaptive cellular responses ($CD4^+$ and $CD8^+$) are also induced after vaccination and are highest within 2 weeks.

There are three different strains (17D, 17DD and 17D-213) being used to produce the YFV vaccine[65]. The difference between these strains is the number of passages they were subjected during their obtention. For example, strain 17D was obtained after 235 passages in chicken embryonic tissues, while 17DD is subjected to a higher number of passages (287). The 17D-213 is produced with 240 passages. A previous study has shown that such differences in the number of passages do not produce significant variations in the strains[66]. The percentage of homology identified between 17D and 17DD was 99.9% at DNA level[66]. At the protein level, these strains presented minimal differences in the glycosylation sites of the viral envelope[66].

An investigation carried out with 1,087 volunteers aiming to compare the response induced by the 17D and 17DD vaccines demonstrated that these variations were not capable of generating major differences across the vaccines outcomes, especially in relation to the protection induced in terms of antibody titers and seroconversion rates[67]. Furthermore, genetic stability between vaccines is quite high even when they are produced on a large scale[68]. To date, there are

only six research institutes responsible for this vaccine production. These producers are located in the United States (17F-204, YF-Vax, Sanofi-Pasteur), France (17D-204, Stamaril, Sanofi-Pasteur), Senegal (17D-204, Pasteur Institute, Dakar), China (17D- 204, Tiantan, Wuhan Institute of Biological Products), Russia (17D-213, Chumakov Institute of Poliomyelitis and Viral Encephalitis) and Brazil (17DD, Fiocruz – Fundação Bio Manguinhos)[65].

The vaccination against YFV is successfuly conducted in several countries and diverse follow up studies have been conducted in these populations to better understand the kinetics and durability of the vaccine's protective response[69-71]. So far, these studies have shown that, after immunization, the YFV vaccine virus starts to replicate and a rapid humoral immune response is elicited, with neutralizing antibodies being detected within 10 days in 90% of the vaccinees. The neutralizing antibody titers continue to rise during the 30 days following vaccination, and 95% of the vaccinees present seroconversion and protection status[72-75]. These studies attributed the rapid seroconversion of the vaccinees to the pro-inflammatory profile induced by the YFV vaccine, which contributes to activation of cells from both innate and adaptive system[10, 71].

Reports about the cellular dynamics in response to YFV vaccine have described the plasmablast's peak of expansion between 7 and 14 days after vaccination, while memory B cells are detectable as early as 14 days, peaking between 3 and 6 months[7, 48, 76]. These cells produce IgM and IgG antibodies which are the main components of the adaptive response. The IgM antibodies are the first to be secreted and they can persist in the serological repertoire by several months and even years after vaccination[77] (Figure 3). Persistence of IgM antibodies is associated to the transient viremia and its neutralizing potential is explained by the multivalent binding to the virus[78-79]. According to previous studies, 65% of the YFV vaccinees produce IgM that peaks at 2 weeks after vaccination, while 60% of the individuals present IgG that is usually detected at 4 weeks following vaccination[10, 80]. These antibodies can activate citotoxic mechanisms, direct neutralization of the virus, inhibit the viral binding and entry into the host cells, trigger the clearance of infected cells through complement-mediated lysis and activate Fc-γ receptor-dependent viral clearance[81].

The YFV vaccine is obtained after a long process of production based on chicken embryos using pathogen-free eggs[82]. To overcome the time consuming

limitation, the World Health Organization (WHO) approved the use of the fractional dose (1/50 of the standard dose)[83]. A recent comparative report on the immune response triggered by the standard and fractional dose, found same outcome of protection, specially in terms of neutralizing antibodies[10]. This evidence highlights the effectivity and feasibility of YFV vaccine administration, specially in endemic areas with low vaccination coverage due the stock shortage. However, further studies are needed to better investigate the duration of the immune response and specificities of the antibodies.

2.4 Epidemiology and pathogenicity of the yellow fever disease in Brazil

Spite of the availability of the YFV vaccine and its excellent results, infections and outbreaks caused by the YFV virus are still recurrent worldwide, with high mortality rates in the region of Americas and Africa[84]. This may be associated to low vaccination coverage, favorable climatic conditions and the propagation of the transmission vector[85]. In Brazil, YFV reemergence has threatened millions of people over the last decades[86]. This scenario is worsened by the fact that up to date there is no specific treatment to the YFV disease.

From 1980 to present, the YFV virus has spread throughout the country (Figure 4). The most severe outbreak was recorded in the southeast region, especifically in Minas Gerais, between 2016 and 2019. In this period, 2,551 cases of yellow fever were reported and 772 deaths were registered. This represented a 3 fold increase in the number of cases and 1.5 more deaths in comparison to past years (1980-2015)[6, 87-88]. In 2020, YFV cases persisted in Minas Gerais and expanded to the central region of the country, in the states of Goiás and Distrito Federal[89-90]. The circulation of the YFV continued in Brazil in 2021, reaching the South and Southern regions (States of Rio Grande do Sul, Paraná and Santa Catarina)[91-92]. In 2022, the virus was detected in the North (Pará and Tocantins) and Southeast (São Paulo), raising concerns of a possible new outbreak[93]. In the period between 2023 to present, there were four cases of YFV disease in Brazil, two in the North (Amazonas and Roraima) and two in the Southeast region (São Paulo and Minas Gerais). Three of the four reported cases resulted in death, even though two of these individuals had been vaccinated against YFV[94].

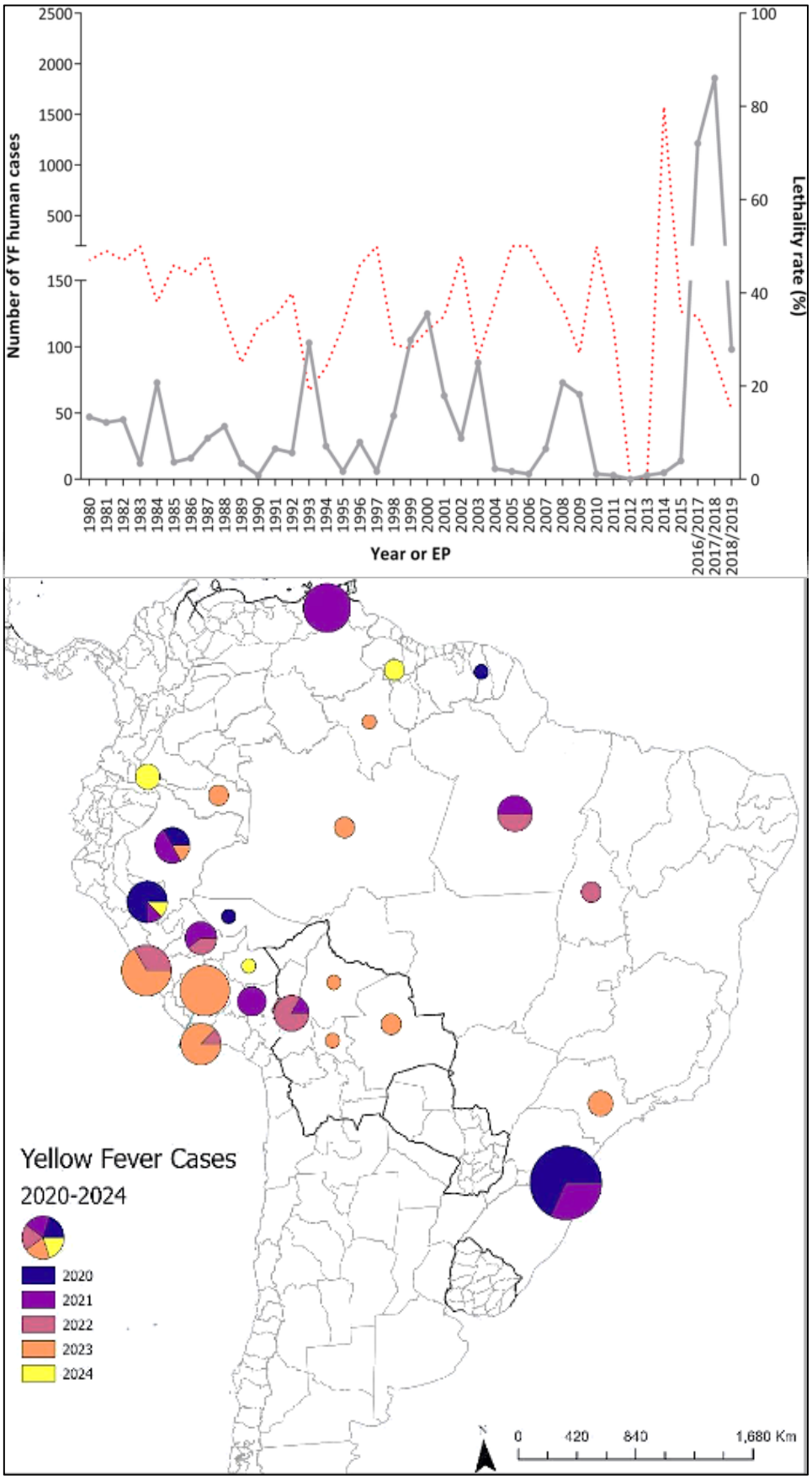

Figure 4. Incidence of YFV disease in Brazil and in the Region of Americas over the decades[95-96]. Top graph showing the number of human cases of YFV disease (grey line) and lethality rate (red dotted line) between 1980 and 2019. Bottom graph represents the geographic distribution of human YFV cases reported in the region of Americas between 2020 and March 2024.

It is possible that distinct YFV lineages were involved in these infections, since it has been observed the co-circulation of more than one YFV lineage in the country during this time[97-98]. Recently, it was reported that the neutralization potency of the YFV vaccine-derived antibodies is reduced against the emergent Brazilian strain[99]. This finding could explain the recent deaths caused by YFV in vaccinated individuals[94]. Although there is only one serotype of YFV virus, seven different genotypes of this pathogen have been identified worldwide[6]. In Brazil, the predominant genotype is the South American YFV I, which has five different sublineages (1A-1E)[100-102]. Molecular studies about YFV found that 1E sublineage was responsible for the 2016-2019 outbreaks. Analysis of the genomes of this sub-lineage identified mutations that led the replacement of nine amino acid residues in highly conserved regions of non-structural proteins involved in virus replication (NS3 and NS5). The impact of these mutations was associated with greater potential of viral infection, transmissibility and, consequently, virus spread[103-104].

Usually, the YFV transmission is critical during the summer season (between December and May), when the climatic conditions are favorable for *Aedes*, *Haemagogus* and *Sabethes spp.* mosquitoes' reproduction[1]. These vectors propagate YFV mainly through two distinct cycles, named sylvatic and urban. In the sylvatic cycle, *Haemagogus* and *Sabethes spp*. mosquitoes become infected with YFV after feeding on the blood of infected non-human primates. Afterwards, these vectors start spreading the virus in nature by biting healthy primates. Yet, these vectors can vertically transmit the YFV virus between themselves[105]. In the urban cycle, *Aedes aegypti* or *Aedes albopictus* mosquitoes become infected after feeding on the blood of an infected individual. So, just as happens in the sylvatic cycle, these infected mosquitoes spread the YFV virus across humans[106-107].

YFV has already been shown to be capable of spreading systemically, infecting various cell types[108-110]. Along with this viscerotropic process of the YFV disease, several clinical manifestations can be observed. These symptoms appear after an incubation period that varies from 3 to 6 days[75]. Firstly, manifestations are flu-like and, as the disease progresses, nausea, headaches, vomiting, photophobia and myalgia may also appear[111]. Although most of the patients recover after these symptoms, in some cases, the disease can progress to a second stage that can last up to two days, leading to a severe condition[112]. This worse stage may occur to 15% - 25% of the infected individuals, and multiple dysfunctions that can result in

death may be observed, such as hepatic syndromes, cardiovascular disorders, renal dysfunctions and even hemorrhagic fever[6, 113]. Studies have pointed out some factors that contribute for the development of these severe conditions, including the viral load, host immunity status, age and comorbidities[114-115]. In Brazil, the yellow fever mortality rate related to these severe conditions has reached 40%, exceeding the global average that varies between 5 and 10%[116].

2.5 Biological aspects of the YFV virus

2.5.1 Origin and replication

The increased yellow fever cases in the recent years have encouraged many scientists across the world to fill the gaps in the knowledge involving the YFV virus. For example, the molecular aspects of the life cycle of this pathogen have been the extensively studied in several investigations that aim to find specific targets for future therapeutics[59, 110, 117]. Overall, the YFV virus belongs to the *Flavivirus* genus and shares diverse biological aspects to Dengue (DENV – Dengue Virus), Zika (ZIKV – Zika Virus), the Japanese Encephalitis virus (JEV – Japanese Encephalitis Virus), West Nile Fever virus (WNV) and Tick-Borne Encephalitis Virus (TBEV)[3].

It is well known that after the virion be introduced in the host by the mosquitoes bite, it initiates the interaction with the cell receptor that enables its entry into the host cell[110]. Many receptors have been identified as mediators of *Flavivirus* internalization in different cells, such as the C Type Lectins (CLR) - CLEC5A, DC-SIGN/L-SIGN, phosphatidylserine receptors (TIM and TAM), laminin receptors, heat shock proteins (hsp70), αvβ3 integrin receptors, G protein-coupled receptor kinase 2 (GRK2) and the mannose receptor[118-125]. The variety of receptors implies in the infection of a broad range of cell types, in the tropism for certain tissues and in the elevated pathogenicity[126].

Alternatively, flaviviruses can penetrate the host cell through non-neutralizing antibodies. Upon recognition of the viral particles and interaction to Fcγ receptor[127], these antibodies activate the virion endocytosis. The acidic environment of the endosomal vesicle triggers conformational changes on the viral particle, enabling the fusion of the viral envelope with the endosome membrane[126]. Following this fusion, the capsid is disassembled and the nucleocapsid releases the virion RNA into the cytoplasm[128]. Then, the RNA is translated into a polyprotein

that is a precursor of viral proteins before its cleavage by proteases[129].

Part of the viral proteins (the non-structural proteins) is responsible for the replication of the viral genome[129] and once this process is done, the new sintetized viral RNA is packaged with the translated structural proteins forming the nucleocapsid[130]. This, in turn, is involved by a lipid bilayer derived from the host reticulum membrane during the viral budding process. Then, structural proteins are assembled to the surface of the particle and the immature virion is formed[130]. These immature virions head to Golgi where they become mature after the partial proteolysis of the structural proteins carried out by furin enzymes[131-133]. This process is important to virions acquire infectiveness, since the consequent structural rearrangement will enable the fusion of viral particles with endosomal vesicles under the influence of reduced pH[133]. The mature virions finally move towards the secretory pathway and leave the cellular environment via exocytosis[129]. The whole process is summarized in the Figure 5.

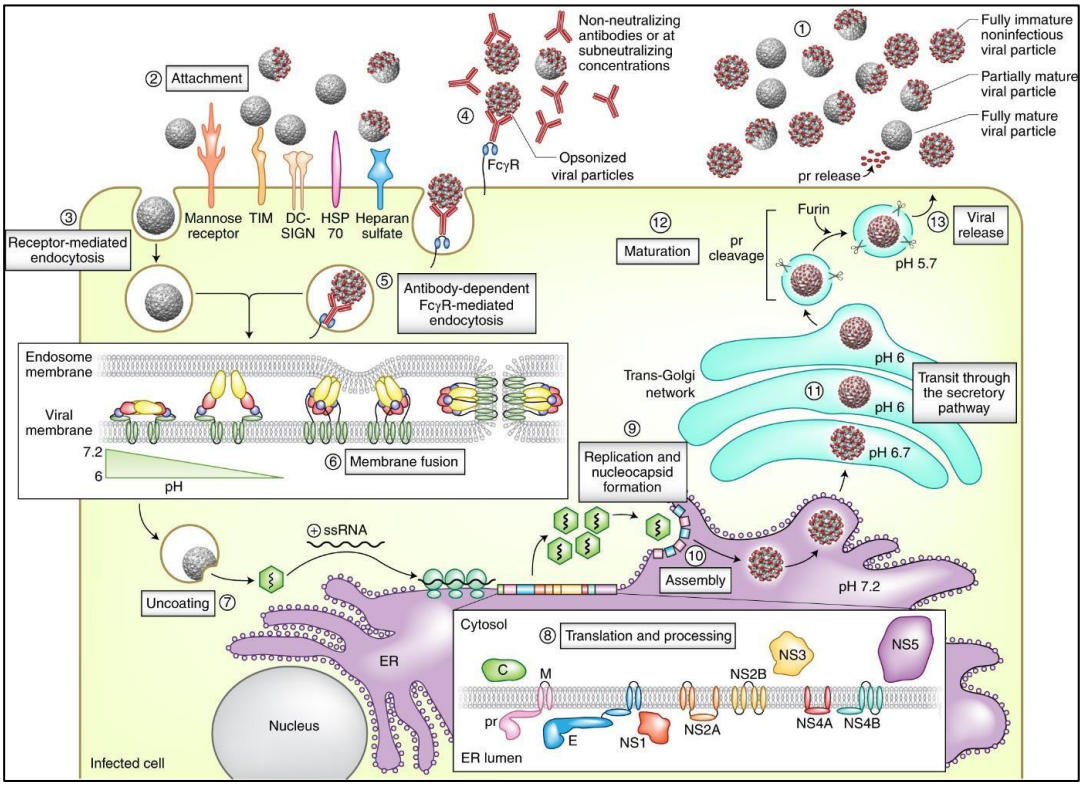

Figure 5. Flavivirus replication cycle[127]. 1. Viral particles can be released at different degrees of maturation. 2. Virions can interact with different receptors depending on the cell type and the specificity of the pathogen for certain ligands. 3. Binding to the cellular receptor activates endocytosis, leading to virion internalization. 4. Alternatively, virions can penetrate into the cell through non-neutralizing antibodies. 5. Viral particles are opsonized via Fcγ receptor-mediated endocytosis. 6. The acidic pH of the endosomal vesicle activates the conformational change of the viral particle proteins, enabling the fusion of the virus with the endosomal membrane. 7. Next, viral RNA is released into the

host cell's cytoplasm. 8. The translation of viral proteins takes place in the endoplasmic reticulum. 9. Replication of the viral genome occurs in the reticulum. 10. After replication, the nucleocapsid is formed through the packaging of the viral genome with the newly synthesized viral proteins. 11. The nucleocapsid takes the secretory pathway to Golgi complex. 12. Immature virions undergo maturation process through proteolytic cleavage of the viral envelope. 13. Mature virions are released from cell via exocytosis.

2.5.2 Structural organization

The recent advances on structural biology have brought valuable understanding about the flaviviruses structure organization. High-resolution electron cryomicroscopy images from many studies[12, 133-137] permitted to elucidate details of the viral particles. Overall, flaviviruses are structuraly described as smooth and spherical virions of 50 nm size and containing a lipid bilayer that forms the envelope. Internally, these virions are comprised of the nucleocapsid that holds the positive single-stranded RNA measuring approximately 11kb[127, 129, 133-134]. As mentioned previously, this RNA encodes a polyprotein of 3,388 amino acids, in which three structural proteins and seven non-structural proteins are derived[127] (Figure 6). The seven non-structural proteins are: NS1, NS2A, NS2B, NS3, NS4A, NS4B, and NS5, which are involved in the processes of replication, assembly and evasion of the innate immune response during infection[134]. The three structural proteins: capsid (C), precursor membrane glycoprotein/membrane protein (prM/M) and the envelope protein (E) are involved with viral pathogenicity[138-139].

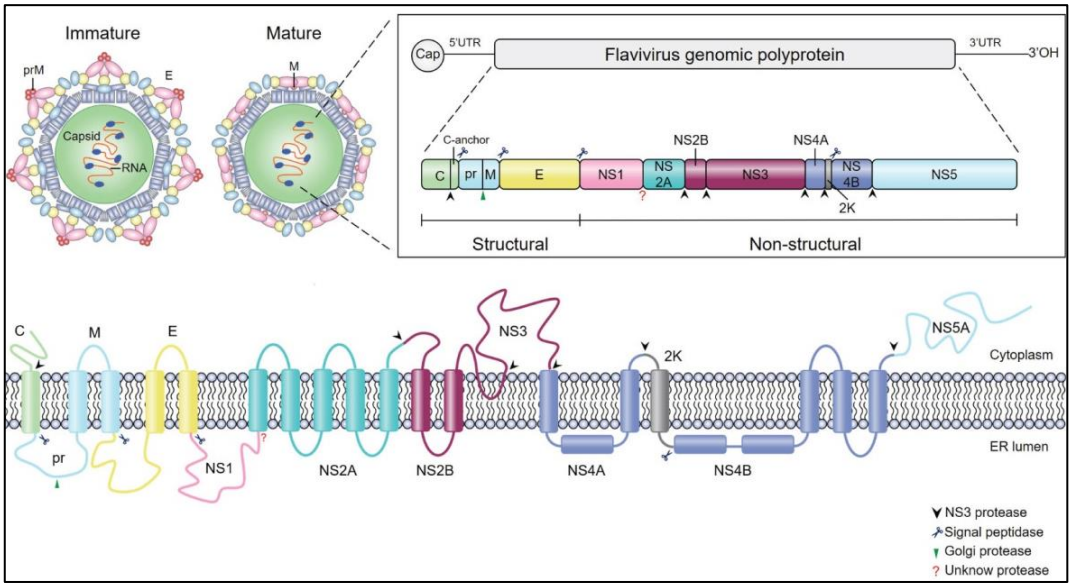

Figure 6. Flavivirus structure, genome and polyprotein organization[141]. Top-left: Immature and mature forms of the viral particles. Top right: flavivirus RNA genome encodes a polyprotein that generates three structural (C, E and prM) and seven non-

structural proteins (NS1, NS2A, NS2B, NS3, NS4A, NS4B and NS5). Bottom: Sites of polyprotein cleavage performed by viral and host cell proteases.

The non-structural NS1 protein is conserved among the flaviviruses, sharing an average of 53% homology between DENV and ZIKV viruses[142]. This molecule it is a hexameric protein, comprised of 352 amino acids and 300 kDa molecular weight (between 46 and 55 kDa per monomer depending on the glycosylation pattern)[141, 143]. It is highly immunogenic and plays a key role in the virus replication[141]. A fraction of this protein can be secreated by the infected cells and circulates in the bloodstream of the infected individuals inducing endothelial disorders and proinflammatory cytokines that increase the flavivirus pathogenicity[143-144].

NS2A is a transmembrane protein which is responsible for both RNA replication and virion assembly[145]. Likewise, NS2B (14 kDa) is also involved in both processes by being part of the replication machinery and serving as cofactor of NS3 during the virion assembly[145]. NS3 is another component of the replication complex that works as an helicase enzyme and its activity is regulated by NS4A and NS4B proteins[145]. Basically, both NS4A and NS4B participate of the replication process by enhancing NS3 helicase activity[145]. The last non-structural protein, NS5, is responsible for RNA methylation and addition of RNA capping[145]. Therefore, although all seven non-structural proteins are components of the the replication complex, only NS3 and NS5 develop enzymatic activity and represent the core of the replication machinery. The others are regulatory proteins of the replication process, with some of them also having additional roles in the virion assembly and in the interaction with signaling molecules to get away from the immune response[141, 145]. As example, there are the NS1, NS2B, NS3 and NS5 that can act suppressing the interferon I (IFN-I) response by targeting host signaling molecules[146].

The mature virion has 180 copies of the E (55 kDa) and M (8 kDa) proteins associated with the envelope[139] (Figure 7). The arrangement of these structural proteins in the mature viral particle confers a smooth and icosahedral shape to the viral surface[12, 139]. The E protein represents one of the most important structures of flaviviruses, since the interaction of this molecule with the target receptor triggers the virus entry into the cell host[147]. Furthermore, this protein is involved in many other aspects of viral pathogenesis, such as the variety of hosts,

the tropism of the virus for certain types of tissue, as well as its virulence[148].

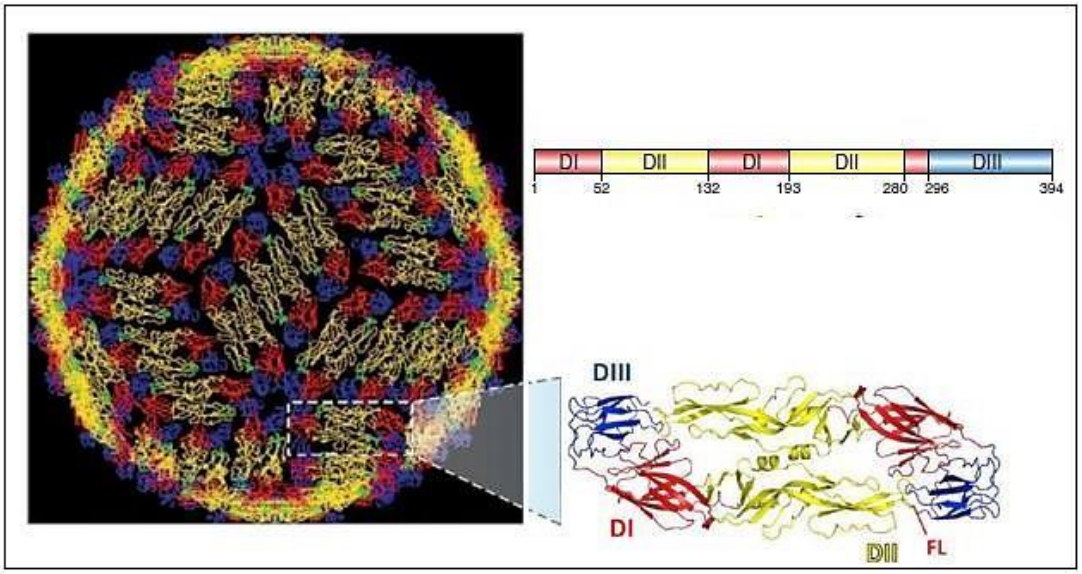

Figure 7. Schematic representation of E protein on the viral particle surface. Left: Arrangement of 180 E-protein subunits on the flavivirus particle. Bottom-right: an expanded view of the E dimer protein (PDB: 1OAN) showing the three domains (I – red, II – yellow and III – blue) and the fusion loop (FL) at the tip of DII. Top-right: primary sequence of E protein highliting the three domains positions.

Basically, the glycoprotein E is comprised by 500 amino acids in its monomer primary sequence. At the three-dimensional arrangement, the E protein structure is formed by two monomers in head-to-tail position, forming a homodimer[133]. Each monomer contains three functional and structural domains: DI, DII and DIII[12-13]. The first domain (I) is called central for being located between the extension of domain II and domain III. The domain II is considered the largest of the three domains and contains a conserved region called fusion loop (FL). This loop is hydrophobic and plays an important role in the fusion of the virion to the host cell membrane. For this reason, domain II is also known as the fusion domain. The third and final domain (III) has a globular shape and it contains the binding site for the host receptor[147, 149] (Figure 7).

A previous study detailed the structural dynamics of the YFV E protein by resolving its crystallographic structure[147]. One of the results highlighted the similarity of YFV E conformation to the other flaviviruses[147]. The homology between E proteins from different flaviviruses had already been described before, and the identity degree varies approximately between 40% and 80%[142, 150-151] (Figure 8). The highest homology of E protein (78.4%) was reported between DENV1 and DENV3. By contrast, the E protein from DENV4 was the most

distant serotype within DENV serocomplex, since its homology with DENV1 (63.3%), DENV2 (62.8%) and DENV3 (63.4%) was considerably low in comparison to others (66.1% DENV1-DENV2 and 66.3% DENV2-DENV3)[150]. Distantly related serotypes, such as DENV and ZIKV, have shown even lower E protein homology (between 51% and 54%)[152-153]. Regarding the YFV E protein homology to other flaviviruses, a previous study has shown that this antigen is closer to TBEV than DENV, ZIKV, WNV and JEV[154].

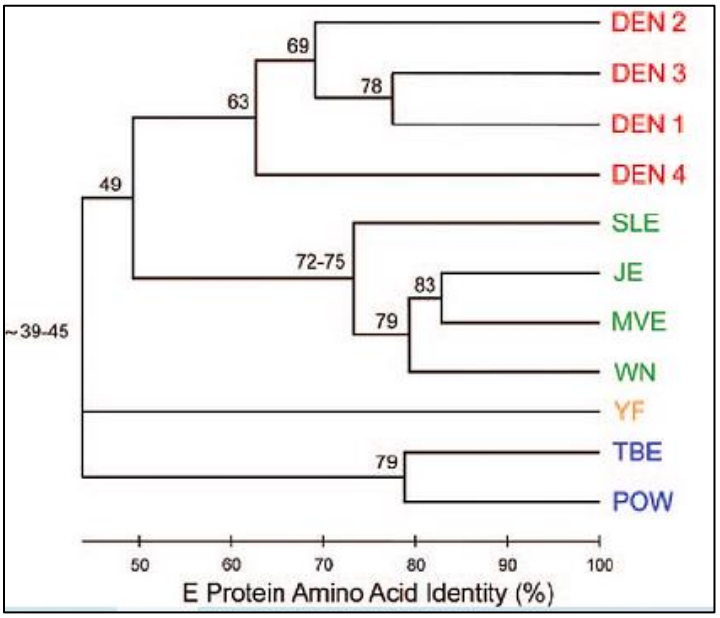

Figure 8. E protein amino acid identity among the different flaviviruses[151]. Colors represent the distinct serotypes: red – DENV, green – JEV, SLE, MVE, orange – YFV, blue – TBE, POW (Powassan).

The prM protein has around 164-168 amino acids and its cleavage by furin enzymes results in the removal of the N-terminal "pr" peptide, leaving only the M protein with approximately 93 amino acids[155]. The association of pr peptide to M protein has been shown to prevent conformational changes before the virion transition to mature state[156]. Additionally, its function is similar to a chaperon, controling the proper folding of E protein[12, 137]. A recent study has shown that this protein is able to inhibt the antiviral signaling and consequently, contribute for flavivirus pathogenicity by supressing IFN-I production[157].

The structure of the mature virion is very dynamic upon intracellular pH changes and this phenomenon results in buried areas that affects the epitope accessibility[151, 158-160]. Studies have describe this as "viral breathing" that impacts in the antibody responses including in the aspects of specificity, neutralization

potency and cross-reactivity[11, 151, 159-161]. In addition to pH, thermostability of some viral strains also can determine changes in the morphology and, consequently, the viral breathing[159-162]. Past investigations have shown that certain DENV viruses are less stable upon temperature increase, exhibiting transient structural oscillations[160, 162]. Taken together, this structural flexibility has determinant implications for adaptive immunity evasion.

2.6 Implications of flavivirus antibody cross-reactivity

Most of the flaviviruses are medically relevant due their potential of infectivity to humans[3]. The genetic and antigenic similarities among these flaviviruses allowed their organization in 8 serocomplexes and 17 independent viruses[163]. Serocomplexes were defined by the ability of an immune sera against one flavivirus cross-neutralize others[163-164]. For instance, there are four DENV serotypes (DENV1-4) and different degree of cross-reactions between these viruses are commonly observed in pre-immune individuals sera[165-166]. In addition to cross-reative responses within the same serocomplex, studies have also described this phenomenon between distantly related viruses. For instance, polyclonal immune sera from previous DENV experienced individuals were found to cross-react to ZIKV virus[152, 167-168]. Moreover, the polyclonal sera from ZIKV infected patients with vaccination history against TBE and/or YFV showed neutralizing activity against DENV[169]. Likewise, cross-reactive antibodies isolated from YFV vaccinees showed to prevent congenital neurological dysfunctions in ZIKV-infected mice[170]. Furthermore, another study discovered that anti-DENV and anti-ZIKV antibodies were able to neutralize the YFV virus[171].

The global spread of flaviviruses increases the frequency of co-circulation of related viruses[97, 172] (Figure 9). As consequence, humans become more vulnerable to experience multiple infections through different flaviviruses[84, 172-173]. The impact of these exposures during lifetime is the induction of a flavivirus memory immune response that can influence the course of subsequent infections[142, 166-169, 171, 174-175]. Beside of the cross-protection, these outcomes can lead to increased disease severity[14, 142, 171, 175-177].

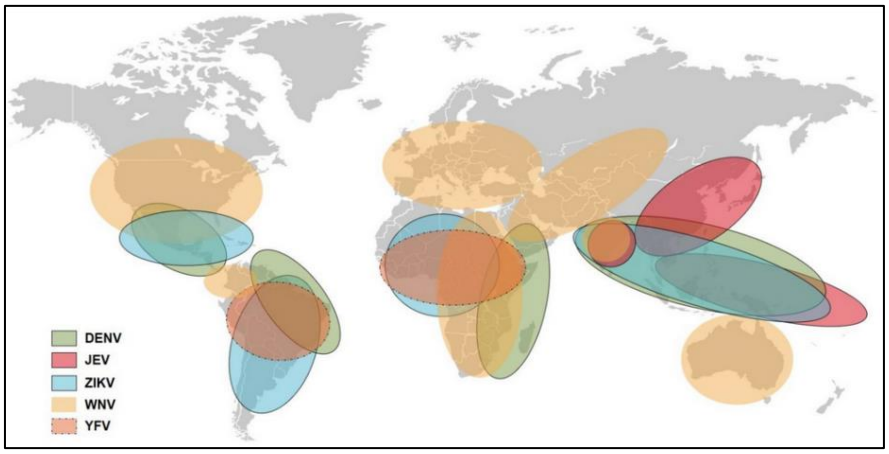

Figure 9. Co-circulation and distribution of DENV, JEV, ZIKV, WNV and YFV worldwide[172].

Over the years, epidemiological studies have linked these cross-reactive antibodies to augmented infection via a mechanism which is best known as antibody-dependent enhancement (ADE)[177-178] (Figure 10). In this process, pre-existing IgG antibodies from past infections with related viruses may interact with the heterologous virus in a weakly/non neutralizing way. Nevertheless, these antibodies bound to the virus can activate its opsonization in antigen-presenting cells by targeting the Fcγ receptor. Inside of these cells and still active, the virus can replicate, resulting in increased viral load and amplification of the infection[127, 178].

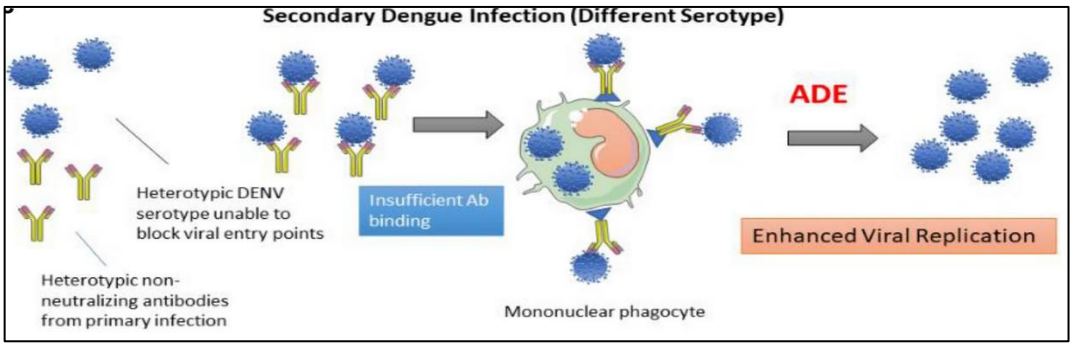

Figure 10. Antibody-dependent enhancement (ADE) in DENV[178]. Non-neutralizing antibodies elicited during primary infection recognize the heterologous DENV serotype during secondary infection. However, these antibodies are unable to neutralize the different DENV serotype that enhances the virus infection and replication into cells leading to increased risk of dengue severity.

Recently was found that prior ZIKV infection increases the risk of Dengue disease by subsequent infection with serotypes 2, 3 and 4[175]. On top of that, anti-YFV antibodies were capable of increasing the viral load *in vitro*[179-180] and *in vivo*[181]. Another study has found that pre-existing immunity against TBEV

influenced YFV vaccine response towards the production of cross-reactive IgG with potential to enhance DENV infection[14]. The determinants for either cross-protection or disease enhancement are the antibody concentration, binding affinity and specificity[177, 182-183]. Early studies on the nature of antibody cross-reactivity observed that antibody titers from previous vaccination or natural infection decay over the time to subneutralizing concentrations that impact the functional responses to different flaviviruses[177, 182].

It is already known that the antibody stoichiometry relies on the epitope[182]. These antibodies are mostly within E, prM and NS1 proteins, which represent the immunodominant antigens in the immune response against flavivirus[184]. Among these antigens, the E protein contains the majority of the epitopes that are recognized by the neutralizing antibodies[48, 64, 147, 185-190]. Using anti-YFV antibodies, it was possible to map these epitopes within domains I (aa E-153/158), II (aa E-71/72, E-173) and III (E-305/325, E-380) of the YFV virus E protein[59, 189, 191-192].

The distinct antigenic sites on DI, DII and DIII can determine the functional activity and serological specificity of the antibody responses[148, 193-194]. Overall, DI has epitopes that are predominantly recognized by either virus-specific or cross-reactive antibodies that lack neutralization activity[148, 194]. DII presents epitopes for the recognition of antibodies that mostly exhibit cross-reaction to other flaviviruses and display low or none neutralization characteristics[148, 151, 194]. DIII in turn, contains epitopes that induce a highly specific and protective response through neutralizing antibodies[195-196]. For instance, a previous report found that DENV1 pre-immune individuals developed ZIKV immunity by eliciting antibodies that bind to DIII[197]. There are also complex quaternary epitopes that span more than one of these domains in the surface of the E homodimer[39, 185, 198-202]. Previously, it was found that anti-YFV antibodies targeting these quaternary epitopes formed between DI and DII represent a significant fraction of the neutralizing response[185]. Likewise, these quaternary epitopes have also been characterized in human antibody repertoires against DENV[39, 198-199], WNV[201], JEV[202] and ZIKV[200, 203].

Another important region involved in these antibody-mediated cross reactions is the FL at the tip of the DII[11, 163, 187, 204]. Antibodies targeting this region likely display weak neutralization potency and increased risk of disease

enhancement[148, 204]. Similarly, epitopes on prM protein have been also associated to this phenomenon[156, 205]. Studies have also linked the NS1 protein to the development of cross-reactive antibodies that display a wide range of neutralization potency[206-207].

The content of these proteins in the viral particle is determined by its maturation state[127, 136]. During maturation, the efficiency of the proteolysis may vary according to the cell type, and sometimes, it is possible that viral particles are not fully mature[135-136, 160]. Consequently, partial matured viruses may be released with varied prM content that affects the antigen presentation and production of antibodies[127, 136]. This was demonstrated by a study that found distinct prM content in viral particles produced in insect, tumor cell lines and human dendritic cells[39, 127, 205]. Therefore, the structural diversity of the viral particles may impact the quality of antibody responses, including the cross-reactivity.

Alternatively to epitope diversity, cross-reactions may be product of B cell development, since the refinement of the antibody specificity is obtained after processes that involve GC reactions, such as affinity-maturation and SHM[208]. Studies have shown that antibodies lacking critical processes of affinity-maturation and SHM tend to present poly/cross-reactive properties due to the suboptimal avidity and affinity against the heterologous antigen[209-212]. This fact increases the probability of ADE during the secondary exposure[210]. The involvement of GC-independent B cells in the production of unmutaded and cross-reactive IgG antibodies has become more evident with characterized antibody responses from repertoire studies[48, 209].

On the other hand, there are studies suggesting that repeated antigen stimulation, such as repeated DENV infections or SARS-CoV-2 vaccination/breakthrough infections, triggers extensive SHM reactions that also contribute to cross-reactivity and polyreactivity with potent neutralizing activity[213-214]. The explanation to this is the memory B cells recall after antigen reencountering[214]. Repertoire studies have also linked cross-reactivity to preferential use of certain VH genes[215-216]. For example, it has been shown that anti-ZIKV mAbs strikingly use IGHV3-23 gene segment. Among the amino acid residues which are codified by this gene, there is a tyrosine at 58 position (Y58) that interacts with DIII from ZIKV E protein and contributed to the cross-reactive binding to WNV by targeting the same epitope[215]. Therefore, as the knowledge in

the antibody genotype-function increases, our understanding about adaptive immunity wises to elucidate the impact of these cross-reactions on disease pathology and vaccinology.

3. SIGNIFICANCE

Currently, there is no specific treatment against infections caused by flaviviruses and prevention through vaccination represents the main strategy for controlling virus spread and disease severity. However, there are only available vaccines against YFV, JEV, TBEV and DENV[64-65]. Even though, vaccination against DENV is restricted to some groups of individuals given the risk of disease enhancement caused by cross-reactive immunity[217-218]. This is the main reason why the design of safe and protective vaccines against flaviviruses have been challeging. Therefore, it is absolutely necessary to better understand the antibody responses against flaviviruses to overcome this difficulty and find therapeutic tools.

The study of the antibody repertoire can provide a comprehensive knowledge of the adaptive immune response at the molecular level, especially in the context of the antibody diversity between different groups of individuals and/or experimental conditions. In this investigative process, relevant properties of the humoral response are considered, aiming to identify how differences between populations, ages, time of infection and recovery affect the immune responses[219]. At the same time, monoclonal antibodies can be identified and isolated from human repertoires to be used as treatment against these infections[37-39].

Particularly in this study, the analysis of the antibody repertoire elicited by the YFV vaccine throw light on the immune complexity of populations from endemic countries such as Brazil, where DENV, ZIKV and YFV co-circulate and cause recurrent infections. This is extremely relevant since the relative frequency, abundance and longevity of type-specific and cross-reactive antibodies are not well understood[13]. By identifying these aspects, this study brings on important viral elements that could impact the development of vaccines against flaviviruses. Therefore, this work opens perspectives for the development of new therapeutics against the disease.

4. OBJECTIVES

4.1 Main Objective:

To analyze the antibody repertoire elicited after the vaccination against YFV, elucidating the impact of the endemic area, especially the co-circulation of DENV and ZIKV, on the humoral responses, including the existence of cross-reactive antibodies.

4.2 Specific Objectives:

- To obtain samples from YFV vaccinees before and after vaccination with the 17DD-YF vaccine;
- To determine the reactivity and neutralizing capacity of vaccinees sera samples against YFV, DENV and ZIKV;
- To analyze the diversity, expansion level, SHM, germline gene usage and CDRH3 properties of the B cell receptor (BCR) antibody repertoire of vaccinees.
- To verify the abundance of the cross-reactive antibody lineages against DENV2 and ZIKV in the serological repertoire.

CHAPTER 1

Dynamics, persistence, magnitude and specificity of the antibody responses upon 17DD-YF vaccine boosting

Abstract

Pre-existing cross-reactive immunity can determine the course of a heterologous flavivirus infection, leading to either protection or disease enhancement. Although the 17DD-YF vaccine is highly effective in conferring long-term immunity, studies have shown the need for booster doses in endemic areas. Here, we characterize the dynamics of the B cell repertoire following the 17DD-YF booster dose and investigate its impact on the antibody kinetics and specificities. A combined analysis of serology and BCR sequencing was used to identify molecular features of the antibody repertoire in four vaccinated donors from an endemic area. Our findings indicate that at day 7 and 14, YFV booster vaccination primes a rapid expansion of both pre-existing BCR lineages as well as new lineages without extensive affinity maturation. However, the magnitude and persistence of these latter lineages in the repertoire are reduced after 28 days. We also observed that repertoires are greatly predominated by expanded IgA lineages that may be not associated with predictors of disease severity, but protection. Additionally, we identified expanded lineages containing high CDRH3 amino acid sequence identity to DENV and/or ZIKV characterized antibodies, suggesting the influence of the flavivirus co-circulation in the vaccine outcomes. Therefore, these findings unveil the complexity of the antibody responses upon YFV revaccination and their implications for dictating protection in susceptible populations.

Keywords: Flavivirus Immunity; Immunoglobulin Repertoire; Antibody Response; B Cell Receptor.

5. INTRODUCTION

Several studies have shown that major protective elements elicited by the YFV vaccine are T cells and neutralizing antibodies (nAb)[8]. Following vaccination, nAbs can be detected within a few days[7, 10, 72] and memory B cells are also observed as early as 14 days after vaccination and peaking between three and six months later[7, 48]. nAbs can persist in the vaccinee's serological repertoire up to 35 years[9] and most of them target the E protein[48, 188] which is structurally dynamic, reflecting the availability of the antigenic sites for interaction with these antibodies, and consequently, their biological function[158].

The YFV vaccination induces antibodies that target the DII and DIII domains of the E protein, including a highly conserved epitope located at the tip of the DII domain that includes the fusion loop (FL)[12, 48]. The FL is poorly accessible in the molecular organization of the E homodimer, and that is the main reason why most of the anti-FL antibodies are cross-reactive but weakly neutralizing[11, 135]. It has also been observed that immunization elicits antibodies directed to quaternary epitopes situated between the DI and DIII domains[39]. Antibodies that recognize these dimeric quaternary epitopes commonly display strong neutralization potential[39], and since these quaternary epitopes are also present in other flaviviruses, some of the nAbs may cross-neutralize even distantly related viruses[39, 168, 220].

Different degrees of cross-reactivity between distinct flaviviruses (for example, between YFV and tick-borne encephalitis (TBE), YFV and DENV, DENV and ZIKV) have been observed in sera from both convalescent patients following infection and from vaccinated individuals[174, 220-221]. Notably, this cross-reactive immunity can impact the course of a secondary infection and the immune response in the context of repeated vaccinations against different flavivirus[14, 174]. It is noteworthy that, a recent study reported a negative influence of pre-existing YFV vaccine derived immunity on the neutralizing antibody response to tick-borne encephalitis (TBE) vaccination[174]. The opposite was also observed in TBE-vaccinated individuals who generated weak neutralizing IgG that cross-reacted to YF17D vaccine antigen, in such a way as to enhance the virus infection in vitro via antibody-dependent enhancement (ADE)[14].

Here, we investigated the antibody response to 17DD-YF vaccine

elucidating the impact of the revaccination and co-circulation of different flaviviruses (ZIKV and DENV1-4) on the antibody repertoire fingerprints. We analyzed the antibody repertoire of 4 volunteers sampled before (T0), 7, 14, 28, and 180 days after vaccination against YFV. Our findings show that pre-immunity may drive the magnitude and persistence of antibody responses. We also described important molecular features of the expanded repertoire lineages that may be associated with the antibodies' specificities and neutralization capacity. Overall, this work sheds light on the impact of co-circulation and pre-existing antibodies on YFV vaccine outcomes.

6. MATERIALS AND METHODS

6.1 Human Subjects

Study was approved by the institutional Ethics Committee – Federal University of Minas Gerais, under protocol number CAAE: 08301112.9.0000.5091. Informed consent form and an epidemiological questionnaire (Supplemental Information 1) were obtained before any sample collection and kept anonymized. Subjects enrolled in this study consisted of three women and one man (n=4), aged between 20 and 45 years old and originally from Belo Horizonte, Minas Gerais – Brazil. All participants were vaccinated with YFV-17DD vaccine and a total of 4 ml of venous blood was obtained from each subject before vaccination and on days 7, 14, 28, and 180 following vaccination. Samples were processed by centrifugation at 1,300 rpm and room temperature to separate plasma. Peripheral Blood Mononuclear Cells (PBMC) were also isolated using Ficoll-Paque^{TM} gradient centrifugation and cryopreserved in FBS 90% / DMSO 10%. Both plasma and PBMCs aliquots were stored at -80 ºC until further analysis.

6.2 Indirect ELISA Assay

Indirect ELISA assay was carried out to confirm the presence of antibodies against YFV, DENV1-4, and ZIKV in plasma from vaccinated subjects. Serological tests (IgG) for all flaviviruses were performed at the Flavivirus Laboratory of the Oswaldo Cruz Institute (Rio de Janeiro) using in-house YFV and ZIKV ELISA assay and PANBIO dengue IgG indirect Elisa (Brisbane, Australia).

6.3 Neutralizing Antibody Quantification

Quantification of neutralizing antibody against YFV, DENV1-4 and ZIKV in inactivated (56 ºC/30min.) plasma samples collected from all donors in each time point - 0, 7, 14, 28, and 180 days after YFV-17DD vaccination were performed by the Immunomolecular Analysis Laboratory of Bio-Manguinhos/Fiocruz. Both YF- and DENV-nAb levels were quantified using the micro-focus reduction neutralization test (mFRNT) in 96-well plates, and nAb titers were expressed as the highest serum dilution resulting in 50% focus reduction ($mFRNT_{50}$)[222]. Briefly, samples were serially diluted from 1:3 to 1:729

(dilution factor = 3), followed by the addition of virus suspension (YFV-17D-213/77 vaccine virus; D1- West Pac 74; D2- S16803; D3- CH53489 or D4-341750) containing approximately 100 PFU, resulting in final dilutions of 1:6 to 1:1458 (dilution factor = 2). Plates were incubated at either 37 °C (YFV) or 35°C (DENV) for 2 hours in a 5% CO2 atmosphere for neutralization. The mixtures (diluted samples + virus) were then transferred onto pre-formed confluent Vero CCL-81 cell monolayers for mFRNT-YF or Vero NIBSC cell monolayer, for mFRNT-DENV1-4, both with 2 x 10^5 cells/well. Carboxymethylcellulose (CMC) was added to each well before final incubation only for mFRNT-YF. The plates were then incubated for 48 hours at either 37°C (mFRNT-YF) or 35°C (mFRNT-DENV1-4) with 5% CO_2. Subsequently, cells were fixed with a solution of ethanol and methanol (1:1), followed by incubation with 4G2 HRP-conjugated monoclonal antibody for 2 hours at 35°C in a 5% CO_2 atmosphere. True Blue Dye substrate was added, and after incubation, monolayers were washed, dried, and imaged using an automated acquisition system[223]. Focus were manually counted, and samples with titers ≥ 1:100 and ≥ 1:30 were considered seropositive to YFV and DENV, respectively.

The $PRNT_{90}$-ZIKV (PRNT - plaque reduction neutralization test) was conducted using Vero CCL-81 cells to assess the presence of nAb against ZIKV in samples. Briefly, samples were serially diluted from 1:5 to 1:15,625 (dilution factor = 5), followed by the addition of 60 µL of ZIKV suspension containing approximately 100 PFU, resulting in final dilutions of 1:10 to 1:31,250 (dilution factor = 2)[224]. Plates were incubated at 37 °C for 1 hour in a 5% CO_2 atmosphere for neutralization. For the adsorption step, 100 µL of dilution mixture was added to monolayers in 24-well plates, previously prepared with 2 x 10^5 cells/well, and incubated for 1 hour at 37 °C with 5% CO_2. Subsequently, supernatants were discarded, and monolayers were overlaid with semi-solid medium (sE199 plus 2% CMC), then incubated for 4 days at 37 °C in 5% CO_2. Cell monolayers were fixed with formalin solution (5%) and stained with crystal violet for plaque counting. Plates were photographed using BioSpot® Software Suite (CTL - Cellular Technology Limited, USA), and plaques were manually counted. nAb titers were expressed as the highest serum dilution that resulted in 90% plaque reduction, with samples exhibiting titers ≥ 1:140 were considered seropositive to ZIKV, since the samples were positive for other flavivirus[224].

6.4 Antibody BCR Repertoire Sequencing

6.4.1 RNA Extraction

To perform the antibody BCR repertoire analysis, frozen PBMC obtained from each donor before (T0) and on days 7 and 14 after vaccination, were briefly thawed in water bath at 37 °C degree and kept on ice. Samples were resuspended in 1 ml of Trizol and incubated at room temperature for 5 minutes, after washing them in 10 ml of DPBS by centrifugation (500 x g for 10 minutes at 4 °C). Cells were reincubated at the same conditions following addition of 200 µl of chloroform and vortex homogenization. Afterwards, samples were centrifuged at 12,000 x g for 15 minutes at 4 °C to form a three-phase solution.

The aqueous phase and an equivalent volume of isopropanol were transferred to 1.5 ml eppendorf. Samples were gently homogenized by inversion and incubated overnight at -20 °C. The RNA was obtained by centrifuging samples in the next day at 12,000 x g for 15 minutes at 4 °C. The supernatant was discarded and the tube containing the RNA pellet was resuspended in 1 ml of 70% ethanol to be washed by centrifugation at 12,000 x g for 10 minutes at 4 °C. After one more wash step, the supernatant was discarded and the remaining ethanol was left to evaporate from the RNA pellet at room temperature. Finally, samples were resuspended in 30 µl of DEPC water and the RNA concentration was measured by Nanodrop and Qubit RNA BR Assay kit (Thermo Fisher Scientific). The extracted RNA was frozen at -80 °C until use.

6.4.2 Isolation and Amplification of VH Antibody BCR Transcripts

The resulting RNA (500 ng) was used for first strand cDNA synthesis using the SuperScript IV enzyme (Thermo Fisher Scientific). IGVH amplification of IgG, IgA and IgM were amplified using the set of primers listed at Table 1 in two different combinations: firstly, 0.2 mM of forward primers (1 to 8 from Table 1) were used with 0.1 mM of each IgG and IgA reverse primers (9 and 10 from Table 1). Secondly, 0.2 mM of forward primers (1 to 8; Table 1) were used with 0.2 mM of IgM reverse primers (11 from Table 1). All reactions were prepared using 0.2 units (U) of Platinum™ Taq DNA Polymerase High Fidelity (Invitrogen), 1X High Fidelity PCR Buffer solution, 0.2 mM of dNTPs, 1 mM of MgSO4, and 2 µL of cDNA in a final volume of 50 µL. The PCR reaction was

conducted using the following conditions: 2 min at 95 °C; four cycles of 94 °C for 30 s, 50 °C for 30 s, 68 °C for 1 min; four cycles of 94 °C for 30 s, 55 °C for 30 s, 68 °C for 1 min; 22 cycles of 94 °C for 30 s, 63 °C for 30 s, 68 °C for 1 min; 68 °C for 7 min; hold at 4 °C. Products were analyzed on 1% agarose gel stained with Sybr Safe (Invitrogen). Bands were excised and purified with PCR clean-up Gel extraction (NucleoSpin - Macherey-Nagel) following the manufacterer's instructions. Purified DNA was quantified by Nanodrop and Qubit DNA High Sensitivity kit (Thermo Fisher Scientific).

Table 1 Primer sequences employed for the amplification of antibody-heavy chains (IGVH).

	Name	Sequence (5' to 3')
1	VH1-fwd	**TCGTCGGCAGCGTCAGATGTGTATAAGAGACA**GCAGGTCCAGCTKGTRCAGTCTGG
2	VH157-fwd	**TCGTCGGCAGCGTCAGATGTGTATAAGAGACA**GCAGGTGCAGCTGGTGSARTCTGG
3	VH2-fwd	**TCGTCGGCAGCGTCAGATGTGTATAAGAGACA**GCAGRTCACCTTGAAGGAGTCTG
4	VH3-fwd	**TCGTCGGCAGCGTCAGATGTGTATAAGAGACA**GGAGGTGCAGCTGKTGGAGWCY
5	VH4-fwd	**TCGTCGGCAGCGTCAGATGTGTATAAGAGACA**GCAGGTGCAGCTGCAGGAGTCSG
6	VH4-DP63-fwd	**TCGTCGGCAGCGTCAGATGTGTATAAGAGACA**GCAGGTGCAGCTACAGCAGTGGG
7	VH6-fwd	**TCGTCGGCAGCGTCAGATGTGTATAAGAGACA**GCAGGTACAGCTGCAGCAGTCA
8	VH3N-fwd	**TCGTCGGCAGCGTCAGATGTGTATAAGAGACA**GTCAACACAACGGTTCCCAGTTA
9	IgG-rev	**GTCTCGTGGGCTCGGAGATGTGTATAAGAGACA**GAGGGYGCCAGGGGGAAGAC
10	IgA-rev	**GTCTCGTGGGCTCGGAGATGTGTATAAGAGACA**GCGGGAAGACCTTGGGGCTGG
11	IgM-rev	**GTCTCGTGGGCTCGGAGATGTGTATAAGAGACA**GGTTGGGGCGGATGCACTCC

The bold sequences constitute elements of the Illumina adaptor sequences. The design of the annealing region in primers was based on McDaniel et al [43].

6.4.3 Library Preparation and Sequencing

Sequencing libraries were constructed with 50 ng of each amplicon and using the Nextera XT DNA Library Prep Kit (Illumina) according to the manufacturer's instructions. The P5 and P7 indexes and adapters were incorporated into the 500 bp amplicons by the overhang adapters added to the primers. All reactions were set in a total of 50 µl under the following conditions: 3 min at 95 °C; 12 cycles of 94 °C for 30 s, 55 °C for 30 s and 68 °C for 1 min; 68 °C for 5 min; and hold at 4 °C. Products were purified using of Agencourt AMPure XP

beads and the final concentration of the library was quantified using the Qubit DNA High Sensitivity kit (ThermoFisher Scientific). The size and quality of the amplicons were confirmed using the High Sensitivity DNA Kit (Agilent) run on the Bioanalyzer 2100 (Agilent). The VH amplicon library containing the indexes with the final concentration of 18 pM of IgM and 18pM of IgG/IgA samples from the four individuals repertoires were submitted for sequencing in 2×300 paired-end Illumina MiSeq platform.

6.5 Bioinformatic Analysis

6.5.1 Raw Reads Processing and Sequence Annotation

Raw Illumina MiSeq output reads were pre-processed and annotated using pRESTO[225] and Change-O[226] packages from Immcantation framework, Biopython[227], and IgBlast[228]. 3'-5' and 5'-3' raw reads were joined using the pRESTO AssemblePairs module, with a minimum overlap of 50 nucleotides. The generated sequences were quality filtered using the Biopython Bio.SeqIO.QualityIO module, retaining those with average phred score ≥30.

The pRESTO MaskPrimers module was employed to find on sequences the primers of the IGHV gene and constant region (Table 1, without Illumina adapters). The option score was used, so sequences were kept intact. If IGHV gene or constant region primers were not found, the sequence was filtered out. Sequence annotation was performed with the AssignGenes module from Change-O together with IgBlast to verify similarities between sequences and human germline genes. IMGT human germline reference database was used as reference for V, J, and D gene, as well as their numbering system[229]. After that, Change-O MakeDB module was run to organize the annotation into tabular .tsv files in the MiAIRR format[230]. These files contain information of V, D, J genes and alleles, framework (FW), complementary regions (CDR) sequences, and functional status of the sequence (productive or unproductive). For each PBMC sample (four donors, three times each), it was generated two files, one containing IgM annotated productive sequences and other containing IgG and IgA annotated productive sequences. Based on previously annotated constant region primers, IgA and IgG productive sequences, that were amplified and sequenced together, were splitted into isotype files. Thus, three files from each sample (donor/time) were used in the following analysis. Each one of these files corresponds to a repertoire isotype.

6.5.2 Lineage Definition and Frequency Calculation

To perform lineage analyses, all productive sequences from all samples with the same VJ segment, CDRH3 length and having approximately 90% similarity were grouped into clonotypes using the tool Yclon[231]. The default parameters were used for clonotyping, generating clusters with 91% of similarity between the nucleotide sequences. In order to calculate the frequency of a lineage in an isotype repertoire, the number of sequences grouped in this lineage was divided by the total number of sequences that belongs to this isotype repertoire and multiplied by 100. The level of expansion of a lineage was determined by this frequency. If a lineage represented 0.1% or more of an isotype repertoire, it was considered expanded.

6.5.3 Persisting-Expanded and New Expanded Lineages Definition

In order to track B cell recall responses upon boosting vaccination, for each isotype repertoire, we grouped B cell lines that pre-existed in the repertoire (T0) in a steady-state, remained in the T7 and/or T14, and were expanded (≥ 0.1% frequency) after boost YFV vaccination. These lineages were defined as "persisting-expanded". Similarly, we grouped expanded B cell lineages (≥ 0.1% frequency) that just were identified after vaccination (T7 and/or T14). These lineages were characterized as "new expanded lineages".

To identify the proportion of persisting-expanded and new expanded lineages among the top 50 most expanded lineages of the T14 repertoire, we filtered all expanded lineages (≥ 0.1% frequency) that comprised the IgG, IgM and IgA repertoires according to their frequency level (descending order). The top 50 lineages were selected and identified as persisting or new expanded lineages.

6.5.4 Repertoire Characterization

Repertoire parameters, such as diversity, clonal expansion, size, gene segment usage, somatic hypermutation frequency, and composition and amino acid groups of CDRH3, were analyzed in R studio. Diversity was defined by the Shannon-Wiener index calculated as in McCune et al.[232]. Gene segments and gene subgroups were defined by taking the first assigned gene segment to each sequence from the IgBlast output. After that it was possible to evaluate the frequencies of gene segment usage, gene subgroups, and the combination of V(D)J

genes in each repertoire. Somatic hypermutation frequency was defined as one minus the v gene identity assigned by IgBlast, multiplied by 100. R studio was also used to generate the clonal expansion diagram that considered the clonal expansion frequency as a measure to set the expansion state of the IgG, IgA and IgM repertoires.

6.5.5 Comparative Analysis with Known Antibodies

We used the “search by keyword” function of The Patent and Literature Antibody Database (PLAbDab)[54] available in July 2024 with "DENV|Dengue|ZIKV|Zika|YFV|Yellow Fever" expression to acquire a list of known antibodies that bind to DENV, ZIKV, and YFV. To this list, we added the antibodies obtained from Wec et al[48]. To verify if any CDRH3 from this list had at least 80% amino acid identity to any expanded sequence, we translated the nucleotide sequence of the heavy chain sequences from the list and renumbered them using ANARCI[233] to standardize the CDRH3 region definition. Following that, we used PairwiseAligner module from Biopython[227] to make a pairwise alignment of each CDRH3 sequences from the literature list with each sequence from the repertoire, counting the number of amino acid matches. If this count, divided by the larger CDRH3 from the analyzed pair of sequences, is equal or greater than 80%, we would identify them as having similar enough CDRH3. In order to get epitope information of each literature match, we consulted the reference hits’ patent and/or pdb registration according to data availability.

6.6 Statistical Analysis

Statistical analysis were conducted in GraphPad Prism version 9.0.0 (GraphPad Software Inc., La Jolla, CA, USA). Shapiro-Wilk test was performed to determine the normality of the data, followed by Mann-Whitney test. Non-parametric Mann–Whitney U tests and analysis of variance tests (anova and Kruskal–Wallis H tests) were used to determine the statistical significance. The mean of each donor-specific paramenter, followed by the average mean of all four donors, as well as the standard deviation were used to compare antibody repertoires differences.

7. RESULTS

7.1 Booster 17DD-YF vaccination induces discrete and transient antibody response that does not significantly interfere in the neutralization of DENV1-4 and ZIKV.

Healthy donors (n=4) originally from a region with great incidence of YFV outbreaks received a single standard dose of 17DD-YF vaccine. All participants self-reported a history of vaccination against YFV before this study (> 10 years) (Table 2). Blood samples were collected before (T0) and on days 7, 14, 28 and 180 post-vaccination (Fig. 11A). Polyclonal sera from each donor at the five time points were analyzed by Indirect ELISA against YFV, DENV, and ZIKV to verify the longitudinal dynamics of the antibody response to YFV vaccine and the detection of antibodies reactive to DENV and ZIKV viruses.

Table 2. Overview of the study participants and their baseline immune status.

				Total n=4					
Donor	**Sex**	**Age**	**Past YFV vaccination**	**YFV**	**DENV1**	**DENV2**	**DENV3**	**DENV4**	**ZIKV**
				mFRNT$_{50}$/PRNT$_{90}$ Serosivity					
D1	F	38	Yes	--	--	--	--	--	--
D2	M	23	Yes	++	++	++	++	++	--
D3	F	24	Yes	--	++	++	++	++	--
D4	F	41	Yes	++	++	--	++	++	--

F; female. **M**; male. --; negative. **++**; positive. Soroneutralization cut-off for positive mFRNT$_{50}$ results: ≥ 1:100 (YFV), ≥ 1:30 (DENV1-4); PRNT$_{90}$ ≥ 1:140 (ZIKV).

Overall, most of the donors (50% to 75%) presented detectable levels of YFV and/or DENV antibodies before vaccination (T0), while just donor 2 had high titer of anti-ZIKV antibodies before immunization (Table 2, Fig. 11B-C). Interestingly, this donor presented transient decay in the anti-ZIKV IgG titer after immunization, reaching similar antibody levels (mild antibody reactivity to ZIKV) to the other subjects on day 180 (Fig. 11D). Contrastingly, all donors anti-DENV IgG titer was increased post-vaccination, reaching the highest detection levels at the day 180 (Fig. 11C). Moreover, we detected similar antibody' kinetics against YFV among donors after the vaccination, in which anti-YFV IgG titer peaked two weeks post-vaccination with gradual decline to baseline levels during the first 6 months of monitoring (Fig. 11B).

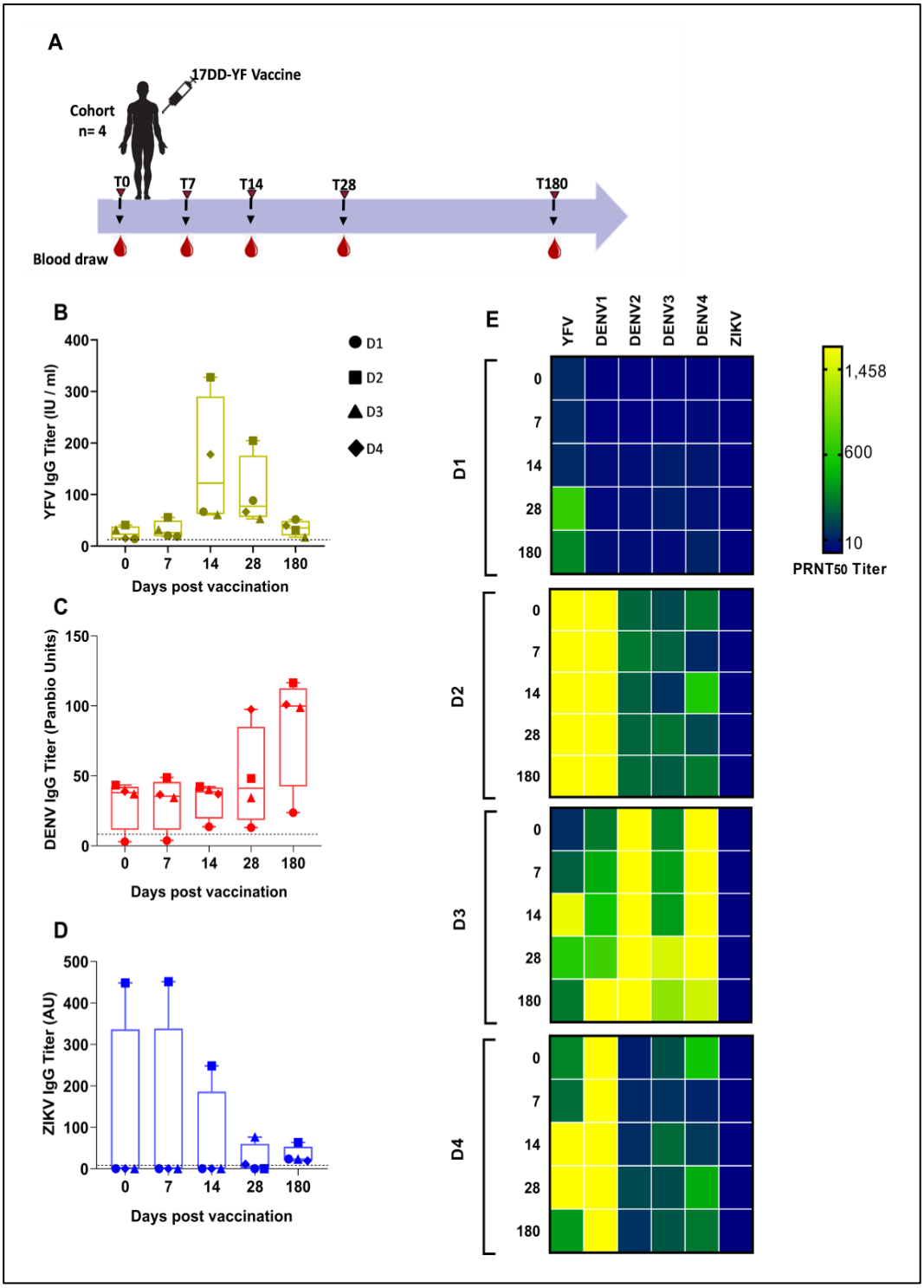

Figure 11. Longitudinal flavivirus antibody responses. **A** Schematic representation of YFV vaccination and longitudinal blood sampling. 17DD-YF vaccine was used to immunize four healthy donors against yellow fever virus. Blood draws were performed before (T0), 7, 14, 28 and 180 days following vaccination to obtain both plasma and PBMCs from each donor at each time point. **B-D** IgG responses against YFV (B), DENV (C) and ZIKV (D). Binding levels were measured using indirect ELISA and the data was expressed as mean IU/ml for YFV, Panbio Units for DENV and AU for ZIKV. Dot lines represent the cut-off for positivity. **E** Neutralizing antibody titers against YFV, DENV1-4, and ZIKV presented by each donor at distinct time points. Results were obtained by performing soroneutralization assay and cut-off criterion for positive mFRNT results were: ≥ 1:100 (YFV), ≥ 1:30 (DENV1-4), and PRNT results ≥1:140 (ZIKV).

We next performed a neutralization assay (either $mFRNT_{50}$-YFV and DENV or $PRNT_{90}$-ZIKV) to test if the antibody kinetics are reflected in the circulating levels of nAbs. These assays were carried out to YFV, ZIKV, and DENV 1-4, and, corroborating the ELISA data, three of the donors showed an increase in the YFV nAb titer during the second (day 14) and fourth week (day 28) after vaccination followed by waning out to day 180 (Fig. 11E). The results also revealed heterogeneity in the anti-YFV response among the donors, which may be attributed to variations in their prior immune status (Fig. 11E, Table 2). By contrast, there was no detectable neutralization of ZIKV. However, all donors displayed a varying degree of neutralizing antibody response to DENV 1-4 that did not correlate to the pattern observed in DENV ELISA. Unlike in the DENV indirect ELISA in which binding titers notably increased post-vaccination, the anti-DENV nAb titer appeared unaffected by vaccination, except for donor 3, who showed an increase in nAbs against DENV-1 and DENV-3 following vaccination (Fig. 11E). In sum, these data indicate a pre-existing immunity to YFV and/or DENV that changed after YFV vaccine boosting. Also, YFV antibodies of revaccinated individuals rapidly decay during the 6 months following immunization. Likewise, neutralization titers waned after 28 days post-vaccination (out to day 180), but they remained higher than their pre-revaccination levels. Nevertheless, a similar trend was not seen with nAb titers against DENV1-4 and ZIKV.

7.2 Revaccination against YFV primes a rapid expansion of antibody repertoires at 14 days with great predominance of IgA.

During revaccination, both naïve and memory B cells (MBC) are activated, resulting in the production of antibodies with different specificities. Prior studies have described that plasmablasts usually peak between 10 and 14 days after revaccination against YFV[13]. Therefore, we sequenced the VH region of the BCR transcripts from samples obtained 0, 7, and 14 days after vaccination, to verify the dynamics of the antibody response upon boost vaccination dose. In this process, IgG, IgM and IgA antibody heavy chain and variable region (VDJ exon), as well as the constant region fragment were analyzed to access the dynamics of the IGHG, IGHM and IGHA clonotype repertoires over time and the summary of the data obtained after sequencing is shown in the Table 3.

Table 3. Summary of the repertoire sequencing analysis.

Donor	Time	Isotype	Raw reads (IgG+IgA and IgM)	Number of annotated sequences	Number of Productive unique sequences	Number of Lineages	Number of Persisting-Expanded Lineages	Number of New Expanded Lineages
1	0	IgA	817,06	349,640	294,721	43,263	56	0
1	0	IgG		111,266	102,657	28,692	20	0
1	0	IgM	772,246	456,415	438,276	144,365	3	0
1	7	IgA	491,344	60,853	59,025	16,084	10	87
1	7	IgG		115,778	110,733	24,480	1	83
1	7	IgM	784,359	555,437	498,120	96,891	4	21
1	14	IgA	769,071	416,364	310,494	26,957	84	114
1	14	IgG		146,206	124,873	23,817	45	124
1	14	IgM	602,074	390,752	371,511	133,714	7	10
2	0	IgA	779,902	289,392	255,099	35,599	82	0
2	0	IgG		157,038	149,259	28,438	73	0
2	0	IgM	840,755	480,008	468,386	204,411	1	0
2	7	IgA	646,452	232,003	225,847	45,671	46	56
2	7	IgG		80,008	79,458	26,082	19	55
2	7	IgM	949,483	670,207	562,135	103,952	16	61
2	14	IgA	724,127	420,192	326,501	21,273	59	125
2	14	IgG		114,823	101,006	12,232	35	162
2	14	IgM	816,536	533,760	471,165	94,946	18	52
3	0	IgA	553,743	197,203	184,882	40,129	77	0
3	0	IgG		70,200	68,839	25,033	37	0
3	0	IgM	674,862	336,539	329,684	133,655	11	0
3	7	IgA	665,123	226,799	214,656	52,515	23	94
3	7	IgG		108,909	107,178	40,007	7	70
3	7	IgM	756,075	534,105	491,875	157,838	3	15
3	14	IgA	560,225	292,489	213,562	27,811	24	146
3	14	IgG		170,938	145,045	32,772	14	141
3	14	IgM	590,317	352,936	334,215	105,805	10	30
4	0	IgA	856,416	334,527	301,707	52,893	58	0
4	0	IgG		125,176	120,574	39,029	19	0
4	0	IgM	792,673	453,542	443,994	271,870	2	0
4	7	IgA	937,116	354,906	326,479	54,746	19	118
4	7	IgG		106,293	103,408	32,486	15	108
4	7	IgM	689,117	455,863	435,937	190,979	2	8
4	14	IgA	726,480	388,328	308,385	36,451	42	134
4	14	IgG		151,487	133,976	29,289	31	132
4	14	IgM	691,220	446,350	381,600	58,969	30	102

Overall, the number of raw reads obtained per IgG and IGA samples ranged from 491,344 to 937,116, while IgM samples raw reads ranged from 590,317 to 949,483 in the three time points. The average of productive reads which were obtained after the data's pre-processing ranged from 28.51% to 41.50% for IgA samples, 14.55% to 18.63% for IgG, and 54.34% to 62.76% for IgM. These productive reads resulted in the obtention of 28,123 - 42,971 IgA lineages, 24,527 - 30,763 IgG lineages, and 98,358 - 188,575 IgM lineages which were analyzed to access the dynamics of the repertoires over time (Table 3).

Formely, this analysis permitted us to identify lineages that are shared across the different time points in each IgG, IgA and IgM repertoires, indicating the persistence of B cells and possible recall response after the YFV booster dose (Fig. 12A).

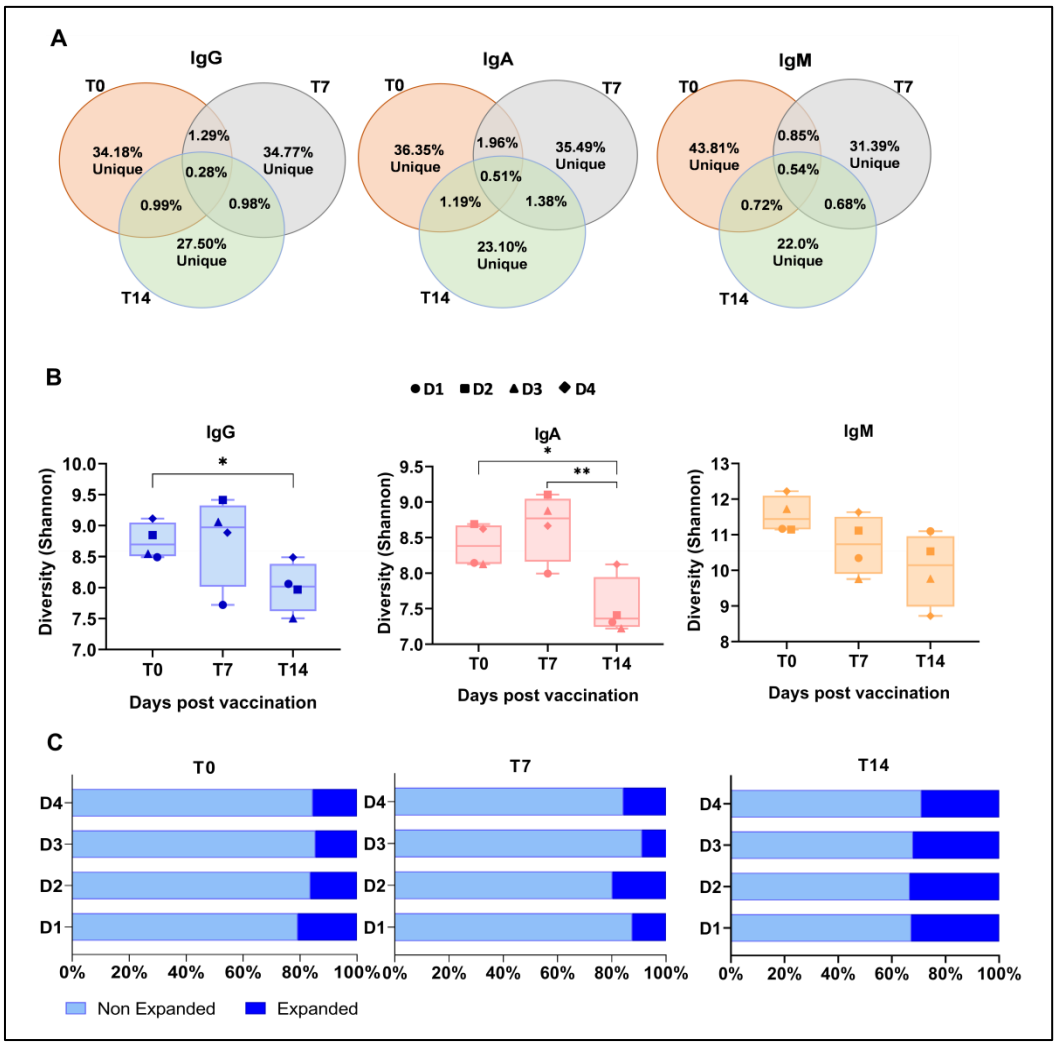

Figure 12. Dynamics of repertoire diversity and expansion following 17DD-YF vaccine boost. **A** Average of IgG, IgA and IgM lineages across donors that are and are not shared between the indicated time points 0, 7 and 14 days after vaccination. **B** Diversity of IgG (B), IgA (C) and IgM (D) repertoires was assessed by Shannon diversity index at 0, 7 and 14 days following vaccination. **C** Proportion of expanded and non expanded IgG, IgA and IgM lineages in each vaccinee repertoire at 0, 7 and 14 days after 17DD-YF booster dose. Lineages were classified into non expanded (< 0.1%) and expanded (≥ 0.1%) according to their frequencies in the repertoire. *p < 0.01 and ** p ≤ 0.005.

Diversity levels can indicate the state of B cell repertoire response, since antigen-specific stimuli increase clonal expansion of a limited number of antigen-specific clonal lineages and, consequently, reduce diversification of the repertoires. We interrogated how booster vaccination against YFV affects the diversity and expansion of the repertoire in the first two weeks following immunization.

Interestingly, we observed that all donors had their repertoire diversity decreased on day 14 for all isotypes (Fig. 12B). We also verified that IgH repertoires presented greatest expansion levels on day 14, and the proportion of the expanded lineages on this day represented 30% of the total repertoire (Fig. 12C). Further, we analyzed the degree of expansion of the IgA, IgG and IgM, lineages across each time point (Fig. 13).

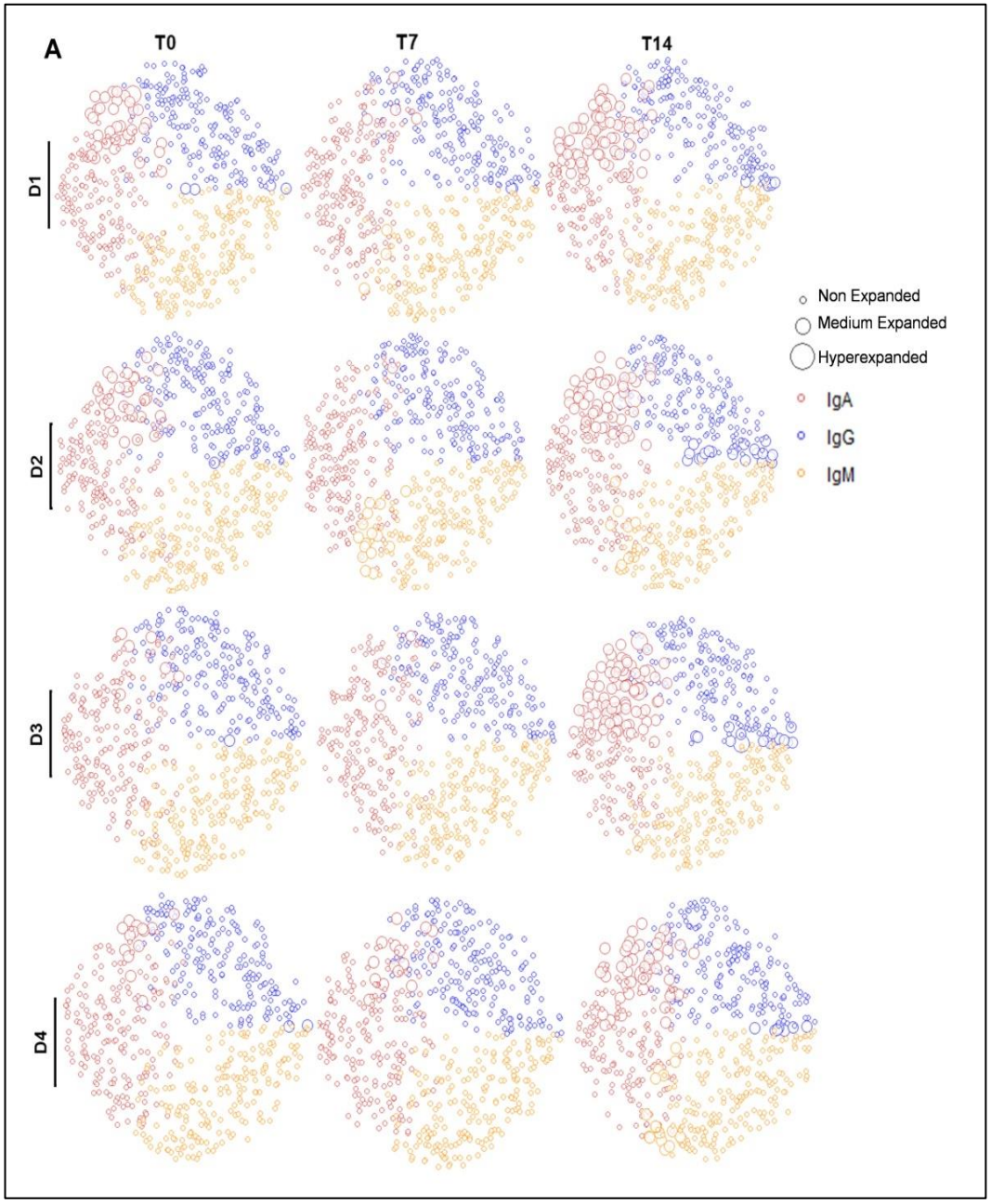

Figure 13. Overview of the repertoire expansion state over the two weeks after 17DD-YF boosting. Diagram representing the top 200 most frequent B cell lineages from each IgG, IgA and IgM repertoire. Each circle represents a B cell lineage with size proportional to its frequency in the repertoires at 0, 7 and 14 days after revaccination. Expansion levels were defined as non expanded for lineages presenting frequency below to 0.1%, medium

expanded for lineages with frequency between 0.1% and 1% and hyperexpanded for lineages presenting frequencies greater than 1%.

Interestingly, we see that IgA lineages and to a lesser extent IgG lineages demonstrate increased clonal expansion on day 14 after boosting (Fig. 13). Taken together, these longitudinal changes are suggestive of a robust response to YFV revaccination, that can be summarized by a decrease in circulating B cell repertoire diversity, caused by significant clonal expansion , mostly of IgA B cell lineages.

7.3 Persistent B cell lineages dominate the immune repertoire 14 days post-vaccination

Aiming to explore in detail the dynamics of the clonal expansion in the repertoire after revaccination, we tracked each clonal lineage across time to determine whether some of these lineages were recalled and kept stable in the repertoire. We had already detected lineages being shared across time points (Fig. 12A) and to verify whether these persistent B cells were related to the vaccine response, we defined that if a lineage that pre-existed in the repertoire (T0) in a steady-state, remained in the T7 and/or T14, and were expanded (≥ 0.1% frequency) after vaccination, this lineage would be considered as “persisting-expanded”.

Less than 30% of the lineages were found to be persistent in the entire expanded repertoire (Fig. 14A). The majority of these persisting-expanded lineages were identified as IgA, while IgG and IgM tended to present lower persistence (Fig. 14B). Thus, the expanded repertoire seems to be dominated (> 70%) by lineages detected only after YFV boost vaccination (T7 and/or T14) (Fig. 14A). Although this outcome can be related to sampling that affected the non-detection of these lineages at the time before and after vaccination, we can observe that all donors presented similar proportion of both lineages (persisting and new lineages) in their repertoires, suggesting that these individuals are similarly responding to the YFV boost vaccination (Fig. 14A). Yet, we identified that most of these newly expanded lineages (persistent or new) are IgA and IgG (Fig. 14B-C) and this was not surprising, since we had observed a greater involvement of IgA and IgG lineages in the expanded repertoire (Fig. 13).

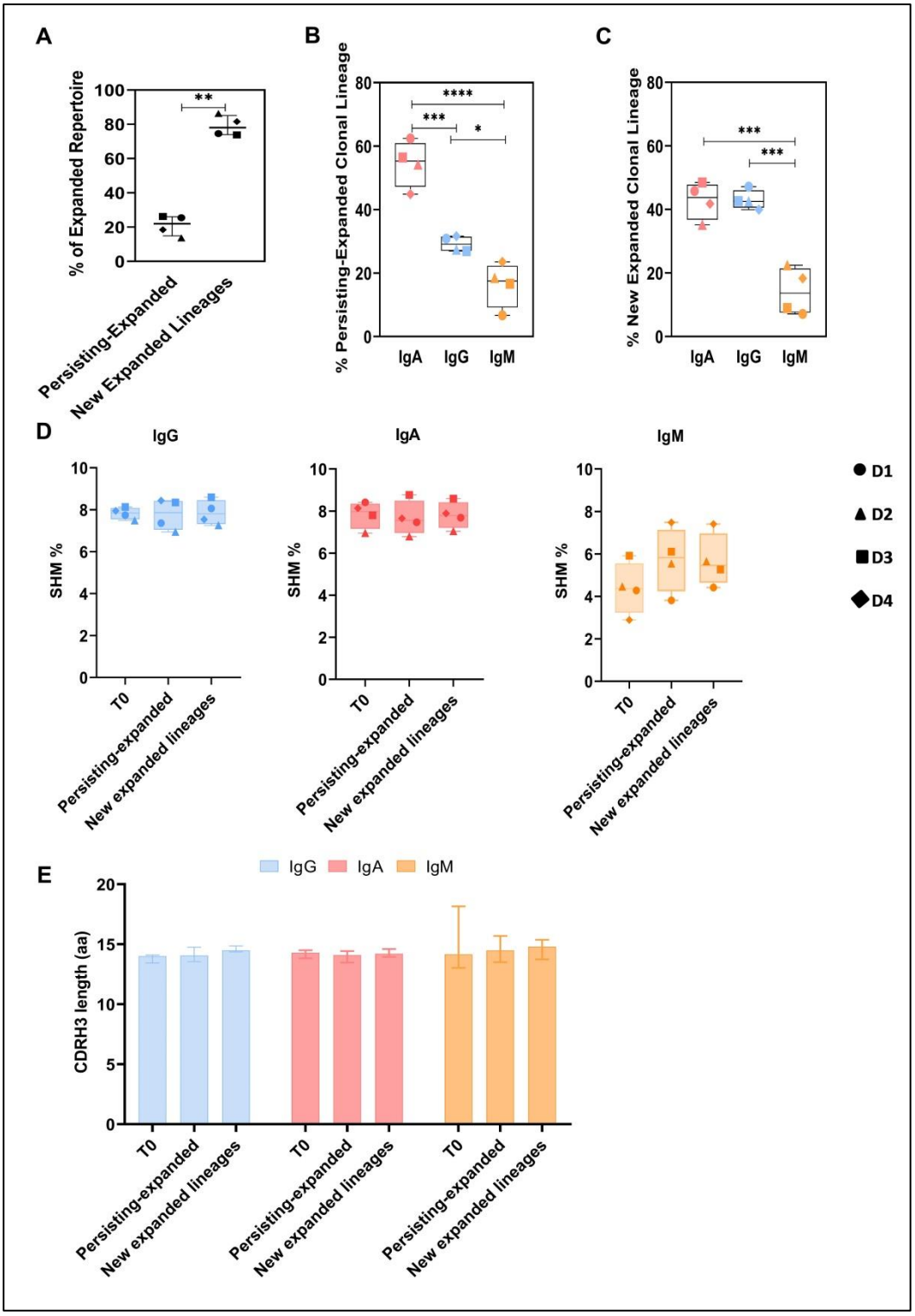

Figure 14. Analysis of persisting-expanded and new lineages. **A** Proportion of persisting-expanded and new expanded lineages found in the repertoires on day 7 and 14. **B-C** Proportion of persisting-expanded and new expanded lineages according to the isotype. **D** SHM average loads presented by IgG, IgA and IgM clonal lineages found in expanded repertoire on day 0 and on T14 by persisting-expanded and new expanded lineages. **E** CDRH3 average length of clonal lineages. *$p < 0.05$, ***$p \leq 0.001$, ****$p \leq 0.0001$.

We next teased out the molecular characteristics of these lineages to find out their nature, since the development of these cells will reflect the effectiveness

of the vaccine immune response. Overall, both persisting-expanded and new expanded lineages presented similar SHM loads (median level ranging from 6 and 8%) and CDRH3 length (approximately 15 amino acids) that did not significantly differ from the time before vaccination (Fig. 14D-E). Interestingly, the donor 1 who was considered non-immune to any of the flaviviruses prior to vaccination, had the IgM repertoire with the lower level of SHM. Interesting to note that the donor 1 who was considered non-immune to any of the flaviviruses prior to vaccination, had the IgM repertoire with the lower level of SHM.

The germline gene usage was compared in these lineages to verify a preferential VH convergence, suggestive of B cell activation and expansion, despite similar SHM and CDRH3 length. Throughout clonal expansion, a large diversity of V gene segments are non-uniformly utilized by both B cell populations (Fig. 15). Moreover, most of the gene segments used by the persisting and new expanded lineages had similar proportions of use on day 0, suggesting no preferential VH gene usage upon YFV boost vaccination.

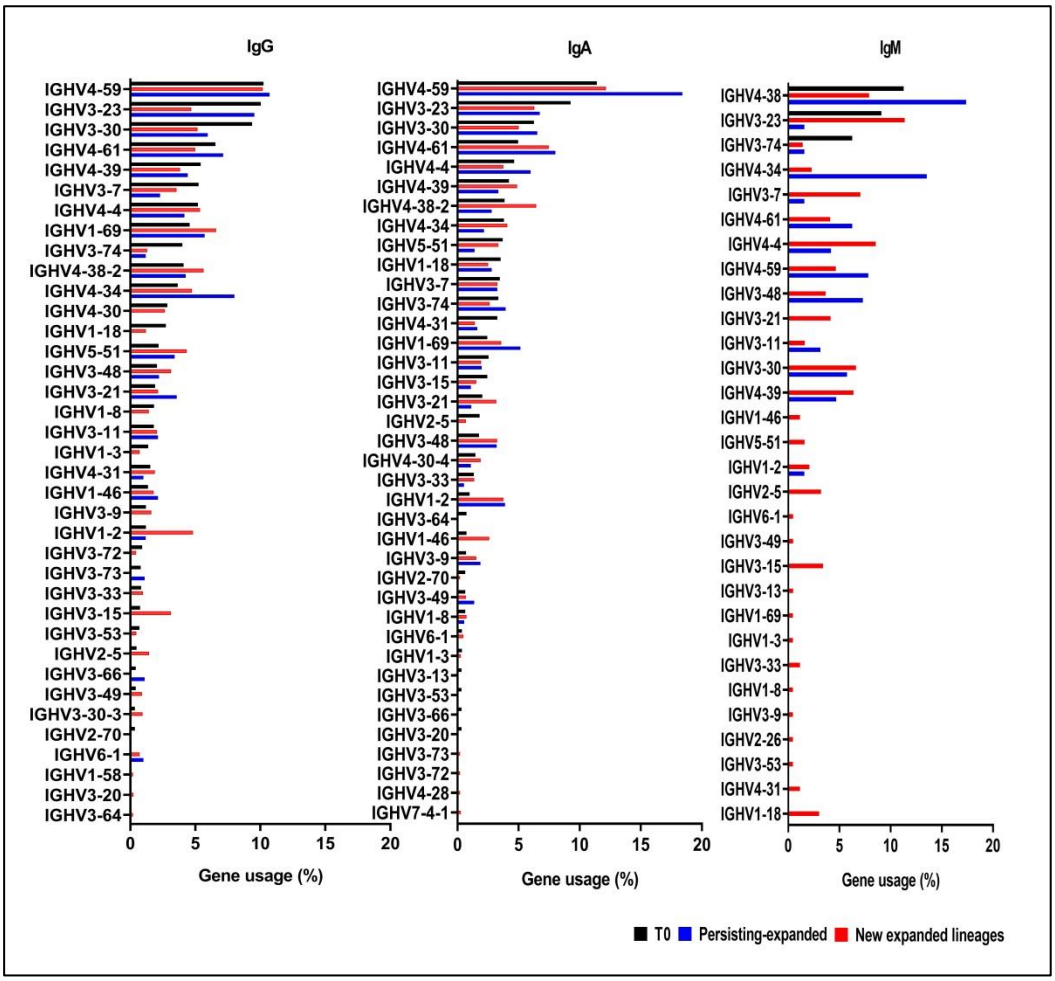

Figure 15. VH germline gene average of usage of persisting-expanded and new expanded

lineages. Gene segments present in more than 50% of the donors were considered for representation.

We selected the top 50 most expanded clonal lineages from T14 repertoire to verify the abundance of the persisting-expanded and new expanded lineages among these B cells. We found that persisting-expanded cells comprise a substantial parcel of the top 50 most expanded clonal lineages in most donors, except donor 3 (Fig. 16). Hence, although persisting-expanded lineages represent less than 30% of the expanded repertoire, these cells have a significant contribution to the expansion levels of the repertoire.

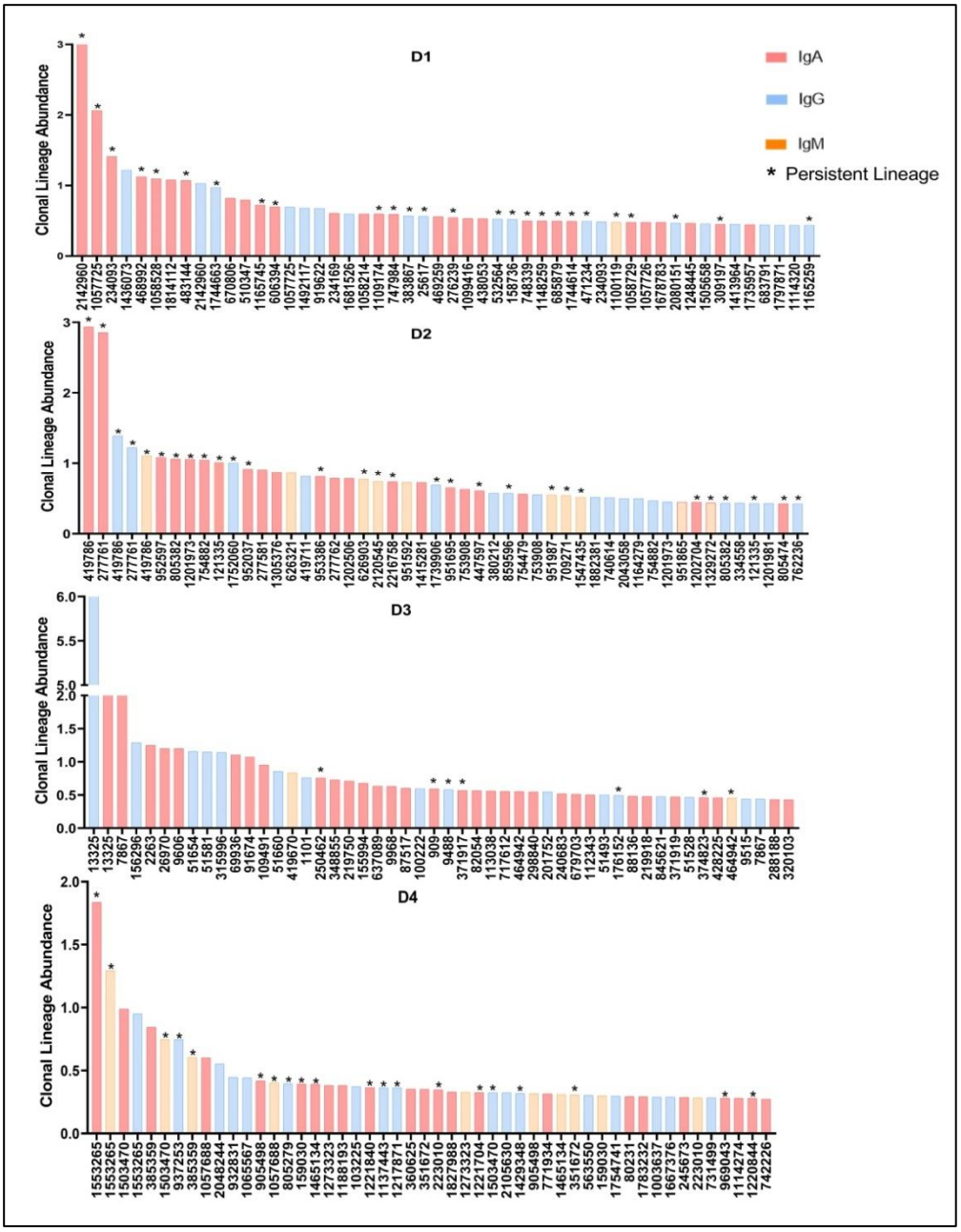

Figure 16. Representative histogram of the top 50 most expanded clonal lineages (IgG, IgA and IgM) that comprise the YFV vaccinees' repertoire at 14 days after vaccination.

Bars indicate the relative frequency of each lineage in the repertoire and * shows the persistent lineages.

7.4 YFV vaccinees' repertoires tend to present cross-reactive lineages

A comparison of the BCR repertoire sequences against a dataset of mAbs with binding experimentally confirmed to YFV, DENV and ZIKV was carried out to determine whether the lineages that comprise the repertoire of the vaccinees may display cross-reactivity. The CDRH3 region of the expanded lineages of IgG, IgA, and IgM repertoires from each individual were queried to the antibodies database[48, 54]. Matches were considered for all sequences alignment greater than 80%. This analysis provided us with more information regarding the specificity of the lineages from repertoires after YFV revaccination.

Overall, 57,626 CDRH3 unique sequences matched to known characterized flavivirus' antibodies CDRH3 sequences of the database. These sequences are clustered in 17,425 unique lineages, in which 27 were expanded and 17,398 were non-expanded after the vaccination (Table S.1). The larger matches of non-expanded lineages to the characterized antibodies reveals that the vaccinees' repertoire contains DENV and/or ZIKV specific lineages that did not expanded upon YFV vaccine booster.

Among the 27 expanded lineages, 11 were IgG, 13 IgA, and 3 IgM. Most of these lineages had their binding profile described by previous studies to DENV(Fig. 17A, Table S.1). A small portion of the discovered hits of antibodies were identified as displaying cross-reactivity to the three flaviviruses: YFV, DENV and ZIKV (Fig. 17A). To know whether these cross-reactive B cells belonged to persisting-expanded or new expanded lineages, we tracked the proportion of discovering hit lineages assigned to each B cell population, finding that most of these matched IgG, IgA and IgM lineages came from new expanded lineages (Fig. 17B). This surprisingly outcome reveals that 17DD-YF booster may induce cross-reactive lineages apart from the recall of the pre-existing cross-reactive cells.

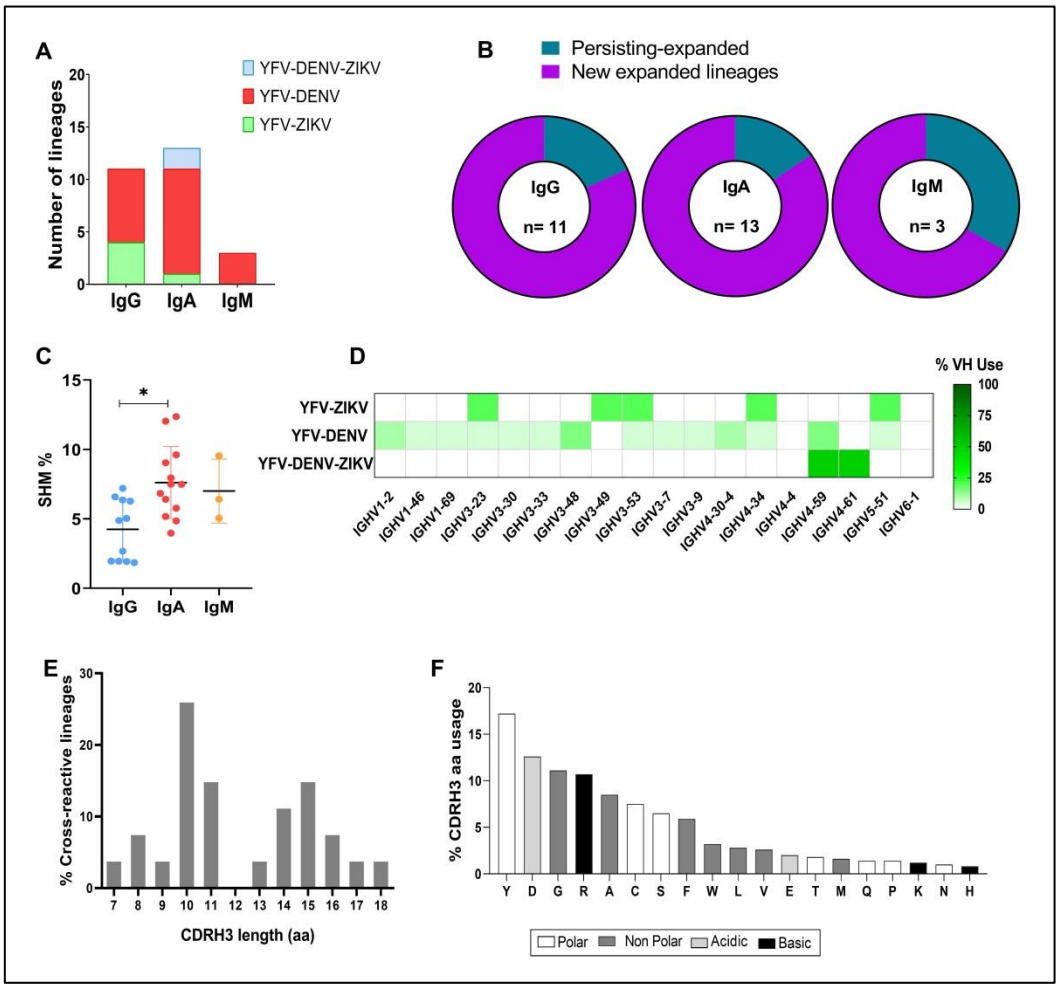

Figure 17. Analysis of putative anti-flaviviruses antibodies present in the analyzed repertoires. **A** Number of discovered hits that display specificity to YFV and cross-reactivity to ZIKV, DENV or ZIKV and DENV. **B** Fraction of cross-reactive lineages that are either persisting-expanded or new expanded lineages. The number in the center of the pie chart shows the total number of lineages belonging to the isotype. **C** SHM rates of IgG, IgA and IgM lineages that may display cross-reactivity. **D** VH germline gene usage of cross-reactivity lineages. **E** CDRH3 length distribution of lineages that may present cross-reactivity to DENV and/or ZIKV. **F** Physicochemical properties and amino acid usage of the cross-reactive lineages CDRH3.

To discover potential features suggestive of antibody cross-reactivity between YFV, DENV and/or ZIKV, we examined the expanded lineages hits by comparing molecular patterns related to SHM loads, VH gene usage, CDRH3 length and amino acid composition. By checking the SHM rates, we observed a varying degree of hypermutation on these cross-reacting lineages (Fig. 17C). The average of hypermutation rates were 4.5 for IgG, 7.5 for IgA and 6 for IgM (Fig. 17C). Usually, the average of SHM in healthy individuals is 2.83 ± 0.23% for IgM, 7.24 ± 0.07% for IgG and 8.37 ± 0.23% for IgA[50]. Regarding the VH gene

segments usage by the expanded lineages which were found in this study as displaying cross-reactivity profile, we observed a restrict list of germlines genes being used by these lineages (Fig. 17D).

Next, the distribution of the CDRH3 length in these lineages was checked and results show this distribution ranging from 7 to 18 amino acids length, with the largest proportion of the IgG, IgA, and IgM lineages presented 10 amino acids length in the CDRH3 (Fig. 17E). The physicochemical properties and amino acid composition of the CDRH3 in these lineages showed that these cross-reactive BCRs are very hydrophilic due the high content of polar amino acids, such as tyrosine, cysteine and serine (Fig. 17F).

Taken together, we showed that the repertoire of the vaccinees contains lineages that are reactive to DENV and/or ZIKV, and some of these lineages undergo expansion upon YF-17DD boosting. Also, the majority of these lineages show considerable affinity maturation state that may be important to the affinity interaction to these antigens.

7.6 Majority of the discovered anti-flaviviruses antibodies in the YFV vaccinees' repertoire may bind to DIII domain and fusion loop (FL) of the envelope protein

We sought to know what epitopes are targeted by the cross-reactive lineages and whether there is an immunodominance hierarchy in these lineages. By collecting the data from the characterized mAbs that comprised the database used here to discover the cross-reactive lineages of this study, we were able to point out two structural antigens that are possibly targeted by these mAbs: E and prM proteins (Fig. 18A). In agreement to the publish literature, most of the mAbs seem to have their antigenic sites located in the E protein and seeking to better elucidate where these epitopes are located its structure, we observed the majority of the mAbs reacting with DIII domain (28.57%) and fusion loop (FL) at the tip of DII (21.42%) (Fig. 18A). We also verified a considerable portion of mAbs having epitopes that crosslink E protein and prM (17.86%) DI and DII (3.57%) (Fig. 18A). We verified the relationship between epitope and neutralization potency based on experimental data provided by the published literature of the original characterized mAbs. Interestingly, a small fraction of the mAbs targeting epitopes within FL and DI was described as weakly neutralizing, while those targeting DIII and quaternary

epitopes within DI and DII were described as strong neutralizing antibodies (Fig. 18B). This outcome may suggest the 17DD-YF booster may elicit nAbs against ZIKV and DENV.

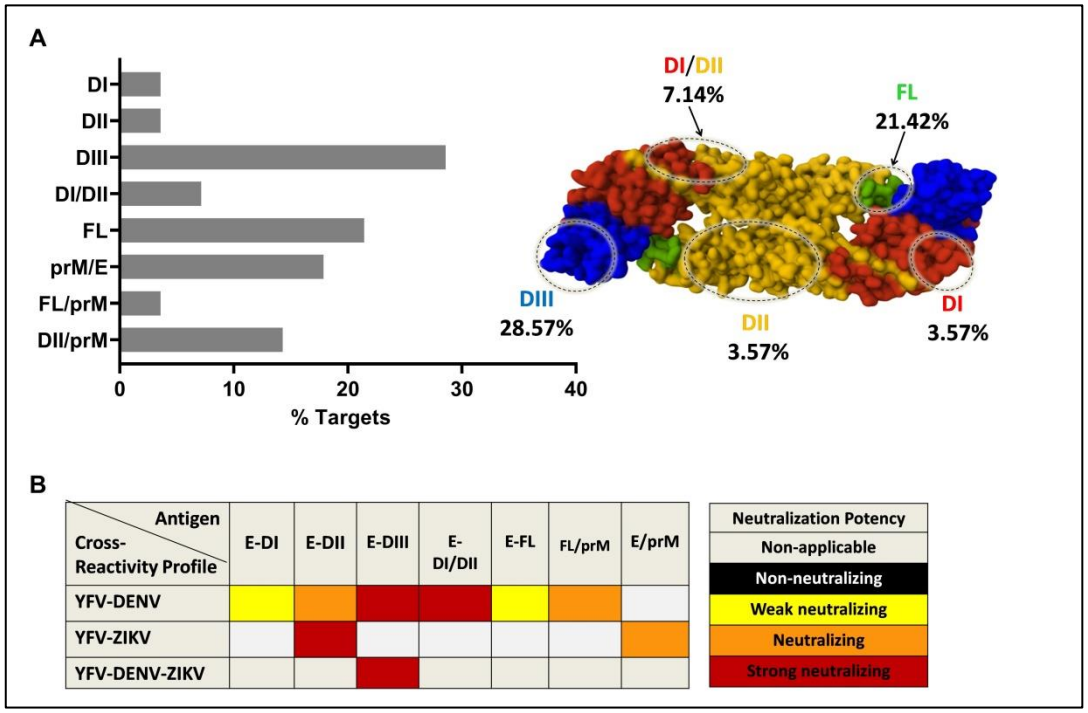

Figure 18. Antigenic sites and functional properties of the lineages elicited by 17DD-YF vaccine booster. **A** Antigenic sites targeted by cross-reactive lineages. Crystal structure of YFV E dimer (Protein Data Bank ID code 6IW2) represented as space filling model. Domains I, II and III are highlighted in red, yellow and blue respectively, in each monomer. FL is colored in green. Labels show the proportion of the mAbs targeting epitopes within each structural region. **B** Prediction of neutralization potential of each mAb according to data in published literature.

8. DISCUSSION

The global emergence of flaviviruses over the past several decades has threatened millions of people and became a major public health issue worldwide. The lack of specific anti-viral treatments and in some cases, flavivirus vaccines, worse the disease's care and control. Gaps in the knowledge about flavivirus antibody responses are mostly driven by the complexity of the immune interplay between sequential exposures and repeated vaccinations. YFV vaccine is highly efficient to generate neutralizing antibodies that last for a long period of time after a single dose[9]. However, the need of boosting is still controversial and studies have encouraged the YFV revaccination each 10 years in endemic countries such as Brazil[71, 74, 236]. This fact along with the co-circulation of ZIKV and DENV viruses in the country, collaborate with the development of pre-immunity that may alter specificities and functionalities of the antibodies, leading to either cross-protection or disease enhancement in the context of reexposure to a distinct flavivirus[237].

The present investigation analyzed the antibody repertoire of four healthy donors with a history of vaccination against YFV and originally from an endemic area with co-circulation of DENV, ZIKV, and YFV viruses. Our findings provided supportive evidence of the dynamics and landscape of the humoral response to 17DD-YF boosting. In addition, we assessed the effects of pre-existing immunity on the magnitude and persistence of the antibody responses. This work also gathered evidences of the existence of lineages with cross-reactivity profile to DENV and ZIKV in the repertoire post 17DD-YF revaccination.

Consistent with past works[7, 15, 48, 237-238], we observed that YFV antibody binding and neutralization peak titer corresponded to the same day when the highest clonal expansion of the repertoires was observed following booster (T14). However, the magnitude and persistence of the humoral response were weakened after 28 days of the revaccination. Interestingly, this antibody kinetics was observed in three of the four individuals who presented pre-immunity to any of the flaviviruses: YFV, DENV and ZIKV. Contrastingly, we observed that donor 1, who did not show any immunity to all tested flaviviruses before vaccination, presented a distinct antibody dynamic following the immunization. In this donor, the seroconversion to YFV was observed at 28 days after vaccination and the

magnitude of the nAbs titers persisted at least the day 180. Yet, the IgM repertoire of this donor presented a lower level of SHM < 2% in comparison to other donors, highlighting the influence of the pre-immunity on the recruitment of B cells. To this respect, we observed that pre-immune donors presented a varying degree of antibody reactivity to DENV1-4 and ZIKV over time, and this fact contributes to the great heterogeneity of the immune responses observed in this cohort.

We believe that pre-existing immunity related to either YFV vaccination history and/or past heterologous exposure without warning signs (WS) may be affecting the dynamics, persistence, magnitude and specificity of 17DD-YF booster antibody response. These outcomes are in line with early studies describing that repeated vaccinations against YFV elicits a discrete increase in nAb due to pre-immunity that prevents the vaccine replication virus and, consequently, inhibits the stimuli for B cell activation[15, 238-239] and that baseline immunity, influenced by prior exposure to infectious diseases can reduce nAb titers post-vaccination as result of frequent exposure to infectious diseases[240]. One of the hypotheses behind this fact is the immune complex formed between pre-existing antibodies and the vaccine antigen could impair the antigen presentation[241]. Conversely, Campi-Azevedo[71] observed an upregulation in the magnitude of the nAb levels that persisted up to 10 years after the secondary vaccination. Such distinct findings may be closely related to the specific population characteristics. Hence, it is clear that booster dose recommendation should consider the role of pre-existing immunity elicited by the effect of co-circulation and/or individual heterogeneity, on vaccine outcomes. The importance of these variables has been noted by many studies evaluating trends and bias towards vaccine efficacy[70, 242].

To our knowledge, this is the first study to describe the kinetics, diversity and clonal expansion of the antibody repertoire upon YFV booster vaccination. Many immune aspects of YFV vaccination have been extensively studied and elucidated, including the B and T cell development after primary and secondary immunization using approaches that combine serological and flow cytometry in low-throughput sequencing data[7, 15, 48, 243]. Nevertheless, these studies did not consider subjects from endemic regions and their pre-existing immunity. Given the difficulties that underlie such complex understanding, here, we performed a high-throughput BCR sequencing technology to longitudinally characterize the antibody repertoire responding cells to 17DD-YF vaccine booster. Although the antibody

response against flaviviruses is best known by the production of highly persistent IgM nAbs[48, 78, 244-245], in this work, analysis of the B cell dynamics revealed a high predominance of expanded IgA lineages and few IgG and IgM lineages at the early stages following vaccination. This finding corroborates previous reports that found IgA-expressing plasmablasts as the dominant lineages in the repertoire between 14 and 16 days of subjects' primary DENV infection[246-247].

To date, it is still unclear the role of IgA on anti-flaviviruses immunity. Few investigations demonstrate that IgA is capable of neutralizing DENV without triggering ADE due to its low affinity for its Fc receptor[248-249]. In addition to that, it was discovered that these IgA antibodies can antagonize IgG-mediated ADE by competing with DENV-reactive IgG for the same epitope[249]. In light of these findings, we believe that prevalence of IgA antibodies in the YFV vaccinees repertoire may contribute to the protective and non-pathologic responses of the YFV vaccine. This idea is supported by a previous study that did not find any evidence of the risk of dengue severe disease in subjects from an endemic area with YFV vaccination status[250].

Our results also showed a considerable proportion of pre-existing lineages in the repertoire that expanded upon revaccination. Analysis of the molecular features of these IgG, IgA and IgM persisting-expanded lineages and newly expanded lineages pointed out several similarities in terms of SHM levels, CDRH3 length (approximately 15 amino acid length) and preferential use of IGHV3 and IGHV4 gene families. Wec et al.48 when analyzing the BCR repertoire from subjects who were vaccinated for the first time against YFV and from a non-endemic flavivirus area observed that vaccinees presented antibody repertoire with low SHM rate, short CDRH3 (10 amino acid length) and a strikingly use the IGHV3-72 germline 14 days after the primary vaccination against YFV. Similarly, our study showed that during the secondary vaccination, the antibody repertoire appears to place a priority on the rapid generation of lineages from both persisting-expanded and newly expanded lineages without extensive affinity maturation.

Serological cross-reactivity between YFV and other flaviviruses is commonly observed in subjects with past history of flavivirus infection or vaccination[14, 48, 169, 174, 251]. In addition to observe this phenomenon, our study reported the presence of cross-reactive lineages in the peripheral B cell repertoire of the YFV vaccinees. Although the majority of these lineages were not expanded

in the repertoire after vaccination, suggesting possible past exposure to DENV and/or ZIKV by the vaccinees, we were able to observe some of the matched lineages under expansion after vaccination. Most of these expanded lineages had their epitopes predicted within the DIII domain and FL of the E protein, according to their characterized antibodies hits[48, 147, 184, 252].

Studies on antibody cross-reactivity attribute the occurrence of these reactions on conserved sequences that comprise either linear or conformational epitopes on different antigens[253-255]. In primary YFV vaccinees, the majority of the isolated mAbs were characterized as non-neutralizing and had their epitopes mapped within the FL[48]. Similarly, our epitope prediction pointed out this highly conserved region as one of the main targets of the discovered lineages. Spite of its conservation across flaviviruses, the FL is usually poorly accessible due the viral breathing, and this has strong implications for the antibody's responses[11].

It is well understood that structural arrangement is as important as sequence identity to predict epitopes and determine antibody cross-reactivity[256-257]. By predicting the structural arrangement of each CDRH3 from discovered lineages, we could identify 21 sequences having a very close match to their reference hits. Although the CDRH3 sequence homology was not very high, we can speculate that these antibodies may target the same epitope. For a long time, sequence homology was linked to functional activity, however, computational studies based on structural data have shown that sequence-distant antibodies but structurally similar can target the same epitope[235, 258].

Despite of the low number of hits which may be the consequence of the limited database composition of characterized antibodies, we could provide some validation of the existence of these cross-reactive antibodies in the YFV vaccinees' repertoire. Yet, this result highlights the need for deep characterization of these antibodies in terms of abundance in the serum, epitope mapping and functionality. Noteworthy, it does not completely mean that other matches are not binders, indeed, they might display cross-reactivity, since the number of YFV published characterized antibodies is still very low and results of our *in silico* analysis might be under estimated, although it is necessary to validate this hypothesis.

There are few limitations related to this study, including sampling, and anti-YFV specific antibody isolation that affects the identification of persisting and new lineages of the repertoire, the intervals between prior flavivirus exposure and

immunizations that may impact the immunogenicity of the booster dose. Also, longer timing after vaccination could yield different antibodies responses since affinity maturation process has been proved to continue up to 9 months after boost[48]. Moreover, the small cohort size (n=4), the use of bulk PBMC samples, and the lack of information regarding circulating antibodies restricts our conclusions and statistical power. Further studies are needed to integrate cellular and serological specific anti-YFV antibody repertoire results and better clarify the complexity of the flaviviruses antibody responses.

9. CONCLUSION

In summary, this work provided comprehensive insights into the kinetics, dynamics, magnitude, and persistence of the antibody responses upon 17DD-YF vaccine boost. We evaluated the implications of the DENV and ZIKV co-circulation in the secondary YFV vaccine response, especially to the development of cross-reactive lineages that tend weak neutralize and strong neutralize DENV and/or ZIKV by targeting FL and DIII epitopes on the E protein respectively. Although we are aware of the need to further investigate these antibodies abundance and persistence in the serological repertoire, here we tracked the molecular basis of the antibody response, providing valuable understanding of the features associated with the elicitation of YFV vaccine immunity. Altogether, this knowledge may contribute to vaccine design, mainly in the aspects involving antibodies specificities, target antigenic sites and population heterogeneity related to the epidemiological context of the region.

CHAPTER 2

Assessing the serological antibody repertoire that is reactive to DENV2 and ZIKV in the YFV vaccinees

Abstract

Subsequent exposures to flaviviruses are governed by pre-existing antibody responses that relies on concentration and specificity, and this has strong implications for disease severity and vaccine development. Understanding the composition of the serological antibody repertoire and its relationship to clonally expanded B cell repertoire is important for elucidating the impact of potentially cross-reactive antibody responses in primed groups. In the current study, we evaluated the molecular composition of the serological repertoires from YFV vaccinees that is reactive to DENV2 and ZIKV at 180 days after vaccination. Using a proteomic approach (Ig-seq) combined to BCR sequencing data (BCR-seq) of the antibody transcripts, we show that secreted antibody molecules reactive to DENV2 and ZIKV comprise a substantial fraction of the serological repertoire, with an average of ~35% of these antibody lineages pre-existing the YFV vaccination. We also found that although all donors presented an increased reactivity to ZIKV on day 180, the total antibody binding activity does not correlate to neutralization. Most of the individuals also presented this behaviour in DENV antibody responses. We profiled these antibody lineages, detecting a great influence of the DENV2 and ZIKV co-circulation on the activation of naive B cells for the generation of low SHM antibodies. Additionaly, we observed that pre-immune donors tend to present more non affinity mature antibodies than non pre-immune donors. Taken together, we found evidence that flavivirus co-circulation and pre-immunity may influence the complexity, quality and effectiveness of the YFV vaccine antibody responses.

Keywords: YFV vaccine; Antibody cross-reactivity; Flaviviruses; Serological repertoire.

10. INTRODUCTION

The nature of the antibody responses against flaviviruses is very controversial across populations presenting pre-immunity and it should be carefully addressed[259]. The magnitude, persistence, cross-reactivity, and possibility of ADE are some of the many concerning aspects related to the flaviviruses humoral immunity and plenty of research has been done to elucidate their relationship with temporal changes dictating protection or severe disease risk [175, 177, 220, 259]. Valuable insights of these studies have unveiled the antibody stoichiometry to trigger ADE following heterotypic exposure and this phenomenon was associated with cross-reactive antibody wanning effect over time[177, 182]. This effect has been observed in both natural infection and vaccine-derived immunity. For example, a past work has shown that DENV naïve children who were immunized with the licensed dengue vaccine, Dengvaxia, presented increased risk of severe dengue disease after DENV breakthrough infections[218]. Recently, ZIKV antibodies elicited during a primary infection had their cross-reactivity to DENV increased one year after the natural infection and this activity was attributed to the affinity maturation process that increases the B cell breadth[220].

Previously, we observed that YFV vaccinee's cellular repertoire tend to present cross-reactive lineages to DENV and/or ZIKV, and this outcome was correlated to the observed serological IgG binding activity to the three viruses. Given the fact that circulating IgG is a result of clonally expanded and differentiated B cells, after a continuous process of diversification, genetic recombination and clonal selection that involve GC reactions, and these reactions have been observed between 6 and 9 month following YFV vaccination[48], we speculate what is the molecular composition of the IgG anti-DENV2 and anti-ZIKV proteome of the YFV vaccinees at 180 day of the vaccination. Our hypothesis is that the abundance of DENV2 and ZIKV reactive IgG in the sera of the YFV vaccinees at 180 days can affect YFV vaccine antibody response, since the continous activation of the immune system by the co-circulation of the three viruses in the endemic area impacts the generation of persistent and affinity mature IgG.

To date, there are no studies providing detailed molecular characterization of the serological antibody repertoire following the YFV vaccination. The current

knowledge about the YFV antibody responses was mostly provided by indirect investigations involving serologic approaches with YFV vaccinee's plasma and B cell repertoire. In sum, these studies, including ours, have described the cross-reactivity between YFV vaccine-derived antibodies and related flaviviruses, such as DENV and ZIKV. However, it still lacks a deep dissection of the humoral response that constitutes the polyclonal sera after vaccination against YFV. This analysis is essential to understand the durability and quality of the immune responses, especially in terms of abundance of antigen-specific antibody in the serum, which can inform the real impact of pre-existing flavivirus immunity in either protection or risk of disease enhancement in endemic populations. In addition, the assessment of the molecular characteristics of the serological repertoire can lead to a comprehensive understanding of the cross-reactive antibody landscape induced by the YFV vaccine in the context of endemicity.

Therefore, in this section we aim to characterize the molecular composition of the serological repertoire of the YFV vaccinees that is reactive to DENV2 and/or ZIKV at 180 days after vaccination. We verified that circulating IgG reactive to DENV2 and ZIKV constitutes a considerable fraction of the antibody responses of the YFV vaccinees' repertoire. Moreover, we found evidences that pre-immunity to flaviviruses may influence the YFV vaccine effectiveness. Our results also suggested that DENV2 and ZIKV co-circulation is constantly priming the immune system of the individuals and the consequence is the generation of low-affinity and cross-reactive antibodies.

11. MATERIAL AND METHODS

11.1 Samples

Plasma and PBMC samples were obtained from the four YFV vaccinees as previously described in the section 6.1 from chapter 1. Details of the study participants are included in Table 2.

11.2 Obtention of E-dimer protein antigens from DENV2 and ZIKV

Stabilized E dimer antigens from DENV2 and ZIKV were obtained to perform Indirect ELISA assays and Ig-Seq pulldowns. Recombinant E dimer from DENV2 (15 mg) containing the substitution A259C[260] was purchased from PEP-MX Core -UNC Chapell Hill. Dimeric E dimer protein from ZIKV was obtained after transiently transfecting the SC12 construct[261] (kindly provided by Kuhlman lab) into Expi 293-F cells (Thermo Fisher) for expression according to the manufacturer's instructions. Cells were grown in suspension for 5 days shaking at 37 °C, 8% CO2 and after this period, cell culture was harvested, centrifuged and the supernatant containing the protein was retained. Supernatant was passed through a 0.22 µm filter and submitted for purification in a Ni-NTA resin (Qiagen) as previously described[261]. Elution fractions were analyzed by SDS-PAGE and those containing ZIKV E dimer protein were pooled, concentrated using 10,000 MWCO Vivaspin centrifugal spin columns (Sartorius) and buffer-exchanged into PBS using Zeba spin columns (Thermo Fisher). Aliquots of 1 mg protein were frozen and stored at -80 °C until use.

11.3 Size exclusion chromatography (Superdex S-200)

ZIKV E-dimer and an IgG1 sample were separately submitted to a size exclusion chromatography (Superdex S-200 column, GE Technologies) in which the column was previously equilibrated with 2 column volumes (CV) of PBS. Elutions were carried out in the same buffer and the eluted protein fractions were pooled, and concentrated to 1ml volume by using a Vivaspin 30K MWCO (Merck Millipore) which was centrifugated at 5,000 x g, 4º C. Samples were aliquoted and stored at -80 ºC until use.

11.4 Expression and Purification of the Control mAbs - mAb11, C8, and C10

Previous characterized anti-flavivirus monoclonal antibodies: mAb11[262],

C8[39] and C10[39] were expressed to be used as experimental controls. These antibodies are cross-reactive and recognize epitopes within FL (mAb 11) and quaternary structures formed between FL and DIII on E protein (C8 and C10)[39, 262]. In summary, plasmid constructions containing the heavy and light chains of the human mAbs were transfected into Expi 293-F cells (Thermo Fisher) for expression according to the manufacturer's instructions. Culture supernantant containing the expressed antibodies was collected after 5 days as described in the section 11.2. Purification of each mAb was performed in affinity chromatography and using a gravity column (Pierce™ Disposable Column - Thermo Fisher Scientific) packed with 1.5ml of hydrated Protein G Plus Agarose 50% slurry resin (Pierce Thermo Fisher Scientific), and equilibrated with Dulbecco's PBS. Supernatants were previously clarified by centrifugation and filtration on a 0.22 µm filter and then loaded in to the affinity column. Mabs were eluted after a washing step of 20 column volumes (CV) using Dulbecco's PBS, followed by 5 CV of 100 mM glycine pH 2.7. The eluted mAbs were immediately neutralized to a neutral pH using 1ml of 1M Tris-HCl pH 8.5 and buffer-exchanged into PBS using 10,000 MWCO Vivaspin centrifugal spin columns (Sartorius). The final volume was adjusted to 1ml and sample concentration was determined in the nanodrop at 280nm.

11.5 SDS-PAGE

SDS-PAGE electrophoresis was used to analyze the protein purification results. Samples (3 µg) were run in a 4-12% gel under non-reducing (0.5 mol/l Tris-HCl pH 6.8, 10% glycerol, 10% (w/v) SDS, 0.1% (w/v) bromophenol blue) and reducing conditions (0.5 mol/l Tris–HCl, pH 6.8, 10% glycerol, 10% (w/v) SDS, 0.1% (w/v) bromophenol blue, 5% (w/v) β-mercaptoethanol). The protein marker Precision Plus ProteinTM Dual Color Standards (Bio-Rad Laboratories, Inc.) was used to estimate the molecular weight of the protein bands. Runs were performed at 150 v for 1h in vertical electrophoresis system (CVS10 OmniPage Cleaver Scientific Ltd). Gels were stained using Coomassie blue.

11.6 Indirect ELISA

Indirect ELISA assays were run in 96 well Microplates (Corning®, USA) coated with 4 µg/ml of DENV2 or ZIKV antigens at 4º C, overnight. In the next

day, plates were washed 3x with PBST (PBS, 0.01% Tween 20) and blocked with 2% PBS milk solution. After 2 h incubation at room temperature, plates were washed again as previously, and either plasma samples collected on days 0, 28, and 180 after vaccination or C8 mAb, C10 mAb, and mAb11 were added in serial dilutions (1:25, 1:50, and 1:100 for plasma samples and 10, 5, 2.5 and 1.25 µg/ml for the antibodies). Plates were incubated at room temperature for 1h and then washed as described above. The anti-IgG human horseradish peroxidase (HRP) (Sigma, USA) was diluted to 1:5,000 in 2% PBS milk and added to each well. Plates were incubated in the same conditions as previously and washed 3x with PBST before development with 50 µl per well of 5,5'- Tetramethyl benzidine (TMB) (Sigma, USA). Reactions were quenched after 20 minutes by adding 50 µl/well of 2M sulfuric acid (H2SO4). Plates were read at 490 nm in a microreader plate (Thermo Fisher Multiskan Sky).

11.7 BCR repertoire sequencing

VH repertoire sequencing data was obtained as described in the section 6.4 from chapter 1. Paired VH:VL repertoire sequencing data was obtained at single cell level using T14 PBMCs samples and according to McDaniel et al protocol[43]. To summarize, each cell from a total of $2x10^6$ PBMCs was co-emulsified with oligo (dT) magnetic beads (New England Biolabs) in 19 ml of lysis buffer (100 mM Tris pH 7.5, 500 mM LiCl, 10 mM EDTA, 1% lithium dodecyl sulfate, and 5 mM dithiothreitol) using a custom flow-focusing device (FFD)[43]. Beads were rescued from the emulsion by adding hydrated ether (Sigma-Aldrich, MA) and resuspended in a one-step RT-PCR solution containing the following reagents: 115µl of 10µM APEX common reverse primer mix, 57.5µl of 10µM IgGAMKL constant region reverse primer mix, 9.2µl of 12.5µM human VH framework region 1 (FR1) forward primer mix, 14.9µl of 7.7µM human VL FR1 forward mix (Table 4), 28.75µl of ultrapure BSA (Thermo Fisher Scientific), 287.5µl of 10x concentrated RTX buffer (600 mM Tris-HCl pH8.4, 250 mM $(NH_4)_2SO_4$, 100 mM KCl, and 10 mM $MgSO_4$), 57.5 µl of 0.2 mg/ml exonuclease-deficient version (N210D) of reverse transcription xenopolymerase (RTX)[263], 115µl of SUPERase•In™ RNase Inhibitor (Thermo Fisher Scientific, MA; Cat. AM2694), 57.5 µl of 10mM dNTP (New England Biolabs, MA; Cat. N0447L), 575 µl of 5 M Betaine (Sigma-Aldrich, MA; Cat. B0300-5VL), and 1557.2 µl of H2O.

Resuspended beads were added to a dispersion tube (IKA) pre-filled with 9 ml of the same emulsion oil previously used, and subjected to re-emulsification in an emulsion-dispersing spinner at 600 rpm for 5 min. The emulsion mixture was dispensed in a 96-well PCR plate at 100µl/well and submitted to overlap-extension (OE) RT-PCR reaction under the following conditions: 30 min at 55 °C followed by 2 min at 94 °C; 4 cycles of 94 °C for 30s, 50 °C for 30s, 72 °C for 2 min; 4 cycles of 94 °C for 30s, 55 °C for 30s, 72 °C for 2 min; 32 cycles of 94 °C for 30s, 60 °C for 30s, 72 °C for 2 min; 72 °C for 7 min; hold at 4 °C.

Table 4. Overlap extension (OE) RT-PCR primers for paired VH:VL antibody analysis[43].

Primer Mix Name	Primer ID	Sequence
APEX common	AHX89	CGCAGTAGCGGTAAACGGC
	BRH06	GCGGATAACAATTTCACACAGG
IgGAMKL constant region reverse	hIgM	CGCAGTAGCGGTAAACGGCCGACGGGGAATTCTCACAGGAGACG AGGGGGAAA
	hIgG	CGCAGTAGCGGTAAACGGCGGAGSAGGGYGCCAGGGGGAAGAC
	hIgA	CGCAGTAGCGGTAAACGGCGCTCAGCGGGAAGACCTTGGGGCTG
	hIgLC	GCGGATAACAATTTCACACAGGTTGRAGCTCCTCAGAGGAGGGY GGGAA
	hIgKC	GCGGATAACAATTTCACACAGGCTGCTCATCAGATGGCGGGAAG ATGAAGACAGATGGTGCAG
VH framework region 1 (FR1) forward	HT hVH1	TATTCCCATGGCGCGCCCAGGTCCAGCTKGTRCAGTCTGG
	HT hVH157	TATTCCCATGGCGCGCCCAGGTGCAGCTGGTGSARTCTGG
	HT hVH2	TATTCCCATGGCGCGCCCAGRTCACCTTGAAGGAGTCTG
	HT hVH3	TATTCCCATGGCGCGCCGAGGTGCAGCTGKTGGAGWCY
	HT hVH4	TATTCCCATGGCGCGCCCAGGTGCAGCTGCAGGAGTCSG
	HT hVH4-DP63	TATTCCCATGGCGCGCCCAGGTGCAGCTACAGCAGTGGG
	HT hVH6	TATTCCCATGGCGCGCCCAGGTACAGCTGCAGCAGTCA
	HT hVH3N	TATTCCCATGGCGCGCCTCAACACAACGGTTCCCAGTTA
VL FR1 forward	HT hVK1	GGCGCGCCATGGGAATAGCCGACATCCRGDTGACCCAGTCTCC
	HT hVK2	GGCGCGCCATGGGAATAGCCGATATTGTGMTGACBCAGWCTCC
	HT hVK3	GGCGCGCCATGGGAATAGCCGAAATTGTRWTGACRCAGTCTCC
	HT hVK5	GGCGCGCCATGGGAATAGCCGAAACGACACTCACGCAGTCTC
	HT hVL1	GGCGCGCCATGGGAATAGCCCAGTCTGTSBTGACGCAGCCGCC
	HT hVL1459	GGCGCGCCATGGGAATAGCCCAGCCTGTGCTGACTCARYC
	HT hVL15910	GGCGCGCCATGGGAATAGCCCAGCCWGKGCTGACTCAGCCMCC
	HT hVL2	GGCGCGCCATGGGAATAGCCCAGTCTGYYCTGAYTCAGCCT
	HT hVL3	GGCGCGCCATGGGAATAGCCTCCTATGWGCTGACWCAGCCAA
	HT hVL-DPL16	GGCGCGCCATGGGAATAGCCTCCTCTGAGCTGASTCAGGASCC
	HT hVL3-38	GGCGCGCCATGGGAATAGCCTCCTATGAGCTGAYRCAGCYACC
	HT hVL6	GGCGCGCCATGGGAATAGCCAATTTTATGCTGACTCAGCCCC
	HT hVL78	GGCGCGCCATGGGAATAGCCCAGDCTGTGGTGACYCAGGAGCC

Amplicons were extracted from the emulsions by centrifugation at 16,000 x

g for 30 sec, followed by removal of the upper mineral oil phase and addition of an equal volume of hydrated ether. The mixture was vortexed twice and centrifuged again in the same conditions. The ether layer was removed and the ether addition step was repeated twice to fully break the emulsions. After removing any residual ether by evaporation at room temperature and speed-vac centrifugation during 45 min, the magnetic beads were pelleted and the aqueous layer containing the DNA amplicons was PCR-purified using a PCR purification kit (Zymo Research, CA). and further amplified using a nested PCR, and sequenced using 2x300 paired-end Illumina MiSeq. The DNA was eluted with 2 x 15µl of H_2O and used as template for nested PCR reaction. Nested PCR conditions were optimized by testing three different reactions prepared as follows: 2µl of OE RT-PCR product, 1 µl of 10 µM nested primer mix (Table 5), 0.5 µl of 10mM dNTP, 5 µl of 10x DreamTaq buffer, 0.5 µl of DreamTaq™ Hot Start DNA Polymerase (Thermo Fisher Scientific, MA), and 41 µl of H_2O for each reaction. Reactions were run under the following conditions: 94 °C for 2 min; [94 °C for 30 sec, 62 °C for 30 sec, and 72 °C for 20 sec] x 25, 30, or 35 cycles; 72 °C for 7 min. Results were compared by running a 1% agarose gel and PCR cycles that resulted in a clear single band at ~800bp were choosen as the optimal condition to perform a large nested PCR reaction under the same conditions. The nested PCR products were concentrated in 20µl of H_2O and gel extracted.

Table 5. Nested PCR primers for paired VH:VL antibody analysis.

Primer ID	Sequence
hIgG Nested 4N	NNNN SGATGGGCCCTTGGTGGARGC
hIgM Nested 4N	NNNN GGTTGGGGCGGATGCACTCC
hIgA Nested 4N	NNNN CTTGGGGCTGGTCGGGGATG
hIgK Nested 4N	NNNN AGATGGTGCAGCCACAGTTC
hIgL Nested 4N	NNNN GAGGGYGGGAACAGAGTGAC

Libraries were prepared by attaching Illumina adaptor sequences to the PCR amplicons. Briefly, five distinct reactions with different combinations of primer sets were prepared: (i) hIgGA and IgKL primers, (ii) hIgGA and Linker_VH primers, (iii) IgM and IgKL primers, (iv) IgM Linker_VH primers, and (v) IgKL and Linker_VL primers, as described previously[43-44]. For each reaction, 30ng of nested PCR products were mixed with 25 µl of NEBNext® High-Fidelity 2x PCR Master Mix (New England Biolabs, MA), 4 µl of 10 µM

primer 1, and 4 µl of 10 µM primer 2, with the final volume adjusted to 50 µl with H_2O. Each reaction was amplified under following conditions: 98 °C for 30 sec; [98 °C for 10 sec, 62 °C for 30 sec, and 72 °C for varying extension time - 33 sec for (i), 20 sec for (ii), 33 sec for (iii), 20 sec for (iv), and 20 sec for (v) x varying PCR cycles, specifically 8 cycles for (i) and (ii), and 5 cycles for (iii), (iv), and (v)]; 72°C for 7 min. The PCR product from each reaction was purified and concentrated to 20 µl of H_2O. Subsequently, 50ng of the PCR product from each reaction was mixed with 25 µl of NEBNext® High-Fidelity 2x PCR Master Mix, 6µl of the forward primer (5'-ACCGAGATCTACACGACGACTCGTCGGCAGCGTC-3'), and 6 µl of reverse primers containing unique Illumina adaptor sequences with a final volume adjusted to 50 µl. Then, the PCR reaction was performed as follows: 98 °C for 30 sec; [98 °C for 10 sec, 62 °C for 30 sec, and 72 °C for varying times depending on the reaction (i) 33 sec, (ii) 20 sec, (iii) 33 sec, (iv) 20 sec, and (v) 20 sec] x 8 cycles; and 72°C for 7 min. The PCR products were concentrated in 20 µl of H_2O, and the desired DNA fragments were confirmed by gel electrophoresis. The reaction (i), (ii), (iii), (iv), and (v) resulted in DNA gel bands at ~1100bp, 600bp, 1100bp, 600bp, and 550bp, respectively. After gel extraction, each amplicon was eluted in 30 µl H_2O. Finally, 15 µl of the eluate from each reaction was submitted to the GSAF at UT Austin for sequencing on the Illumina MiSeq platform, with 2x300bp paired-end reads and a minimum of 10^6 reads for each reaction.

11.8 Bioinformatic analysis of BCR-seq data

Raw Illumina MiSeq output sequences from VH sequencing were quality filtered and R1-R2 merged using PEAR 0.9.6 software[264] with default settings except for the following changes: the minimum overlap size, 10 base pair (bp); the maximum possible length, 700bp; the minimum possible length, 50 bp; the maximum proportions of uncalled bases, 1 bp; the number of threads to use, 4[264]. The R1 and R2 stitched VH reads were aligned against IMGT V, D, and J germline genes using MiXCR[265]. Sequences with ≥ 2 reads were clustered into clonal lineages using single linkage hierarchical clustering, with clonality defined by 90% CDR-H3 amino acid identity measured by Levenshtein distance across the CDRH3 amino acid sequences.

Paired-end FASTQ files from the natively paired VH:VL sequencing

(reaction (i)-(v) described above) were quality-filtered using Trimmomatic[266] with the following settings: 5bp sliding window; a cutting when the average quality per base drops below 20; a removal of reads below 100 bp[266]. Similarly, filtered data was V, D, and J annotated using MiXCR, and the resulting R1 and R2 files were stitched together based on the same read ID. Any unproductive reads that contain stop codon or truncated reads were removed, and the resulting productive VH:VL paired reads with a minimum of 2 reads were subjected for a centroid-based UCLUST clustering (USEARCH software 10.0.240) to perform BCR clustering based on > 90% identity across CDRH3 nucleotide sequences[267].

11.9 Ig-Seq repertoire sequencing

11.9.1 IgG purification and digestion into F(ab')$_2$

1ml of plasma sample collected on day 180 was diluted with 1ml of Dulbecco's PBS and submitted to affinity chromatography purification using a gravity column (Pierce™ Disposable Column - Thermo Fisher Scientific) packed with 1.5ml of hydrated Protein G Plus Agarose 50% slurry resin (Pierce Thermo Fisher Scientific) as described in the section 11.4. The purified IgG (3mg) was digested into F(ab')$_2$ fragments by adding 60 µg of IdeS. The mixture was incubated at 37 ^{o}C for 1h.

11.9.2 Antigen enrichment - pulldown

Antigen-specific IgG-derived F(ab')$_2$ was isolated by affinity chromatography and using the recombinant antigen (1 mg of either DENV2 or ZIKV E dimer) coupled to dry N-hydroxysuccinimide (NHS)-activated agarose resin (Thermo Fisher Scientific) as described by Voss et al[268]. Briefly, 50 mg of NHS-activated agarose was resuspended into 1mg/ml of antigen and incubated at room temperature, rotating end-over-end for 1.5h. Following this time, the mixture was left rotating ovenight at 4°C. The coupled NHS agarose was loaded into a 0.8 ml Pierce™ Centrifuge Column (Thermo Fisher Scientific) and washed with 2 CV of Dulbecco's PBS. Unreacted NHS groups were blocked with 1M ethanolamine, pH 8.2 (Sigma, MO, USA) for 20 min at room temperature. DENV2 or ZIKV E-dimers coupled NHS was washed with 12 CV of Dulbecco's PBS by centrifuging at 1000 x g for 30 sec to remove any non-conjugated antigen from the resin. F(ab')$_2$ fragments (10 mg/ml in PBS) were added to the antigen-conjugated NHS

column and the sample was incubated at room temperature during 1.5 h on an end-to-end rotator. Following this step, flow-through was collected by centrifugation at 1000 x g for 30 sec. The column was subsequently washed with 12 CV of Dulbecco's PBS and the $F(ab')_2$ were eluted with 360 µl of LC-MS grade 1% formic acid (Thermo Fisher Scientific) at 1000 x g for 30 sec. For each elution, 30 µl of eluate was immediately neutralized with 20 µl of 1M Tris-HCl, pH 8.0. The elution step was repeated six times. The neutralized samples were tested (25 µl) in an ELISA assay coated with 4 µg/ml of DENV2 or ZIKV to confirm the depletion of antigen-specific F(ab)2 fragments in the flow-through as well as to confirm the elution of antigen-specific F(ab)2 fragments from the affinity column (Figure S.1).

11.9.3 Sample denaturation, reduction, alkylation and trypsin digestion

Fractions containing the flow-through and the eluted $F(ab')_2$ fragments were concentrated in a speed-vac at 45 ^{o}C for approximately 1.5h in aqueous mode until 5µl of final volume was left. Eluates were pooled, 5µl of MS grade H_2O (Fisher Scientific, MA) was added, and 0.2 v/v 1M Tris pH 8.5 / 3 M NaOH were used to neutralize the sample. The final volume was adjusted to 50µl after pH adjustment to between 7.0 and 7.5. Aliquots containing 10µg of each flow-through and eluates were resuspended in 50 µl of MS grade H_2O and submitted for denaturation with an equal volume (50 µl) of 100% 2,2,2-trifluoroethanol (TFE) (Sigma, MO, USA). Samples were then reduced with 1.2 µl of 500mM of TCEP solution (Thermo Fisher Scientific) and incubated at 55 ^{o}C for 1h in a dry shaker. The resulting samples were alkylated with 3 µl of 550 mM iodoacetamide (Sigma, MO, USA) at room temperature in the dark during 30 min. Samples were diluted to a final volume of 1ml with 40 mM Tris-HCl pH 8.0. The trypsin digestion was carried out by adding 2 µg of MS grade Trypsin Gold (Promega) into solution and incubating samples overnight at 37 °C. Trypsin was inactivated by adding 10µl of 100% formic acid.

11.9.4 Bottom-up LC-MS/MS

Trypsin digested peptides were concentrated by speed-vac at 45^{o}C for 3h until less than 20 µl was left. Samples were resuspended in 50 µl of 0.1% formic acid and desalted using Millipore U-C18 ZipTip Pipette Tips following the manufacturer's protocol. The desalted, dried peptides were resuspended in 0.1%

formic acid and submitted to the UT Austin Center for Biomedical Research Support Biological Mass Spectrometry Facility (RRID: SCR_021728) for protein identification by liquid chromatography–tandem mass spectrometry (LC-MS/MS) using a Thermo Ultimate 3000 RSLCnano UPLC coupled to a Thermo Scientific Orbitrap Fusion Tribrid mass spectrometer. LCMS/MS analysis was conducted as follows: (i) samples were loaded onto a C18 analytical column with triplicate injections (25cm x 75 µm inner diameter) packed with 3 µm material (Thermo Acclaim PepMap 100). Peptide separation was performed by using a gradient from 5-45% mobile phase B (0.1% formic acid in acetonitrile) over 120 min total run (ii) MS data was collected on an Orbitrap Fusion (Thermo Fisher Scientific) operated at 3 sec cycle time, 120,000 resolution, scan range 400-1600 m/z, maximum injection time of 60 milliseconds, and 60% RF lens value (iii) centroid MS/MS data were acquired in the linear ion trap using quadrupole isolation followed by HCD (higher-energy collisional dissociation) in topspeed mode with a 3 sec cycle time and (iv) dynamic exclusion of precursors were set after n=2 fragmentation events in 30s window.

11.10 Bioinformatic analysis

LC-MS/MS resulting spectra were searched against databases consisting of the VH and VL sequences. Databases were constructed by concatenating bulk VH (T0, T7, and T14 sequencing data from IgG, IgA and IgM repertoires) and paired VH:VL (T14 sequencing data from IgG, IgA and IgM repertoires) sequencing data (BCR-seq) with either DENV2 or ZIKV E protein sequence[260-261] and common protein contaminants list provided by MaxQuant and an Ensembl version of 73 human protein database. Peptide-spectrum matches for each subject were identified by Thermo Proteome Discoverer 1.4 software (Thermo Scientific). Parameters were set with maximum missed cleavage sites of 2 and the peptide length ranging from 6 aa to 144aa. The average precursor mass and the fragment mass were set to False, while the mass tolerance for matching fragment peaks was set to 5ppm for precursor mass and 0.5Da for fragment mass. The weight of a, b, c, x, y, and z ions were set to 0, 1, 0, 0, 1, and 0, respectively. For dynamic modifications, maximum equal or dynamic modifications per peptide were set to 3 and 4, respectively, and the oxidation (+15.9995Da) was selected as a C-terminal dynamic modification. For static modifications, carbamidomethyl (+57.021Da)

was selected as a C-terminal static modification. The precursor ions area detector node was set for the entire workflow. To set the parameters for the Percolator node, the maximum delta Cn value was set to 0.05, and the target false discovery rate for high-confidence and medium-confidence peptide hits were set to 0.01 and 0.05, respectively, with a validation based on q-value.

Results were filtered for high-confidence peptide-spectrum matches (PSMs) associated with the precursor ions for each peptide. Ambiguous peptides with an average delta mass deviation exceeding 1.5 ppm were excluded. MS data analyses were performed using custom Python scripts[268] and as described by Lavinder et al.[42]. Peptide abundance was quantified as sum of extracted ion chromatography peak area, also known as XIC area. Each VH peptide were assigned to unique antibody lineages using VH BCR-seq data as described above. To measure the abundance of each antibody lineage, we summed the XIC areas of CDRH3 peptides that are uniquely associated with a single IgG lineage and that have PSMs ≥ 2 across triplicate elution injections. Any CDRH3 peptides found in multiple antibody lineages or having only 1 PSM detected across triplicate elution injections were excluded from subsequent analysis.

We compared the XIC areas in the elution and flow-through to determine antigen-specific IgG lineages and non-antigen-specific IgG lineages. Peptides were considered as corresponding antigen-specific IgG lineages when found to be enriched > 2-fold in the elution in comparison to flow-through. We applied the formula: $C_{adj} = C_{default} \times \frac{total\_Elu\_XIC}{total\_FT\_XIC}$, $C_{default}$ = 2, to define the cut-off for antigen-specificity comparison, where $total\_Elu\_XIC$ represents the total elution XIC areas for all CDRH3 peptides, and $total\_FT\_XIC$ represents the total flow-through XIC areas for all CDRH3 peptides. Therefore, when $total\_Elu\_XIC$ for a given IgG lineage equals the $total\_FT\_XIC$, default cut-off is applied and thus any IgG lineages with an $total\_Elu\_XIC$ 2-times higher than the $total\_FT\_XIC$ are defined as antigen-specific IgG lineage ($C_{adj} = C_{default} = 2$). IgG lineages that passed this cut-off were added to the final list of antigen-specific IgG lineages. We classified cross-reactive IgG lineages as those that were identified in both DENV2 and ZIKV eluates. We also defined pre-existing IgG lineages as those that the CDRH3 sequence was detectable in the cellular repertoire data (BCR-seq) in day 0, 7 and 14 after vaccination. The relative abundance (fraction of the serological

repertoire %) of each lineage in the DENV2 or ZIKV repertoire was determined by dividing the sum of the elution XIC areas for a given antigen-specific IgG lineage by the total elution XIC areas for all antigen-specific IgG lineages. To compare the molecular characteristics of the serological repertoires, the representative VH SHM for each clonotype was determined as the average of SHM for VH reads clustered in each IgG lineage. We used the D80 index to perform the plasma IgG repertoire diversity measurements. This index refers to the number of lineages that comprise the top 80% of the repertoire by abundance (by total CDR3 XIC abundance in the elution)[268].

11.11 Statistical analysis

All data was statistically analyzed as described in the section 6.7 from chapter 1.

12. RESULTS

12.1 YFV vaccinees' plasma exhibits reactivity to DENV2 and ZIKV E dimer proteins.

Previously, we had observed an increased reactivity of YFV vaccinees' plasma against DENV and ZIKV at 180 days after vaccination (Figure 11B - chapter 1, Figure 19A) and we sought to determine the fraction of the vaccinees' serological repertoire that is reactive to DENV2 and ZIKV or both viruses at six months of the YFV vaccination. Using plasma samples collected on day 180, we assessed the sorological repertoire of the YFV vaccinees through Ig-seq pipeline[42] that combines LC-MS/MS proteomics of enriched antigen-specific IgG with high-throughput sequencing of BCR heavy chain (VH) and single B cell VH:VL variable region repertoire sequencing (BCR-seq) (Figure 19B).

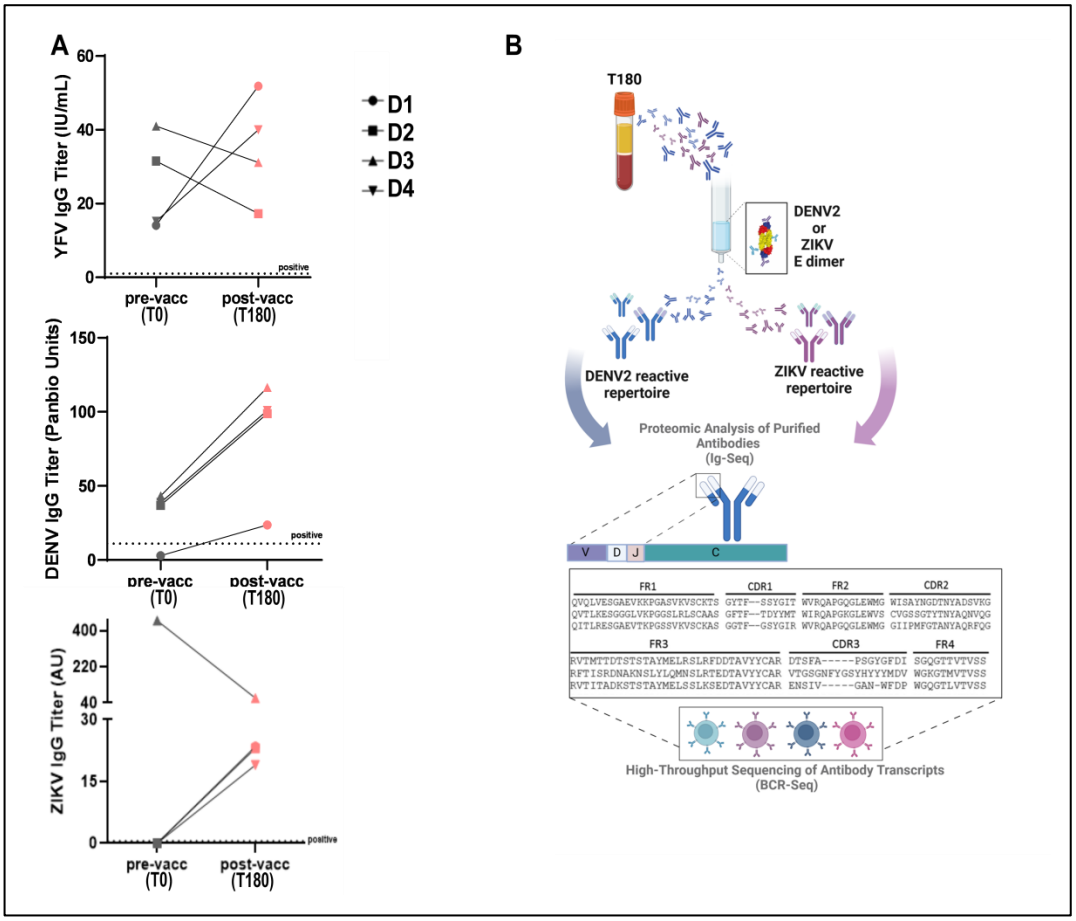

Figure 19. Characterization of the serologic antibody responses to DENV2 and ZIKV at 180 days following YFV vaccination. **A** IgG binding ELISA showing the antibody responses against YFV, DENV and ZIKV before (T0) and after (T180) YFV vaccination of four healthy donors. **B** Ig-seq experimental design. Plasma samples obtained on day 180 from each donor after vaccination against YFV were used to identify the IgG antibody lineages in the serological repertoire reactive to DENV2 and/or ZIKV. Polyclonal IgG was

submitted to affinity purification chromatography with DENV2 or ZIKV E protein dimers. A proteomic analysis of the purified IgG was performed by combining LC-MS/MS and NGS VH and VH:VL pairing of peripheral B cell repertoires (BCR-seq).

We used recombinantly expressed E protein dimers from DENV2 and ZIKV to isolate antigen-specific $F(ab')_2$ fragments from each subject plasma repertoire (Figure 19B). DENV2 dimeric E-protein containing the substitution A259C[260] was purchased from PEP-MX Core - UNC Chapell Hill, while ZIKV E-dimer proteins[261] (~92 kDa) were transiently expressed in mammalian cells and purified using His-tag affinity chromatography as described above (see section 11.2), having yields estimated in 8 mg/ml (Figure 20A).

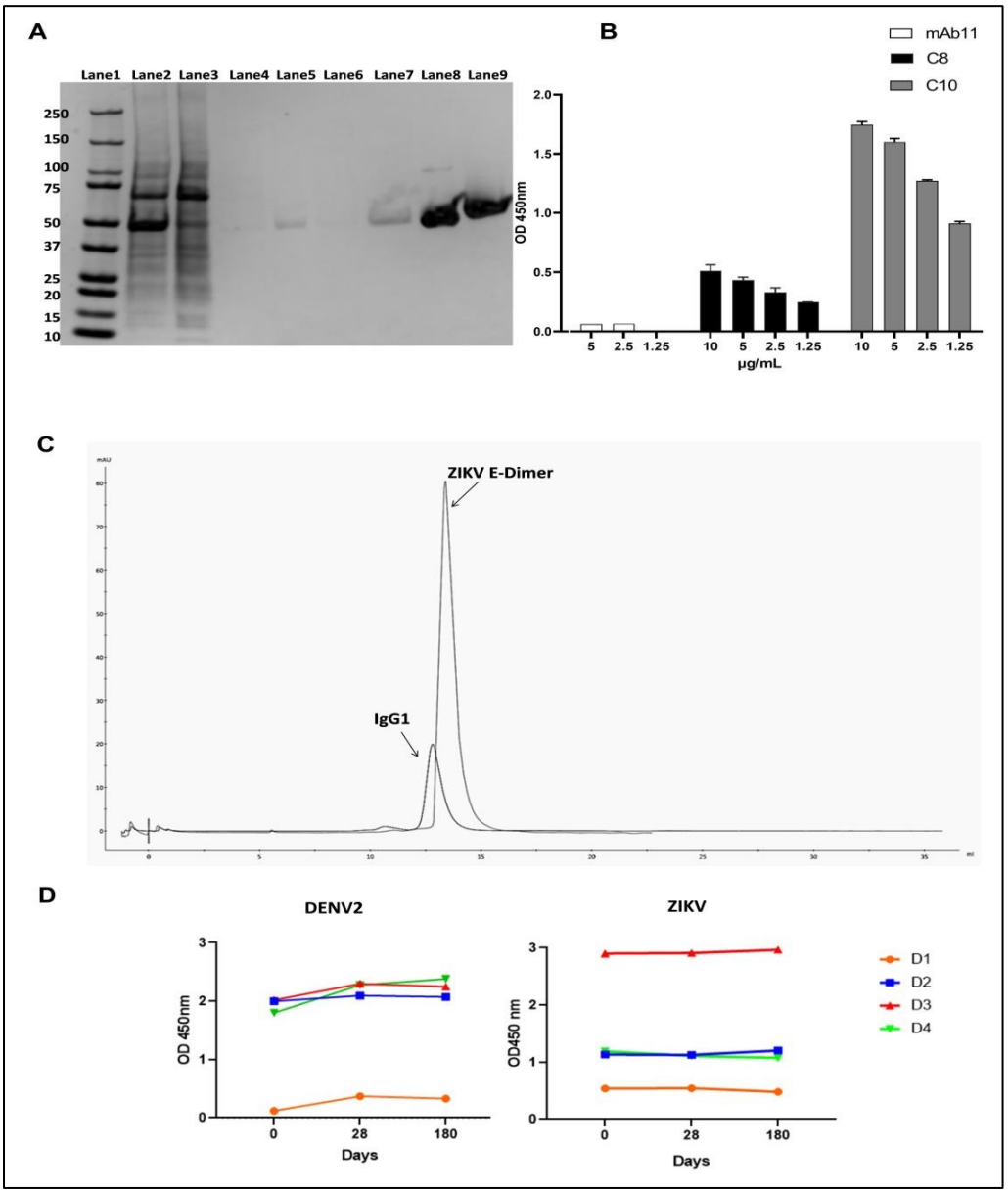

Figure 20. DENV2 and ZIKV E-dimer antigens obtention and reactivity to IgG from YFV vaccinees' plasma. **A** SDS PAGE 4-12% stained with Coomassie blue showing the

expression and purification of the ZIKV E-dimer proteins. Lane 1: molecular weight (M.W.), Lane 2: culture supernatant (input), Lane 3: flow-through (FT), Lane 4-7: wash (W1, W2), Lane 8 and 9: ZIKV E-dimer elutions under non-reducing (NR) and reducing (R) conditions. As ZIKV E-dimers are formed through non-covalent bonds, it is only possible to detect in the gel a single band corresponding to the monomer form (~55 kDa). **B** Indirect ELISA to measure the ZIKV E-dimer recognition by cross-reactive mAbs. C8 and C10 mAbs that target quaternary epitopes within the dimeric E protein were tested in serial dilutions (10, 5, 2.5, and 1.5 µg/ml). We also tested the mAb 11 which recognizes conserved structures in the FL of the E protein in three different dilutions (5, 2.5, and 1.25 µg/ml). Graph represents the absorbance ± SD of the mean for all replicates. **C** Chromatogram showing the retention time of the ZIKV E-dimers (~92 kDa) in comparison to an IgG1 (~150 kDa). Size exclusion chromatography was performed in a Superdex S-200 column equilibrated with PBS. **D** Reactivity of the YFV vaccinees plasma against DENV2 and ZIKV E-dimer antigens. Indirect ELISA assay was performed to detect the polyclonal plasma IgG antibody binding to the recombinant antigens. Tested samples were obtained at 0, 28 and 180 days following vaccination of the 4 subjects. Graph represents the absorbance at 450nm of each individual in each time time point.

Next, we used two cross-reactive antibodies, C8 and C10 mAbs, that target quaternary epitopes on the E-dimer and the mAb 11 that targets the FL of the E protein to confirm the dimeric conformation of the recombinant ZIKV antigens. Results from the Indirect ELISA show that mAbs that target quaternary epitopes were able to bind to ZIKV E-protein, indicating that its homodimeric conformation was successfully obtained (Figure 20B). We further evaluated the presence of any monomeric E-protein in the sample by running a size exclusion chromatography. Using an IgG1 (~150 kDa) as reference to compare the retention time of the samples, we confirmed that the recombinant protein was fully expressed as dimers (Figure 20C).

Next, we tested the YFV vaccinees' plasma obtained on 0, 28, and 180 days after vaccination to measure the reactivity of the samples to DENV2 and ZIKV E-dimers. In comparison to the previous IgG ELISA outcomes, here we observed a distinct binding behaviour of the vaccinees' plasma IgG to the recombinant E-dimers (Figure 20D). Moreover, each individual showed a different recognition pattern of these antigens, highlighting the heterogeneity of the serological antibody responses in the cohort. In sum, we demonstrated that the YFV vaccinees' plasma contain antibodies that recognize DENV2 and ZIKV E dimer proteins. Given the fact that some of the most potent neutralizing antibodies target quaternary epitopes that only exist in context of the dimeric E protein, we interrogate the nature of these antibodies responses against DENV2 and ZIKV at

180 days after the YFV vaccination.

12.2 Serological repertoires of the YFV vaccinees are comprised of cross-reactive antibody lineages between DENV2 and ZIKV at 180 days after the vaccination.

To figure out the composition of the serological repertoire at 180 days of the YFV vaccination, we firstly coupled either DENV2 or ZIKV recombinant E dimers into two separated NHS resin columns to affinity purify the reactive IgG from each donor plasma sample (Figure 19B). Eluates from each pulldown were separately submitted for LC-MS/MS analysis and the resulting MS spectra from each donor's samples were annotated using the respective donor database of bulky BCR sequences obtained by NGS of peripheral B cells isolated at 0, 7, and 14 days following vaccination (BCR-seq) (Figure 19B).

We identified between 19 and 30 unique serum IgG lineages reactive to DENV2, and between 14 and 32 unique serum IgG lineages reactive to ZIKV in the YFV vaccinees serological repertoires (Figure 21A, Table 6). Overall, we did not observe significant differences between the diversity index (D80) of anti-ZIKV antibody lineages (average D80 of ~15 plasma IgG lineages) and anti-DENV2 antibody lineages repertoire (average D80 of ~10 plasma IgG lineages) (Figure 21B). Notably, these repertoires are greatly polarized in terms of relative abundance of the IgG lineages, with more than 50% of the top abundant lineages accounting for 90% of the total abundance in the entire serological repertoire reactive to both antigens (Table 6).

Table 6. Polarization of the serological repertoires reactive to DENV2 and ZIKV.

	Total n=4	
Donor	**DENV2 Ig-Seq**	**ZIKV Ig-Seq**
D1	10/19 (52.63%)	7/14 (50%)
D2	12/19 (63.16%)	17/26 (65.38%)
D3	19/30 (63.33%)	21/32 (65.62%)
D4	11/21 (52.38%)	24/31 (77.42%)

Number of top antibody lineages accounting 90% abundance of the D80 diversity index / Number of the most abundant antibody lineages that comprise 80% (by abundance) of the serological repertoire (D80 diversity index). Parentesis indicate the frequency of the antibody lineages constituting the 90% most abundant lineages of the D80 diversity index.

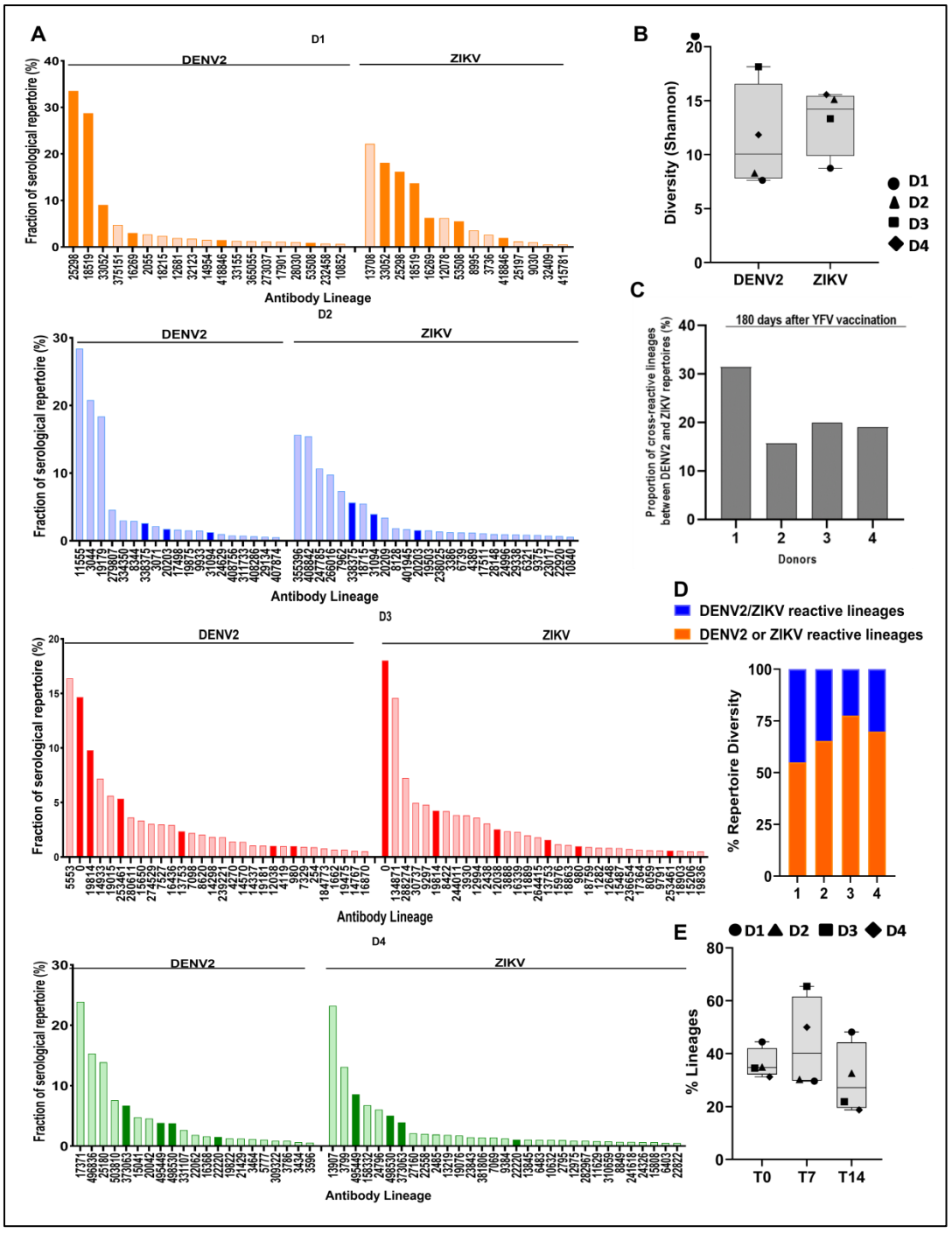

Figure 21. Analysis of DENV2 and ZIKV reactive antibody repertoires from YFV vaccinees' plasma. **A** Representative histograms of each donor's serological repertoire that was found to be reactive to DENV2 and/or ZIKV on day 180. Each bar indicates individual IgG lineages and its height represents the relative abundance (fraction) in the repertoire. Dark color bars represent the overlapping lineages between the two repertoires. **B** Anti-DENV2 and Anti-ZIKV IgG repertoires' diversity was assessed by Shannon index at 180 days following vaccination. **C** Proportion of IgG antibody lineages in the serological repertoire of each donor that are reactive to both DENV2 and ZIKV viruses. **D** Fraction of the repertoires' diversity that is due to the overlapping DENV2/ZIKV IgG lineages (blue) and to lineages that are only reactive to DENV2 or ZIKV (orange). **E** Proportion of DENV2 and/or ZIKV reactive IgG antibody lineages that were detected at early time points in the expanded repertoire (0, 7, and 14 days after vaccination).

Interestingly, some of these lineages were found in overlap in both DENV2 and ZIKV repertoires from all donors (Figure 21A), revealing the presence of cross-reactive antibody lineages between these two viruses in the repertoire of the YFV vaccinees. The abundance of these cross-reactive lineages varies from 18% to 32% across donors (Figure 21C) and represents less than 45% of the entire repertoire diversity (Figure 21D). We investigated whether these lineages reactive to DENV2 and/or ZIKV already existed in the cellular repertoire at earlier time points. Surprisingly, we found between 31% and 45% of these lineages existing before vaccination and an average of 40% and 25% of these antibody lineages were detected on day 7 and 14, respectively (Figure 21E). However, just a few of these lineages were found expanded at 7 and/or 14 days after vaccination (Table 7). Moreover, those expanded lineages presented very low abundance in the serological repertoire at 180 after the vaccination. Therefore, we show that the serological repertoire of the YFV vaccinees contains low abundant and persisting DENV2 and ZIKV cross-reactive antibody lineages that could be result of repeated vaccinations and YFV, DENV, and ZIKV co-circulation in the region.

Table 7. Plasma IgG lineages that contain the same CDRH3 sequence of BCR lineages from the cellular repertoire at 0, 7 and 14 days after the vaccination.

Donor	Lineage	CDRH3 Sequence	Time	Expansion Level in the Cellular Repertoire	Fraction of the Serological Repertoire on day 180 (%)
1	25298	ARGPGIFGVAIPED	T14	Non Expanded	33.56
1	18519	ARAPWGSSSAPYYYFDL	T0 / T14	Non Expanded	28.77
1	33052	VREANY	T0	Non Expanded	9.05
1	375151	VRSGAGSTWGFDS	T7 / T14	Expanded	4.73
1	16269	AKAPDGY	T14	Non Expanded	3
1	2055	ARDVPPRGLWFGEIDGAFDV	T0 / T7 / T14	Non Expanded	2.71
1	18215	ARAIFPFGMDV	T14	Non Expanded	2.40
1	12681	ARGSPETPPH	T14	Non Expanded	1.93
1	32123	AYRRRAGGNYRTDF	T7	Non Expanded	1.78
1	14954	SGREAAAGTLPKENDY	T0	Non Expanded	1.50
1	33155	VRHHNHYRWGFDP	T14	Non Expanded	1.28
1	365055	ARGGVGPPPDYDYIWGTYRRGREFDY	T7 / T14	Non Expanded	1.26
1	273037	ARVDCRSTSCYGEWFDT	T0	Non Expanded	1.18
1	17901	ARAAVLAATRQSDY	T14	Non Expanded	1.13
1	28030	ARRDTNY	T0 / T7	Non Expanded	1.05
1	53508	ARRRYSGYDLDY	T0	Non Expanded	0.87
1	232458	ARIRARQAARPTIGIRTQDY	T7	Non Expanded	0.72
1	10852	ARDQLRNYYADY	T0	Non Expanded	0.64

2	11555	ARDGSDYPLDY	T7	Non Expanded	28.39
2	3044	ARDAYYFHH	T14	Non Expanded	20.80
2	19179	ARDDDSYGPIY	T7	Non Expanded	18.36
2	279807	ARMPGFSYAFFDY	T7	Expanded	4.57
2	**8344**	**AREGDYELDY**	**T0**	**Non Expanded**	**2.91**
2	**338375**	**AREGDYELDY**	**T0**	**Non Expanded**	**2.60**
2	3071	ARDMGGAVAGMWLY	T7	Non Expanded	2.17
2	20203	ARDNYGSGRGFSDY	T0	Non Expanded	1.72
2	17498	AKGQDFGY	T0	Non Expanded	1.64
2	19875	ARDLESESIAARQGGFDY	T0	Non Expanded	1.54
2	9933	ARDLESESIAARQGGFDY	T0	Non Expanded	1.49
2	24629	ARHRRNSLGDRKDVFDI	T14	Non Expanded	0.99
2	408756	AKVVVPETKTGWFDP	T0 / T7 / T14	Expanded	0.77
2	311733	ARIRDWNYDY	T7 / T14	Non Expanded	0.75
2	408286	ARDYSPGWYRGAFDI	T0 / T7 / T14	Expanded	0.66
2	29134	SKQLGIRGYFDS	T14	Non Expanded	0.60
2	407874	AKGGDGYNPALDI	T0 / T7 / T14	Expanded	0.55
3	5553	ARDRLYYYDSSGPFQRYD	T7	Non Expanded	16.39
3	0	ARVPHIVVASAAIQVRFDP	T0 / T7 / T14	Expanded	14.66
3	19814	VRTVDY	T0 / T7 / T14	Non Expanded	9.80
3	14933	ARGTTGRMYLNWFDP	T7	Non Expanded	7.18
3	19015	ATSRYCDSTSCYGAFDI	T0 / T7 / T14	Non Expanded	5.61
3	253461	SRGQSDVYNQGVLEDY	T0	Non Expanded	5.35
3	280611	ARALHTNSWYTQY	T0 / T7 / T14	Non Expanded	3.63
3	15650	ARLGRSSRDLY	T7	Non Expanded	3.35
3	7527	ASKGGSLYNWFDP	T0	Non Expanded	2.99
3	16436	ARRPQWGPFDP	T7	Non Expanded	2.94
3	13753	ARGGKVGATTRFDY	T7	Non Expanded	2.35
3	7098	ARSTILRGVH	T0 / T14	Non Expanded	2.20
3	8620	AKDRATVDY	T0	Non Expanded	2.06
3	14298	ARGNVDRLGYFQKVNYFDL	T7	Non Expanded	1.84
3	4270	ARVAVAGDWFDP	T7	Non Expanded	1.42
3	14570	ARGRIAARPDDFDY	T7	Non Expanded	1.39
3	14337	ARGPGEGTVDY	T7	Non Expanded	1.07
3	19181	GRAYGNRFFDS	T7	Non Expanded	1.05
3	12038	ARDVGLTGDRHFDL	T0 / T7 / T14	Non Expanded	1.02
3	4119	ARLTRYGDPDY	T7	Non Expanded	1.01
3	7329	ARVQYYYDSGSNYYFDY	T0 / T14	Expanded	0.93
3	184773	ATRRGKAFDY	T0	Non Expanded	0.78
3	1662	ARDYGGRLGY	T7	Non Expanded	0.67
3	19475	TTDFSRSYFGS	T0 / T7 / T14	Non Expanded	0.67
3	14767	ARGSGYSYGYFVY	T7	Non Expanded	0.57
3	16870	ARSSTYQLLNRFDP	T7	Non Expanded	0.53
4	17371	ARGGTAAGIGGEDY	T7	Non Expanded	23.88
4	25180	ASGPLKQWGWRGDY	T7	Non Expanded	13.86
4	503810	ARAPINGHFDY	T14	Expanded	7.59

4	373063	ARVRRLYYASGSSLKGVFDS	T14	Expanded	6.68
4	15041	AREDSYDYRYLDS	T14	Non Expanded	4.77
4	20042	ARGYYGSGSALSRRWGFDP	T7	Non Expanded	4.56
4	495449	AREGGFSQSFEY	T7	Expanded	3.83
4	498530	ARVIVVRNYDFWSGFKTGNWFDL	T7 / T14	Expanded	3.76
4	331107	ARRLGELSPLEFDI	T0 / T7 / T14	Non Expanded	2.64
4	22062	ARRALSPYYYDSSGYYYRSAPYDY	T0	Non Expanded	1.85
4	16368	ARFRSTNWFDP	T0	Non Expanded	1.59
4	22220	ARRGTQWLVRLDWFDP	T0	Non Expanded	1.50
4	19822	ARGVVWFGSWYFDY	T7	Non Expanded	1.26
4	21429	ARMHLGFDP	T7	Non Expanded	1.22
4	3464	ARGVDRYGSGRNYWFDP	T7	Non Expanded	1.14
4	5777	ARAVTIFDY	T0	Non Expanded	1.04
4	309322	ARLRSPYFHYYMDL	T0	Non Expanded	0.87
4	3786	AAVKELSFLWVDY	T7	Non Expanded	0.86
4	3434	ARGRVRFNLLG	T7	Non Expanded	0.63
4	3596	ARSTDF	T14	Non Expanded	0.56

Bold highlights the plasma IgG lineage that was found in the cellular repertoire and its CDRH3 sequence identity matched to a known flavivirus anibody.

12.2 IgG lineages reactive to DENV2 and/or ZIKV are low expanded and little hypermutated.

We next interrogated what is the expansion levels of the IgG lineages reactive to DENV2 and/or ZIKV in the repertoires and their affinity maturation state at 180 days after the vaccination. The observed diversity index (D80) for both DENV2 and ZIKV repertoire's IgG lineages (Figure 21B) corroborates to a low clonal expansion state on day 180, as expected. We next assessed the SHM loads of these lineages to gather more information about their affinity maturation state. The average of mutations ranged between 4% and 8% across donors (Figure 22A). Noteworthy, we observed that at least 20% of the each donor's repertoire is consisted of low mutated IgG (Figure 22B) and most of these antibodies represent the top abundant IgG lineages of the serological repertoire (Figure 22C). These results may indicate that a substantial portion of the IgG lineages reative to DENV2 and/or ZIKV did not come from affinity mature B cells and we wondered whether this is actually a mechanism related to the cross-reactivity.

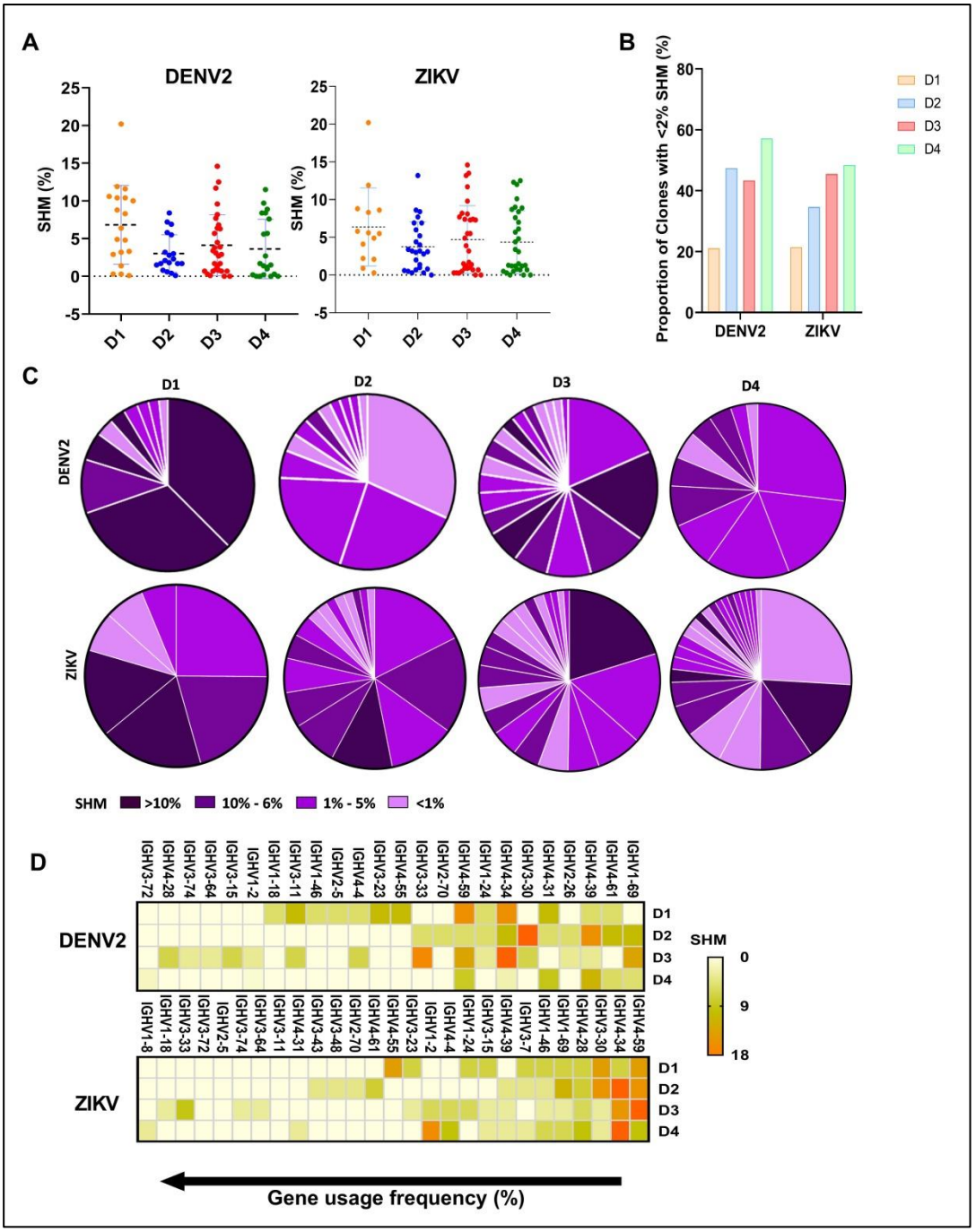

Figure 22. Molecular characterization of the IgG responses to DENV2 and/or ZIKV. **A** SHM levels of secreated IgG that is reactive to DENV2 and/or ZIKV from each donor's repertoire at 180 days after vaccination. Black horizontal lines represent means (dotted) and standard deviation (solid). **B** Proportion of low SHM (< 2%) clones for each donor in the different repertoires (DENV2 and ZIKV). **C** SHM loads of the most abundant IgG antibody lineages from serological repertoires that are reactive to DENV2 or ZIKV viruses. Each fraction of the pie chart represents an antibody lineage that accounts 90% abundance of the D80 diversity index of the serological repertoire. Colors indicate the SHM loads of each represented lineage. **D** Heat map of SHM rates per IGHV gene segment. Bottom arrow indicates the descending order of each gene segment frequency of use by the lineages of DENV2 and ZIKV serological repertoire.

We assessed the VH gene usage in these antibody lineages to verify the preferential involvement of germline segments in low SHM antibodies. First of all, it was observed different VH gene segments being used by these lineages (Figure 22D). Secondly, the less frequent VH gene segments were associated with SHM rates lower 5%, which is considered below of the average for healthy individuals' IgG (7.24 ± 0.07%) (Figure 22D). On the other hand, the most frequent VH gene segments were associated with SHM rates above of the average for healthy individuals' IgG (Figure 22D). For example, lineages that have a greater use of IGHV4-59 and IGHV4-34 contain SHM loads higher than 15%, indicating possible involvement of these gene segments on the hypermutated antibodies. In sum, we showed that plasma IgG lineages reactive to DENV2 and/or ZIKV are low expanded and little hypermutated at 180 days after the vaccination.

12.3 Comparisons of the antibody repertoires at transcriptomic and proteomic level.

The goal of this section was to learn whether the lineages identified at the transcriptome level, encode antibodies (proteomic level) that recognize the DENV2 and ZIKV antigens. To address that, we compared differences and similarities between the anti-DENV2 and/or anti-ZIKV IgG lineages identified in the serological repertoire at 180 days following immunization and the lineages which were found in the cellular repertoire (expanded and non expanded) at early stages after vaccination (T0, T7, and T14) that supposely have reactivity against DENV and/or ZIKV antigens. We found 2 DENV2 plasma IgG lineages with the same CDRH3 sequence (AREGDYELDY) of a non expanded BCR antibody lineage (AREGDYELDY) that was detected as DENV cross-reactive lineage in the repertoire before the vaccination. While this result reveals the existence of the DENV2-specific antibody lineages in the repertoire of the vaccinees, it also shows that these antibodies are very low abundant in the repertoire, representing less than 3% of the serological repertoire abundance (Table 7 data in bold).

Next, we analyzed the SHM loads of the cellular and serological repertoire and we observed that lineages from cellular repertoire have significantly higher SHM loads in comparison to IgG lineages reactive to DENV2 from the serological repertoires, while no significative differences were observed between lineages

from cellular repertoire and anti-ZIKV Plasma IgG antibody lineages (Figure 23A). We also compared the frequency of VH gene usage across the distinct repertoires and we verified a greater diversity of gene segments being used by the cellular repertoire in comparison to the serological repertoires (Figure 23B).

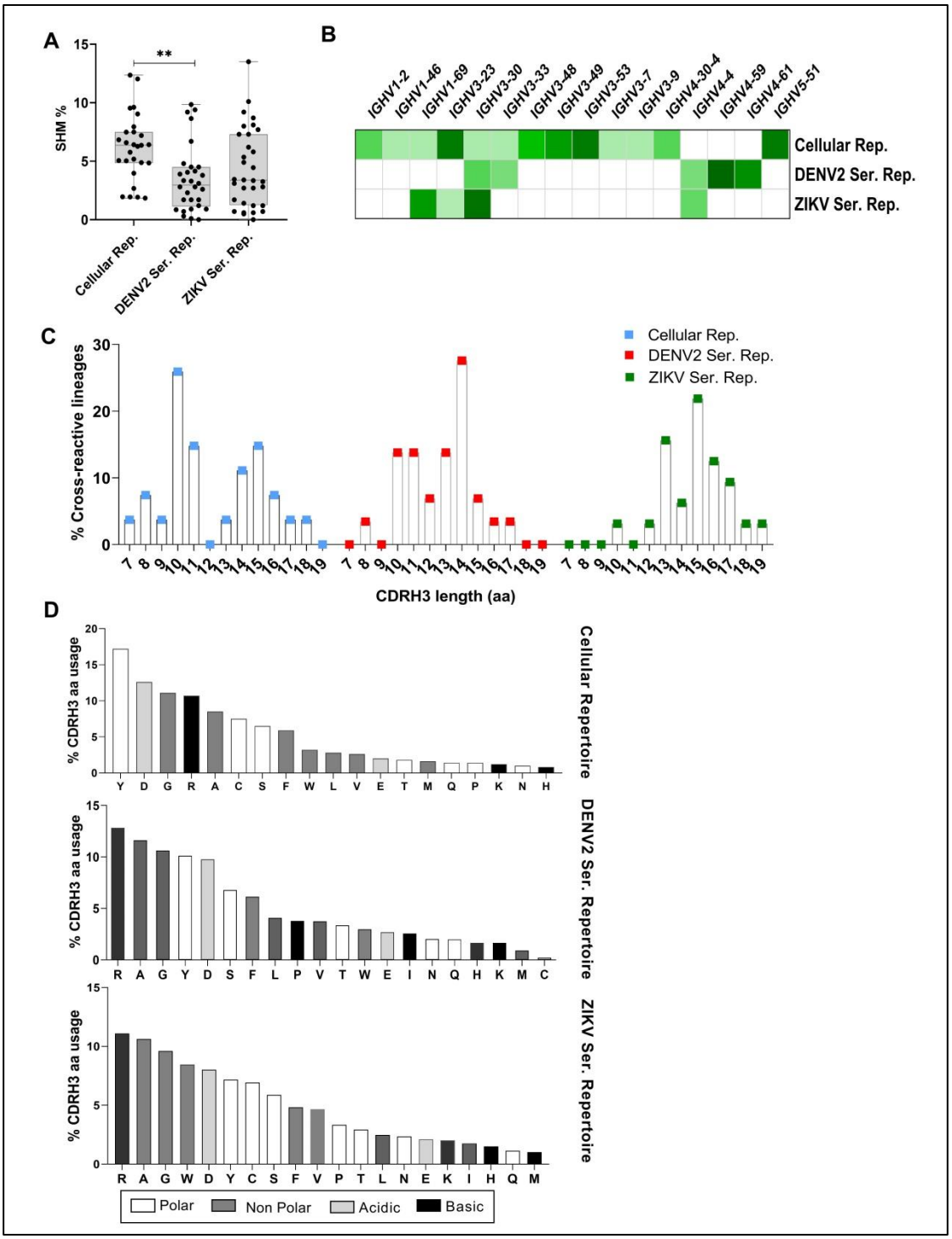

Figure 23. Comparative analysis of cellular (transcriptome) and serological (proteome) repertoires that are reactive to DENV2 and/or ZIKV. **A** Differential SHM levels between cellular (comprised of lineages that matched with known DENV and/or ZIKV antibody sequences – cross-reactive lineages) and sorological repertoires against DENV2 and/or

ZIKV. Data is represented as median of the SHM lineages across the donors in each repertoire. *P* values were calculated by anova test; *, $P < 0.05$; ***, $P < 0.001$. **B** Heat map of IGHV gene segment use in each repertoire. Only common IGHV genes to all repertoires were considered and sorted in ascending order. The median between the four YFV vaccinees was used to show the frequency of use of each segment. **C** CDRH3 length distribution across the different repertoires. **D** Amino acid composition and physico-chemical properties of the CDRH3 of each repertoire.

Particularly, all repertoires use the IGHV3-30 germline gene. On the other hand, IGHV4-4, IGHV4-59 and IGHV4-61 are exclusively used by serological IgG lineages (Figure 23B). Yet, the majority of the DENV2 and ZIKV plasma IgG lineages have longer CDRH3 in comparison to BCR lineages (Figure 23C). Regarding the physico-chemical properties of the CDRH3, plasma IgG lineages are enriched with hydrophobic amino acids, such as alanine, glycin and tryptofan, while BCR lineages present more hydrophilic profile in the CDRH3 (Figure 23D). In conclusion, we have observed distinct molecular characteristics between serological and cellular repertoire lineages that may affect the recognition of the antigens, and therefore, the cross-reactions.

13. DISCUSSION

Understanding the human antibody responses upon vaccination and/or infections is essential to improve the strategies of management during epidemies. Investigations based on B cell transcriptomes have filled important gaps in the knowledge about the immune responses against flaviviruses[48, 269-271]. However, this techique has critical limitations related to the estimation of the protein content in the repertoires. In the present study, an integration of the recently developed technologies for high-throughput paired heavy and light chain (VH:VL) sequencing, BCR heavy chain (VH) sequencing and LC–MS/MS proteomic mass spectrometry of antigen-specific antibodies (Ig-seq) were used for identification and quantification of antibody lineages that are reactive to DENV2 and ZIKV in the plasma of YFV vaccinees at 180 days of the vaccination. We also compared the changes between the cellular (comprised of lineages that matched with known DENV and/or ZIKV antibody sequences – cross-reactive lineages) and serological repertoires that are reactive to these viruses. Our data revealed that YFV vaccinees' plasma are enriched with IgG lineages that are reactive to DENV2 and/or ZIKV at 6 months following the YFV vaccination. Furthermore, we demonstrated that a substantial portion of these representative lineages of the serum response against DENV2 and ZIKV (on average ~35%) pre-existed in the repertoires (T0) and we also observed that the average of this pre-existing lineages that are reactive to both viruses increased at one week after the vaccination (on average ~40%) (Figure 21E). This finding reiforces the existence and persistence of antibody precursor sequences targeting DENV2 and ZIKV in the YFV vaccinees' antibody repertoires.

Circulating IgG has unique characteristcs that only can be analyzed at the proteome level. The Ig-seq method enables the isolation of lineages that target the antigen of interest and this fact accounts for the estimation of the real diversity of the functional repertoires. In this regard, we observed that DENV2 and ZIKV plasma IgG repertoires do not significantly differ in terms of diversity (shannon D80). Interestingly, we verified a considerable proportion of low SHM antibody lineages comprising these serological repertoires. SHM is a well described mechanism which occurs in the GC and produces affinity matured antibodies after the introduction of point mutations in the variable region that encodes the antigen-

binding site. Usually, the average of SHM in healthy individuals is 2.83 ± 0.23% for IgM, 7.24 ± 0.07% for IgG and 8.37 ± 0.23% for IgA[50]. Here, we observed that the average of the SHM loads of the plasma IgG from YFV vaccinees repertoires ranged between 4 and 8% and this finding is in line with a past work that characterized a panel of anti-ZIKV mAbs as having limited SHM (ranging from 3.72% to 7.46%)[153]. Likewise, an early investigation observed a large proportion of low somatic hypermutated B cells during acute dengue virus infection and this was associated with more severe disease[209]. In this work, we believe that YFV, DENV and ZIKV co-circulation in the endemic region is responsible for the continuous activation of the immune system and, therefore, the recruitment of both pre-existing and naïve B cells (non-affinity matured).

During the year of 2021 in Brazil, when samples were collected for this study, there were reports of co-circulation of YFV (11 cases), ZIKV (19,090 cases) and the four DENV serotypes (2,739 cases of DENV1, 1,559 cases of DENV2, 3 cases of DENV3, 10 cases of DENV4, 527,025 cases of unknown serotype) in the country[272]. In the same period, in the state of Minas Gerais, infections caused by YFV were not reported, while 401 cases of ZIKV infections and 22,230 dengue infections were registered, being most of the cased caused by DENV1 (20 cases) and DENV2 (6 cases)[272]. The lack of YFV cases in Minas Gerais may be result of great vaccination coverage, which achieved 74.59% in 2021 and was considered one of the highest of the country in that year[272]. Taken together, this epidemiological data highlights the influence of DENV and ZIKV co-circulation on the antibody responses against the flaviviruses, including in the YFV vaccine, and supports the preliminar idea that constant enviromental stimuli may be affecting the persistence and magnitude of the YFV vaccine outcomes. One example is the distinct behaviour of the YFV antibody titers observed at 180 days after vaccination. Although all donors presented decreasing anti-YFV antibody levels after the day 28, two of them kept the IgG titers above of the pre-vaccination levels on day 180 (Figure 11B - chapter 1, Figure 18A). From these two, only the donor who had not presented pre-immunity to any flavivirus was able to keep the nAb titers increased at this time point (Figure 11E - chapter 1). This outcome reiforces the effect of the pre-immunity on the YFV vaccine antibody responses. At the same time, it emphasizes the complexity of the antibody responses across subjects, in which seems to rely on the individual

exposure's history.

Previously, we had used BCR-seq to identify cross-reative lineages based on the CDRH3 amino acid sequence identity with a database of known DENV and ZIKV antibodies (Figure 17A – chapter 1). Here, we performed a comparative analysis between these lineages from the cellular repertoire and the DENV2 and/or ZIKV plasma IgG lineages from the serological repertoires to figure out their molecular characteristics. We showed that certain VH genes appear to be differentially used between cellular and serological repertoire lineages. Most of the VH genes that we identified in use by the repertoire lineages agrees with previous reports about ZIKV antibodies characteristics[153], including the IGHV3-30, IGHV5-51, IGHV4-30-4 and others found here in either serological or cellular repertoires. We also identified differences involving lineages from both repertoires, such as the length of the CDRH3 and its physico-chemical properties. Among these properties, it is worth of attention the hydrofobicity of the CDRH3 from plasma IgG lineages, that according to an investigation about the molecular basis of the antibody cross-reactivity, combination of critical hydrophobic amino acids enable the formation of π-π stacking interactions that facilitate this sort of cross-reaction with the epitopes[255]. Thus, these characteristics may be correlated to the serum antibody responses observed in terms of binding and neutralization profile.

Finally, results gathered in this study must be considered in light of some limitations, tough. It cannot be excluded that some of the observations may be at least partly due to the methods, since it is well known that a fraction of the serological responses is constituted by antibodies from a memory pool of cells that are not available in the peripheral blood, but in the bone marrow[273] and, therefore, it would not be accessible through BCR-seq analysis. Furthermore, the time gap between the BCR-seq (0, 7, and 14 days) and Ig-seq analysis (180 days) may have affected the abundance of transcripts or antibodies. Yet, the dynamic changes that happened during this timing interval may have been decisive for the generation of the antibodies.

On the other hand, the insights gained with this work could not be provided from classical serology approaches or only using BCR-seq analysis. The former would not be able to detail the individual antibody's characteristics at the molecular level, and the latter cannot inform the antigen-specific antibody lineages

directly involved in the serological response. Therefore, we were able to provide valuable information about the abundance of cross-reactive anti-DENV2 and/or anti-ZIKV-IgG in the plasma of YFV vaccinees spite of this study has analyzed the antibody repertoire of a small cohort. Such understanding unveils the influence of the co-circulation of related flavivirus on the antibody responses and their impact on vaccine outcomes. However, further analysis will be critical to understand the functional activity of these antibodies through their recombinant expression and investigation of their binding and neutralization activity *in vitro* and *in vivo*.

14. CONCLUSION

In this work, using transcriptome and proteome of antibody repertoires, we validated the main hypothesis that populations living in endemic regions with co-circulation of related flaviviruses, such as DENV, ZIKV, and YFV, and after YF vaccination, tend to present cross-reactive antibodies in their repertoire that can affect the YFV vaccine outcomes. Nonetheless, it is necessary to examine the functional properties and individual contribution of these antibodies to better understand their protective/enhancing responses in sequential exposures.

REFERENCES

1. LITVOC, M.N.; NOVAES, C.T.G.; LOPES, M.I.B.F. Yellow fever. **Rev. Assoc. Med. Bras.,** vol.64, n.2, p. 106-113, 2018.

2. CENTERS FOR DISEASE CONTROL AND PREVENTION. **Areas with risk of yellow fever**.[2019]. Available in: https://www.cdc.gov/yellowfever/maps/index.htmlv. Accessed: 2nd Mar 2024.

3. GOULD, E. A. & SOLOMON, T. Pathogenic flaviviruses. **Lancet**, n. 371, p.500–509, 2008.

4. VASCONCELOS, P. F. D. C. Febre amarela: reflexões sobre a doença, as perspectivas para o século XXI e o risco da reurbanização. **Rev. Bras. Epidemiol.** 5, p.244–258, 2002.

5. WHO. **Yellow fever fact sheet.** [2023]. Available in: https://www.who.int/news-room/fact-sheets/detail/yellow-fever. Accessed: 2nd Mar 2024.

6. SILVA, N.I.O.; SACCHETTO, L.; DE REZENDE, I.M.; TRINDADE, G.S.; LABEAUD, A.D.; DE THOISY, B.; DRUMOND, B.P. Recent sylvatic yellow fever virus transmission in Brazil: the news from an old disease. **Virol J.**, 17, p. 1-9, 2020.

7. SANDBERG, J.T.; OLS, S.; LÖFLING, M.; VARNAITĖ, R.; LINDGREN, G.; NILSSON, O.; ROMBO, L.; KALÉN, M.; LORÉ, K.; BLOM, K.; LJUNGGREN, H.G. Activation and Kinetics of Circulating T Follicular Helper Cells, Specific Plasmablast Response, and Development of Neutralizing Antibodies following Yellow Fever Virus Vaccination. **J Immunol.** 207, 4, p. 1033-1043. 2021.

8. STAPLES, J. E.; MONATH, T. P.; GERSHMAN, M. D.; BARRETT, A. D. T. Yellow Fever Vaccines. **Plotkin's Vaccines**, 20, p. 1181–1265. 2018.

9. WIETEN, R.W., JONKER, E.F.F. ; VAN LEEUWEN, E.M.M; REMMERSWAAL, E.B.M.; VISSER, M.P. GROBUSCH; DE BREE J.G. A single 17D yellow fever vaccination provides lifelong immunity: characterization of yellow fever specific neutralizing antibody and T-cell responses after vaccination. **PLoS One,** 11, 0149871, 2016.

10. ABDALA-TORRES, T.; CAMPI-AZEVEDO, A.C.; DA SILVA-PEREIRA, R.A.; DOS SANTOS, L.I.; HENRIQUES, P.M.; COSTA-ROCHA, I.A.; OTTA, D.A.; PERUHYPE-MAGALHÃES, V.; TEIXEIRA-CARVALHO, A.; ARAÚJO, M.S.S.; FERNANDES, E.G.; SATO, H.K.; FANTINATO, FFST, DOMINGUES CMAS, KALLÁS EG, TOMIYAMA HTI, LEMOS JAC, COELHO-DOS-REIS J.G.; DE LIMA, S.M.B.; SCHWARCZ, W.D.; DE SOUZA AZEVEDO, A.; TRINDADE, G.F.; ANO BOM, A.P.D.; DA SILVA, A.M.V.; FERNANDES, C.B.; CAMACHO, L.A.B.; DE SOUSA MAIA, M.L.; COLLABORATIVE GROUP FOR STUDIES OF YELLOW FEVER

VACCINE; MARTINS-FILHO, O.A.; DO ANTONELLI, L.R.D.V. Immune response induced by standard and fractional doses of 17DD yellow fever vaccine. **NPJ Vaccines**. 9, p. 1-54, 2024.

11. REY, F.A.; STIASNY, K.; VANEY, M.C.; DELLAROLE, M.; HEINZ, F.X. The bright and the dark side of human antibody responses to flaviviruses: lessons for vaccine design. **EMBO Rep.,** 19, p. 206–224, 2018.

12. ZHANG, X.; GE, P.; YU, X.; BRANNAN, J.M.; BI, G.; ZHANG, Q.; SCHEIN, S.; ZHOU, Z.H. Cryo-EM structure of the mature dengue virus at 3.5-Å resolution. **Nat Struct Mol Biol**., 1, p.105-110, 2013.

13. HEINZ, F.X. ; STIASNY, K. Flaviviruses and their antigenic structure. **Journal of Clinical Virology**, 55, 4, p. 289-295, 2012.

14. SANTOS-PERAL, A.; LUPPA, F.; GORESCH, S.; NIKOLOVA, E.; ZAUCHA, M.; LEHMANN, L.; DAHLSTROEM, F.; KARIMZADEH, H.; THORN-SESHOLD, J.; WINHEIM, E.; SCHUSTER, E.M.; DOBLER, G.; HOELSCHER, M.; KÜMMERER, B.M.; ENDRES, S.; SCHOBER, K.; KRUG, A.B.; PRITSCH, M.; BARBA-SPAETH, G.; ROTHENFUSSER, S. Prior flavivirus immunity skews the yellow fever vaccine response to cross-reactive antibodies with potential to enhance dengue virus infection. **Nat Commun**., 15, 1696, 2024.

15. BOVAY, A.; NASSIRI, S.; HAJJAMI, H.M.; MONDÉJAR, P.M.; AKONDY, R.S.; AHMED, R.; LAWSON, B.; SPEISER, D.E.; MARRACO, S.A.F. Minimal immune response to booster vaccination against Yellow Fever associated with pre-existing antibodies. **Vaccine,** 38, 9, p.2172-2182, 2020.

16. CYSTER, J.; & ALLEN, C. B Cell Responses: Cell Interaction Dynamics and Decisions. **Cell**, 177, 3, p. 524-540, 2019.

17. MERLO, L. M. F.; & MANDIK-NAYAK, L. Adaptive Immunity. **Cancer Immunotherapy**, p. 25–40. 2013.

18. MARKS, C.; DEANE, C.M. How repertoire data are changing antibody science. **J Biol Chem.**, 295, 29, p. 9823-9837, 2020.

19. MINERVINA, A.; POGORELYY, M.; MAMEDOV, I. T-cell receptor and B-cell receptor repertoire profiling in adaptive immunity. **Transpl Int**, 32, p. 1111-1123, 2019.

20. ROUX, K.H. Immunoglobulin structure and function as revealed by electron microscopy. **Int. Arch. Allergy Immunol.**, 120, p. 85-99, 1999.

21. NORTH, B.; LEHMANN, A.; DUNBRACK, R.L. JR. A new clustering of antibody CDR loop conformations. **J Mol Biol.**, 406, 2, p. 228-56, 2011.

22. KENNETH, B. H.; FOWLER, A.; LUNTER, G.; OLIVER, G. P. The Diversity and Molecular Evolution of B-Cell Receptors during Infection, **Molecular**

Biology and Evolution, 33, 5, p. 1147–1157, 2016.

23. SCHWARTZ, R.S.; SHATTUCK. Lecture: diversity of the immune repertoire and immunoregulation. **N. Engl. J. Med.**, 348, p. 1017-1026, 2003.

24. BRINEY, B.; INDERBITZIN, A.; JOYCE, C.; BURTON, D.R. Commonality despite exceptional diversity in the baseline human antibody repertoire. **Nature,** 566, p. 393–98, 2019.

25. SCHROEDER, H.W. J.R. Similarity and divergence in the development and expression of the mouse and human antibody repertoires. **Dev Comp Immunol.**, 30, p. 119–35, 2006.

26. ZHENG, B.; YANG, Y.; CHEN, L.; WU, M.; ZHOU, S. B-cell receptor repertoire sequencing: Deeper digging into the mechanisms and clinical aspects of immune-mediated diseases. **iScience**, 25, 10, 2022.

27. ALT, F.W.; OLTZ, E.M.; YOUNG, F.; GORMAN, J.; TACCIOLI, G.; CHEN, J. VDJ recombination. **Immunol Today**, 13, p. 306–14, 1992.

28. SCHATZ, D.G.; JI, Y. Recombination centres and the orchestration of V(D)J recombination. **Nat Rev Immunol**., 11, p. 251–63, 2005.

29. TONEGAWA, S. Somatic generation of antibody diversity. **Nature**, 302, p. 575-581, 1983.

30. GLANVILLE, J.; KUO, T.C.; VON BÜDINGEN, H.C.; GUEY, L.; BERKA, J.; SUNDAR, P.D.; HUERTA, G.; MEHTA, G.R.; OKSENBERG, J.R.; HAUSER, S.L.; COX, D.R.; RAJPAL, A.; PONS, J. Naive antibody gene-segment frequencies are heritable and unaltered by chronic lymphocyte ablation. **Proc Natl Acad Sci,** 108, 50, 2011.

31. DAVYDOV, A.N; OBRAZTSOVA, A.S.; LEBEDIN, M.Y.; TURCHANINOVA, M.A.; STAROVEROV, D.B.; MERZLYAK, E.M.; SHARONOV, G.V.; KLADOVA, O.; SHUGAY, M.; BRITANOVA, O.V.; CHUDAKOV, D.M. Comparative Analysis of B-Cell Receptor Repertoires Induced by Live Yellow Fever Vaccine in Young and Middle-Age Donors. **Front Immunol.**, 9, 2309, 2018.

32. BRADDOM, A.E.; BOL, S.; GONZALES, S.J.; REYES, R.A.; MUSINGUZI, K.; NANKYA, F.; SSEWANYANA, I.; GREENHOUSE, B.; BUNNIK, E.M.B Cell Receptor Repertoire Analysis in Malaria-Naive and Malaria-Experienced Individuals Reveals Unique Characteristics of Atypical Memory B Cells. **mSphere,** 6, 2021.

33. HIEPE, F.; DÖRNER, T.; HAUSER, A.E.; HOYER, B.F.; MEI, H.; RADBRUCH, A. Long-lived autoreactive plasma cells drive persistent autoimmune inflammation. **Nat Rev Rheumatol.**, 7, 3, p. 170-8, 2011.

34. BASHFORD-ROGERS, R.J.M.; BERGAMASCHI, L.; MCKINNEY, E.F.;

POMBAL, D.C.; MESCIA, F.; LEE, J.C.; THOMAS, D.C.; FLINT, S.M.; KELLAM, P.; JAYNE, D.R.W.; LYONS, P.A.; SMITH, K.G.C. Analysis of the B cell receptor repertoire in six immune-mediated diseases. **Nature,** 574, 7776, p. 122-126, 2019.

35. HOU, X.; WEI, W.; ZHANG, J.; LIU, Z.; WANG, G.; YANG, X.; DAI, Y. Characterization of T and B cell receptor repertoire in patients with systemic lupus erythematosus. **Clin Exp Rheumatol.** 41, 11, p. 2216-2223, 2023.

36. ZHENG, F.; XU, H.; ZHANG, C.; HONG, X.; LIU, D.; TANG, D.; XIONG, Z.; DAI, Y. Immune cell and TCR/BCR repertoire profiling in systemic lupus erythematosus patients by single-cell sequencing. **Aging,** 12, 13; p. 24432-24448, 2021.

37. WANG, J.; BARDELLI, M.; ESPINOSA, D.A.; PEDOTTI, M.; THIAM-SENG, N.G.; BIANCHI, S.; SIMONELLI, L.; LIM, E.X.Y.; FOGLIERINI, M.; ZATTA, F.; JACONI, S.; BELTRAMELLO, M.; CAMERONI, E.; FIBRIANSAH, G.; SHI, J.; BARCA, T.; PAGANI, I.; RUBIO, A.; BROCCOLI, V.; VICENZI, E.; GRAHAM, V.; PULLAN, S.; DOWALL, S.; HEWSON, R.; JURT, S.; ZERBE, O.; STETTLER, K.; VECCHIA, A.L.; SALLUSTO, F.; CAVALLI, A.; HARRIS, E.; SHEE-MEI, L.; VARANI, L.; CORTI, D. A Human Bi-specific Antibody against Zika Virus with High Therapeutic Potential, **Cell**, 171, 15, 1, p. 229-241, 2017.

38. WU, Y.; WANG, F.; SHEN, C.; PENG, W.; LI, D.; ZHAO, C.; LI, Z.; LI, S.; BI, Y.; YANG, Y.; GONG, Y.; XIAO, H.; FAN, Z.; TAN, S.; WU, G.; TAN, W.; LU, X.; FAN, C.; WANG, Q.; LIU, Y.; ZHANG, C.; QI, J.; GAO, G.F.; GAO, F.; LIU, L. A noncompeting pair of human neutralizing antibodies block COVID-19 virus binding to its receptor ACE2. **Science**, 368, p.1274-1278, 2020.

39. DEJNIRATTISAI, W.; WONGWIWAT, W.; SUPASA, S.; ZHANG, X.; DAI, X.; ROUVINSKI, A.; JUMNAINSONG, A.; EDWARDS, C.; QUYEN, N.T.H.; DUANGCHINDA, T.; GRIMES, J.M.; TSAI, W.Y.; LAI, C.Y.; WANG, W.K.; MALASIT, P.; FARRAR, J.; SIMMONS, C.P.; ZHOU, Z.H.; REY, F.A.; MONGKOLSAPAYA, J.; SCREATON, G.R. A new class of highly potent, broadly neutralizing antibodies isolated from viremic patients infected with dengue virus. **Nat Immunol**, 16, p. 170–177, 2015.

40. ROBINSON, W. Sequencing the functional antibody repertoire—diagnostic and therapeutic discovery. **Nat Rev Rheumatol.,** 11, p. 171–182, 2015.

41. TAN, Y.C.; KONGPACHITH, S.; BLUM, L.K.; JU, C.H.; LAHEY, L.J.; LU, D.R.; CAI, X.; WAGNER, C.A.; LINDSTROM, T.M.; SOKOLOVE, J.; ROBINSON, W.H. Barcode-enabled sequencing of plasmablast antibody repertoires in rheumatoid arthritis. **Arthritis Rheumatol.**, 66, 10, p. 2706-15, 2014.

42. LAVINDER, J.J.; WINE, Y.; GIESECKE, C.; IPPOLITO, G.C.; HORTON, A.P.; LUNGU, O.I.; HOI, K.H.; DEKOSKY, B.J.; MURRIN, E.M.; WIRTH, M.M.; ELLINGTON, A.D.; DÖRNER, T.; MARCOTTE, E.M.; BOUTZ, D.R.;

GEORGIOU, G. Identification and characterization of the constituent human serum antibodies elicited by vaccination. **Proc Natl Acad Sci**, 11, 111, 6, p. 2259-64, 2014.

43. MCDANIEL, J.R.; DEKOSKY, B.J.; TANNO, H.; ELLINGTON, A.D.; GEORGIOU, G. Ultra-high-throughput sequencing of the immune receptor repertoire from millions of lymphocytes. **Nat Protoc.**, 11, 3, p. 429-42, 2016.

44. TANNO, H.; MCDANIEL, J.R.; STEVENS, C.A.; VOSS, W.N.; LI, J.; DURRETT, R.; LEE, J.; GOLLIHAR, J.; TANNO, Y.; DELIDAKIS, G.; POTHUKUCHY, A.; ELLEFSON, J.W.; GORONZY, J.J.; MAYNARD JA, ELLINGTON, A.D.; IPPOLITO, G.C.; GEORGIOU, G. A facile technology for the high-throughput sequencing of the paired VH:VL and TCRβ:TCRα repertoires. **Sci Adv.**, 22, 6, 17, 2020.

45. PRABAKARAN, P.; GLANVILLE, J.; IPPOLITO, G.C. Editorial: Next-Generation Sequencing of Human Antibody Repertoires for Exploring B-cell Landscape, Antibody Discovery and Vaccine Development. **Front Immunol.**, 11, 1344, 2020.

46. GALSON, J.D.; POLLARD, A.J.; TRÜCK, J.; DOMINIC, F. K. Studying the antibody repertoire after vaccination: practical applications, **Trends in Immunology,** 35, 7, p. 319-331, 2014.

47. GUO, S.; ZHENG, Y.; GAO, Z.; DUAN, M.; LIU, S.; DU, P.; XU, X.; XU, K.; ZHAO, X.; CHAI, Y.; WANG, P.; ZHAO, Q.; GAO, G.F.; DAI, L. Dosing interval regimen shapes potency and breadth of antibody repertoire after vaccination of SARS-CoV-2 RBD protein subunit vaccine. **Cell Discov.**, 28, 9, 1, 79, 2023.

48. WEC, A.Z.; HASLWANTER, D.; ABDICHE, Y.N.; SHEHATA L; PEDREÑO-LOPEZ, N.; MOYER, C.L.; BORNHOLDT, Z.A.; LILOV, A.; NETT, J.H.; JANGRA, R.K.; BROWN, M.; WATKINS, D.I.; AHLM, C.; FORSELL, M.N.; REY, F.A.; BARBA-SPAETH, G.; CHANDRAN, K.; WALKER, L.M. Longitudinal dynamics of the human B cell response to the yellow fever 17D vaccine. **Proc Natl Acad Sci**, 117, 12, p. 6675-6685, 2020.

49. MAI, G.; ZHANG, C.; LAN, C.; ZHANG, J.; WANG, Y.; TANG, K.; TANG, J.; ZENG, J.; CHEN, Y.; CHENG, P.; LIU, S.; WEN, H.Q.; LI, A.; LIU, X.; ZHANG, R.; XU, S.; LIU, L.; NIU, Y.; YANG, L.; WANG, Y.; YIN, D.; SUN, C.; CHEN, Y.Q.; SHEN, W.; ZHANG, Z.; DU, X. Characterizing the dynamics of BCR repertoire from repeated influenza vaccination, **Emerging Microbes & Infections**, 12, 2, 2023.

50. ZHANG, Y.; YAN, Q.; LUO, K.; HE, P.; HOU, R.; ZHAO, X.; WANG, Q.; YI, H.; LIANG, H.; DENG, Y.; HU, F.; LI, F.; LIU, X.; FENG, Y.; LI, P.; QU, L.; CHEN, Z.; PAN-HAMMARSTRÖM, Q.; FENG, L.; NIU, X.; CHEN, L. Analysis of B Cell Receptor Repertoires Reveals Key Signatures of the Systemic B Cell Response after SARS-CoV-2 Infection. **J Virol.**, 96, 4, 2022.

51. RAVICHANDRAN, S.; HAHN, M.; BELAUNZARÁN-ZAMUDIO, P.F.; RAMOS-CASTAÑEDA, J.; NÁJERA-CANCINO, G.; CABALLERO-SOSA, S.; NAVARRO-FUENTES, K.R.; RUIZ-PALACIOS, G.; GOLDING, H.; BEIGEL, J.H.; KHURANA, S. Differential human antibody repertoires following Zika infection and the implications for serodiagnostics and disease outcome. **Nat Commun.,** 10, 1, 2019.

52. CORRIE, B.D.; MARTHANDAN, N.; ZIMONJA, B.; JAGLALE, J.; ZHOU, Y.; BARR, E.; KNOETZE, N.; BREDEN, F.M.W.; CHRISTLEY, S.; SCOTT, J.K.; COWELL, L.G.; BREDEN, F. iReceptor: a platform for querying and analyzing antibody/B-cell and T-cell receptor repertoire data across federated repositories Immunol. **Rev**, 284, p. 24-41, 2018.

53. CHRISTLEY, S.; SCARBOROUGH, W.; SALINAS, E.; ROUNDS, W. H.; TOBY, I.T. ; FONNER, J. M.; MIKHAIL, L.K.; MIN, K.; MOCK, S. A.; CHRISTOPHER J.; OSTMEYER, J.; BUNTZMAN, A.; RUBELT, F.; MARCO, D. L.; MONSON, N. L.; SCHEUERMANN, R. H.; LINDSAY, C. G.VDJServer: A cloud-based analysis portal and data commons for immune repertoire sequences and rearrangements. **Front. Immunol**, 9, p. 976, 2018.

54. ABANADES, B.; OLSEN, T.H.; RAYBOULD, M.I.J.; AGUILAR-SANJUAN, B.; WONG, W.K.; GEORGES, G.; BUJOTZEK, A,; DEANE, C.M. The Patent and Literature Antibody Database (PLAbDab): an evolving reference set of functionally diverse, literature-annotated antibody sequences and structures. **Nucleic Acids Research**, 52, D1, p. D545–D551, 2024.

55. ROSENFELD, A.M.; MENG, W.; LUNING, E.T.; PRAK, U.; HERSHBERG. ImmuneDB, a novel tool for the analysis, storage, and dissemination of immune repertoire sequencing data. **Front. Immunol**, 9, p. 2107, 2018.

56. JILG, W.; SCHMIDT, M.; DEINHARDT, F. Vaccination against hepatitis B: comparison of three different vaccination schedules. **J Infect Dis.** 160, 5, p. 766-9, 1989.

57. WEN, G.P.; HE, L.; TANG, Z.M.; WANG, S.L.; ZHANG, X.; CHEN, Y.Z.; LIN, X.; LIU, C.; CHEN, J.X.; YING, D.; CHEN, Z.H.; WANG, Y.B.; LUO, W.X.; HUANG, S.J.; LI, S.W.; ZHANG, J.; ZHENG, Z.Z.; ZHU, J.; XIA, N.S. Quantitative evaluation of protective antibody response induced by hepatitis E vaccine in humans. **Nat Commun.,** 11, 1, 2020.

58. THEILER, M.; SMITH, H.H. The use of yellow fever virus modified by *in vitro* cultivation for human immunization. **J Exp Med.,** v.65, n.6, p.787-800, 1937.

59. LEE, E.; LOBIGS, M. E protein domain III determinants of yellow fever virus 17D vaccine strain enhance binding to glycosaminoglycans, impede virus spread, and attenuate virulence. **Journal of Virology**, v. 82, n. 12, p. 6024–6033, 2008.

60. POLAND, J.D.; CALISHER, C.H.; MONATH, T.P.; DOWNS, W.G.; MURPHY, K. Persistence of neutralizing antibody 30- 35 years after

immunization with 17D yellow fever vaccine. **Bulletin of the World Health Organization**, v.59, n. 6, p.895-900, 1981.

61. MUDD, P.A.; PIASKOWSKI, S.M.; NEVES, P.C.; RUDERSDORF, R.; KOLAR, H.L.; EERNISSE, C.M.; WEISGRAU, K.L.; DE SANTANA, M.G.; WILSON, N.A.; BONALDO, M.C.; GALLER, R.; RAKASZ, E.G.; WATKINS, D.I. The live-attenuated yellow fever vaccine 17D induces broad and potent T cell responses against several viral proteins in Indian rhesus macaques—implications for recombinant vaccine design. **Immunogenetics**, v.62, 127, p. 593–600, 2010.

62. CAMPI-AZEVEDO, A.C.; DE ALMEIDA, E. P.; COELHO-DOS-REIS, J.G.; PERUHYPE-MAGALHÃES, V.; VILLELA-REZENDE, G.; QUARESMA, P.F.; MAIA, M.D.E. L.; FARIAS, R.H.; CAMACHO, L.A.; FREIRE, M.D.A. S.; GALLER, R.; YAMAMURA, A.M.; ALMEIDA, L.F.; LIMA, S.M.; NOGUEIRA, R.M.; SILVA SÁ, G.R.; HOKAMA, D.A.; DE CARVALHO, R.; FREIRE, R.A.; FILHO, E.P.; LEAL, M.D.A. L.; HOMMA, A.; TEIXEIRA-CARVALHO, A.; MARTINS, R.M.; MARTINS-FILHO, O.A. Subdoses of 17DD yellow fever vaccine elicit equivalent virological/immunological kinetics timeline. **BMC Infect Dis.**, 15, 14, 391, 2014.

63. PULENDRAN, B. Learning immunology from the yellow fever vaccine: innate immunity to systems vaccinology. **Nat Rev Immunol,** 9, p. 741–747, 2009.

64. BRANDRISS, M.W.; SCHLESINGER, J.J.; WALSH, E.E.; BRISELLI, M. Lethal 17D Yellow Fever Encephalitis in Mice. I. Passive Protection by Monoclonal Antibodies to the Envelope Proteins of 17D Yellow Fever and Dengue 2 Viruses. **J. gen. Virol.,** v. 67, p. 229-234, 1986.

65. BECK, A.S.; BARRET, A.D. Current status and future prospects of yellow fever vaccines. **Expert Review of Vaccines,** v.14, n.11, p. 1479–1492, 2015.

66. FERREIRA CC, CAMPI-AZEVEDO AC, PERUHYPE-MAGALHĀES V, COSTA-PEREIRA C, ALBUQUERQUE CP, MUNIZ LF, YOKOY DE SOUZA T, OLIVEIRA ACV, MARTINS-FILHO OA, DA MOTA LMH. The 17D-204 and 17DD yellow fever vaccines: an overview of major similarities and subtle differences. **Expert Rev Vaccines**., 17, 1, p.79-90, 2017.

67. CAMACHO, L. A. B.; FREIRE, M. DA S.; LEAL, M. DA L. F.; AGUIAR, S. G. DE .; NASCIMENTO, J. P. DO .; IGUCHI, T.; LOZANA, J. DE A.; FARIAS, R. H. G. Immunogenicity of WHO-17D and Brazilian 17DD yellow fever vaccines: a randomized trial. **Revista De Saúde Pública**, 38, 5, p.671–678, 2004.

68. BARBAN, V.; GIRERD, Y.; AGUIRRE, M.; GULIA, S.; PÉTIARD, F.; RIOU, P.; BARRERE, B.; LANG, J. High stability of yellow fever 17D-204 vaccine: a 12-year restrospective analysis of large-scale production. **Vaccine**, 25, 15, p. 2941-50, 2007.

69. COLLABORATIVE GROUP FOR STUDIES ON YELLOW FEVER

VACCINES. Duration of immunity in recipients of two doses of 17DD yellow fever vaccine. **Vaccine.**, 37, 35, p. 5129-5135, 2019.

70. KAREKO, B.W.; BOOTY, B.L.; NIX, C.D.; LYSKI, Z.L.; SLIFKA, M.K.; AMANNA, I.J.; MESSER, W.B. Persistence of Neutralizing Antibody Responses Among Yellow Fever Virus 17D Vaccinees Living in a Nonendemic Setting. **J Infect Dis.,** 221, 12, p. 2018-2025, 2020.

71. CAMPI-AZEVEDO, A.C.; PERUHYPE-MAGALHÃES, V.; COELHO-DOS-REIS, J.G.; ANTONELLI, L.R.; COSTA-PEREIRA, C.; SPEZIALI, E.; REIS, L.R.; LEMOS, J.A.; RIBEIRO, J.G.L.; BASTOS CAMACHO, L.A.; DE SOUSA MAIA, M.L.; BARBOSA DE LIMA, S.M.; SIMÕES, M.; DE MENEZES MARTINS, R.; HOMMA, A.; COTA MALAQUIAS, L.C.; TAUIL, P.L.; COSTA VASCONCELOS, P.F.; MARTINS ROMANO, A.P.; DOMINGUES, C.M.; TEIXEIRA-CARVALHO, A.; MARTINS-FILHO, O.A.; COLLABORATIVE GROUP FOR STUDIES OF YELLOW FEVER VACCINE. 17DD Yellow Fever Revaccination and Heightened Long-Term Immunity in Populations of Disease-Endemic Areas, Brazil. **Emerg Infect Dis.,** 25, 8, p. 1511-1521, 2019.

72. DE MELO, A.B.; DA SILVA, M.D.A. P.; MAGALHÃES, M.C.; GONZALES GIL, L.H.; FREESE DE CARVALHO, E.M.; BRAGA-NETO, U.M.; BERTANI, G.R.; MARQUES, E.T.J.R.; CORDEIRO, M.T. Description of a prospective 17DD yellow fever vaccine cohort in Recife, Brazil. **Am J Trop Med Hyg.,** 85, 4, p. 739-47, 2011.

73. REINHARDT, B.; JASPERT, R.; NIEDRIG, M.; KOSTNER, C.; L'AGE-STEHR, J. Development of viremia and humoral and cellular parameters of immune activation after vaccination with yellow fever virus strain 17D: a model of human flavivirus infection. **J Med Virol.**, 56, 2, p.159-67, 1998.

74. CAMPI-AZEVEDO, A.C.; COSTA-PEREIRA, C.; ANTONELLI, L.R.; FONSECA, C.T.; TEIXEIRA-CARVALHO, A.; VILLELA-REZENDE, G.; SANTOS, R.A.; BATISTA, M.A.; CAMPOS, F.M.; PACHECO-PORTO, L.; MELO JÚNIOR, O.A.; HOSSELL, D.M.; COELHO-DOS-REIS, J.G.; PERUHYPE-MAGALHÃES, V.; COSTA-SILVA, M.F.; DE OLIVEIRA, J.G., FARIAS, R.H.; NORONHA, T.G.; LEMOS, J.A.; VON DOELLINGER, V.D.O.S. R.; SIMÕES, M.; DE SOUZA, M.M.; MALAQUIAS, L.C.; PERSI, H.R.; PEREIRA, J.M.; MARTINS, J.A.; DORNELAS-RIBEIRO, M.; VINHAS, A.D.E. A.; ALVES, T.R.; MAIA, M.D.E. L.; FREIRE, M.D.A. S.; MARTINS, R.D.E. M.; HOMMA, A.; ROMANO, A.P.; DOMINGUES, C.M.; TAUIL, P.L.; VASCONCELOS, P.F.; RIOS, M.; CALDAS, I.R.; CAMACHO, L.A.; MARTINS-FILHO, O.A. Booster dose after 10 years is recommended following 17DD-YF primary vaccination. **Hum Vaccin Immunother**,12, 2, p. 491-502, 2016.

75. DOUAM, F.; PLOSS, A. Yellow fever virus: Knowledge gaps impeding the fightagainst an old foe. **Trends Microbiol.**, v.26, n.11, p. 913–928, 2018.

76. HUBER, J.E.; AHLFELD, J.; SCHECK, M.K.; ZAUCHA, M.; WITTER, K.;

LEHMANN, L.; KARIMZADEH, H.; PRITSCH, M.; HOELSCHER, M.; VON SONNENBURG, F.; DICK, A.; BARBA-SPAETH, G.; KRUG, A.B.; ROTHENFUßER, S.; BAUMJOHANN, D. Dynamic changes in circulating T follicular helper cell composition predict neutralising antibody responses after yellow fever vaccination. **Clin Transl Immunology**, 9, 5, 2020.

77. MONATH, T. P. C. Neutralizing Antibody Responses in the Major Immunoglobulin Classes to Yellow Fever 17D Vaccination of Humans. **AmericanJournal of Epidemiology**, v.93, n.2, p.122–129, 1971.

78. GIBNEY, K.B.; KOSOY, O.I.; FISCHER, M.; EDUPUGANTI, S.; LANCIOTTI, R.S.; DELOREY, M.J.; STAPLES, J.E.; PANELLA, A.J.; MULLIGAN, M.J. Detection of Anti-Yellow Fever Virus Immunoglobulin M Antibodies at 3–4 Years Following Yellow Fever Vaccination. **Am. J. Trop. Med. Hyg.**, 87, p. 1112–1115, 2012.

79. SINGH, T.; HWANG, K.K.; MILLER, A.S.; JONES, R.L.; LOPEZ, C.A.; DULSON, S.J.; GIUBERTI, C.; GLADDEN, M.A.; MILLER, I.; WEBSTER, H.S.; EUDAILEY, J.A.; LUO, K.; VON HOLLE, T.; EDWARDS, R.J.; VALENCIA, S.; BURGOMASTER, K.E.; ZHANG, S.; MANGOLD, J.F., TU, J.J.; DENNIS, M.; ALAM, S.M.; PREMKUMAR, L.; DIETZE, R.; PIERSON, T.C.; OOI, E.E.; LAZEAR, H.M.; KUHN, R.J.; PERMAR, S.R.; BONSIGNORI, M. A Zika virus-specific IgM elicited in pregnancy exhibits ultrapotent neutralization. **Cell**.,185, 25, p.4826-4840, 2022.

80. BARRETT, A.D.T.; TEUWEN, D. Yellow fever vaccine—how does it work and why do rare cases of serious adverse events take place? **Curr Opin Immunol.**, 21, p. 1–6, 2009.

81. PIERSON, T.C.; FREMONT, D.H.; KUHN, R.J.; DIAMOND, M.S. Structural insights into the mechanisms of antibody-mediated neutralization of flavivirus infection: implications for vaccine development. **Cell Host Microbe**., 4, 3, p. 229-38, 2008.

82. THEILER, M.; SMITH, H. H. The effect of prolonged cultivation *in vitro* upon the pathogenicity of yellow fever virus. **J. Exp. Med.**, 65, p. 767–786, 1937.

83. WHO. **Fractional Dose Yellow Fever Vaccine as a Dose-Sparing Option for Outbreak Response.** [2016]. Available in: https://apps.who.int/iris/bitstream/handle/10665/246236/WHO-YFSAGE-16.1 eng.pdf;jsessionid= 3A0B32C4DACAA3D0BFAEE1A4FF0A609F?sequence=1 Accessed in 23rd Mar 2024.

84. GUBLER, D.J. Human Arbovirus Infections Worlwide. **Ann. N. Y. Acad. Sci.,** 951, p. 13–24, 2001.

85. VASCONCELOS, P. Yellow Fever in Brazil: Thoughts and Hypotheses on the Emergence in Previously Free Areas. **Rev. Saude Publica,** 44, p. 1144–1149, 2010.

86. DE OLIVEIRA FIGUEIREDO, P.; STOFFELLA-DUTRA, AG; BARBOSA COSTA, G; SILVA DE OLIVEIRA, J; DOURADO AMARAL, C; DUARTE SANTOS, J; SOARES ROCHA, KL; ARAÚJO JÚNIOR, J.P; LACERDA NOGUEIRA, M; ZAZÁ BORGES, M.A; PEREIRA PAGLIA, A.; DESIREE LABEAUD, A.; SANTOS ABRAHÃO, J; GEESSIEN KROON, E; BRETAS DE OLIVEIRA, D; PAIVA DRUMOND, B; DE SOUZA TRINDADE, G. Re-Emergence of Yellow Fever in Brazil during 2016-2019: Challenges, Lessons Learned, and Perspectives. **Viruses**, 12, 11, 1233, 2020.

87. BRASIL. Ministério da Saúde. **Monitoramento do período sazonal da febre amarela Brasil 2017/2018.** [2018]. Available in: http://portalarquivos2.saude.gov.br/images/pdf/2018/outubro/08/Informe-FA.pdf Accessed in 23rd Mar 2024.

88. BRASIL. Ministério da Saúde. **Monitoramento de Febre Amarela Brasil 2019 -informe nº 18**. Secretaria de Vigilância em Saúde. [2019]. Available in: https://portalarquivos2.saude.gov.br/images/pdf/2019/junho/13/Informe-de-Monitoramento-de-Febre-Amarela-Brasil%2D%2Dn-18.pdf Accessed in 23rd Mar 2024.

89. BRASIL. Ministério da Saúde. **Situação epidemiológica da febre amarela no monitoramento 2020/2021**. [2021/2022]. Available in: https://gov.br/saude/pt-br/centraisdeconteudo/publicacoes/boletins/boletinsepidemiologicos/edicoes/2021/boletim_epidemiologico_svs_31.pdf Accessed in 23rd Mar 2024.

90. SECRETARIA DE SAÚDE DE MINAS GERAIS. **Febre Amarela.** [2022]. Available in: https://saude.mg.gov.br/febreamarela Accessed in: 23rd Mar 2024.

91. ANDRADE, M.S.; CAMPOS, F.S.; CAMPOS, A.A.S.; ABREU, F.V.S.; MELO, F.L.; SEVÁ, A.D.P.; CARDOSO, J.D.C.; DOS SANTOS, E.; BORN, L.C.; SILVA, C.M.D.D.; MÜLLER, N.F.D.; OLIVEIRA, C.H.; SILVA, A.J.J.D.; SIMONINI-TEIXEIRA, D.; BERNAL-VALLE S, MARES-GUIA, M.A.M.M.; ALBUQUERQUE, G.R.; ROMANO, A.P.M.; FRANCO, A.C.; RIBEIRO, B.M.; ROEHE, P.M.; ALMEIDA, M.A.B. Real-Time Genomic Surveillance during the 2021 Re-Emergence of the Yellow Fever Virus in Rio Grande do Sul State, Brazil. **Viruses,** 13, 10, 1976, 2021

92. BRASIL. Ministério da Saúde/Secretaria de Vigilância em Saúde**. Informe quinzenal sarampo - Brasil, semanas epidemiológicas 43 de 2020 a 1 de 2021**. [2021]. Available in: https://www.gov.br/saude/ptbr/centraisdeconteudo/publicacoes/boletins/epidemiologicos/edicoes/2021/boletim_epidemiologico_svs_4.pdf. Accessed in 23rd Mar 2024.

93. BRASIL. Ministério da Saúde/Secretaria de Vigilância em Saúde. **Monitoramento dos casos de arboviroses até a semana epidemiológica 29 de 2022.** [2022]. Available in: https://www.gov.br/saude/pt-br/centrais-de-conteudo/publicacoes/boletins/epidemiologicos/edicoes/2022/boletim-epidemiologico-vol-53-no29. Accessed in: 23rd Mar 2024.

94. BRASIL. Ministerio da Saúde/Secretaria de Vigilância em Saúde. **Nota informativa conjunta nº 2/2024 - DEDT/DPNI/DEMSP.** [2024]. Available in: https://www.gov.br/saude/pt-br/centrais-de-conteudo/publicacoes/estudos-e-notas-informativas/2024/nota-informativa-conjunta-alerta-sobre-febre-amarela.pdf Accessed in: 23rd Mar 2024.

95. SILVA, N.I.O.; SACCHETTO, L.; DE REZENDE, I. M.; TRINDADE, G. S.; LABEAUD, A.D.; DE THOISY, B.; DRUMOND, B.P.Recent sylvatic yellow fever virus transmission in Brazil: the news from an old disease. **Virology Journal**, 9, 17, 1, 2020.

96. PAN AMERICAN HEALTH ORGANIZATION / WHO**. Epidemiological Update.** Yellow fever in the Region of the Americas. [2024]. Available in: www.paho.org/documents/ 2024-march-21-phe-epi-updateyellow-feveren_0-1 Accessed: 24th July 2024.

97. DELATORRE, E.; SANTOS DE ABREU, F. V.; RIBEIRO, I. P.; GÓMEZ, M. M.; CUNHA DOS SANTOS, A. A.; FERREIRA-DE-BRITO, A.; SEBASTIÃO ALBERTO SANTOS NEVES, M.; BONELLY, I. ; DE MIRANDA, R. M.; FURTADO, N. D.; RAPHAEL, L. M. S.; DE FÁTIMA FERNANDES DA SILVA, L.; DE CASTRO, M. G.; RAMOS, D. G.; MARTINS ROMANO, A. P.; KALLÁS, E. G.; VICENTE, A. C. P.; BELLO, G.; LOURENÇO-DE-OLIVEIRA, R.; BONALDO, M. C. Distinct YFV lineages co-circulated in the central-western and Southeastern Brazilian regions from 2015 to 2018. **Front. Microbiol.,** 10, 1079, 2019.

98. GIOVANETTI, M.; DE MENDONÇA, M. C. L. ; FONSECA, V.; MARES-GUIA, M. A. ; FABRI, A.; XAVIER, J.; DE JESUS, J. G.; GRÄF, T.; DOS SANTOS RODRIGUES, C. D.; DOS SANTOS, C. C.; SAMPAIO, S. A.; CHALHOUB, F. L. L.; DE BRUYCKER NOGUEIRA, F.; THEZE, J.; ROMANO, A. P. M. ; RAMOS, D. G.; DE ABREU, A. L.; OLIVEIRA, W. K.; DO CARMO SAID, R. F.; DE ALBURQUE, C. F. C.; DE OLIVEIRA, T.; FERNANDE, S. F. AGUIAR, C. A.; CHIEPPE, A.; SEQUEIRA, P. C.; FARIA, N. R.; CUNHA, R. V. ; ALCANTARA, L. C. J. ; DE FILIPPIS, A. M. B. Yellow fever virus reemergence and spread in Southeast Brazil, 2016–2019. **J. Virol.,** 94, 2019.

99. HASLWANTER, D.; LASSO, G.; WEC, A.Z.; FURTADO, N.D.; RAPHAEL, L.M.S.; TSE, A.L.; SUN, Y.; STRANSKY, S.; PEDREÑO-LOPEZ, N.; CORREIA, C.A.; BORNHOLDT, Z.A.; SAKHARKAR, M.; AVELINO-SILVA, V.I.; MOYER, C.L.; WATKINS, D.I.; KALLAS, E.G.; SIDOLI, S.; WALKER, L.M.; BONALDO, M.C.; CHANDRAN, K. Genotype-specific features reduce the susceptibility of South American yellow fever virus strains to vaccine-induced antibodies. **Cell Host Microbe**, 30, 2, p. 248-259, 2022.

100. VASCONCELOS, P.F.; BRYANT, J.E.; DA ROSA, T.P.; TESH, R.B.; RODRIGUES, S.G.; BARRETT, A.D. Genetic divergence and dispersal of yellow fever virus. **Emerg Infect Dis.,** v.10, n.9, p. 1578-84, 2004.

101. DE SOUZA, R.P.; FOSTER, P.G.; SALLUM, M.A.; COIMBRA, T.L.;

MAEDA, A.Y.; SILVEIRA, V.R.; MORENO, E.S.; DA SILVA, F.G.; ROCCO, I.M.; FERREIRA, I.B.; SUZUKI, A.; OSHIRO, F.M.; PETRELLA, S.M.; PEREIRA, L.E.; KATZ, G.; TENGAN, C.H.; SICILIANO, M.M.; DOS SANTOS, C.L. Detection of a new yellow fever virus lineage within the South American genotype I in Brazil. **J Med Virol.,** v.82, n.1, p. 175-185, 2010.

102. NUNES, M.R.; PALACIOS, G.; CARDOSO, J.F.; MARTINS, L.C.; SOUSA, E.C. JR.; DE LIMA, C.P.; MEDEIROS, D.B.; SAVJI, N.; DESAI, A.; RODRIGUES, S.G.; CARVALHO, V.L.; LIPKIN, W.I.; VASCONCELOS, P.F. Genomic and phylogenetic characterization of Brazilian yellow fever virus strains. **J Virol.,** v.86, n.24, p. 13263-13271, 2012.

103. BONALDO, M.C.; GÓMEZ, M.M.; DOS SANTOS, A.A.; ABREU, F.V.S.; FERREIRA-DE-BRITO, A.; MIRANDA, R.M.; CASTRO, M.G.; LOURENÇO-DE-OLIVEIRA, R. Genome analysis of yellow fever virus of the ongoing outbreak in Brazil reveals polymorphisms. **Mem Inst Oswaldo Cruz**, v. 112, n.6, p. 447-451, 2017.

104. GÓMEZ, M.M.; ABREU, F.V.S.; SANTOS, A.A.C.D; MELLO, I.S.; SANTOS, M.P; RIBEIRO, I.P.; FERREIRA-DE-BRITO, A.; MIRANDA, R.M.; CASTRO, M.G.; RIBEIRO, M.S.; LATERRIÈRE JUNIOR, R.D.C.; AGUIAR, S.F.; MEIRA, G.L.S.; ANTUNES, D.; TORRES, P.H.M.; MIR, D.; VICENTE, A.C.P.; GUIMARÃES, A.C.R.; CAFFARENA, E.R.; BELLO, G.; LOURENÇO-DE-OLIVEIRA, R.; BONALDO, M.C. Genomic and structural features of the yellow fever virus fromthe 2016-2017 Brazilian outbreak. **J Gen Virol.**, v. 99, n. 4, p. 536-548, 2018.

105. COLLINS, N.D.; BARRETT, A.D.T. Live Attenuated Yellow Fever 17D Vaccine: A Legacy Vaccine Still Controlling Outbreaks In Modern Day. **Curr Infect Dis Rep.,** v.19, n. 3, p. 1-9, 2017.

106. AMRAOUI, F; VAZEILLE, M; FAILLOUX, AB. French *Aedes albopictus* are ableto transmit yellow fever virus. **Eurosurveillance**, v.21, p. 14–16, 2016.

107. MONATH, T. P. Yellow fever: an update. **The Lancet Infectious Diseases,** v. 1,n.1, p. 11–20, 2001.

108. DHIMAN, G.; ABRAHAM, R.; GRIFFIN, D.E. Human Schwann cells are susceptible to infection with Zika and yellow fever viruses, but not dengue virus. **Scientific Reports**, v. 9, n 9951, 2019.

109. LIPRANDI, F.; WALDER, R. Replication of virulent and attenuated strains of yellow fever virus in human monocytes and macrophage-like cells (U937). **Arch Virol.,**v.76, n.1, p. 51-61, 1983.

110. FERNANDEZ-GARCIA , M.D.; MEERTENS, L.; CHAZAL, M.; HAFIRASSOU, M.L.; DEJARNAC, O.; ZAMBORLINI, A.; DESPRES, P.; SAUVONNET, N.; ARENZANA-SEISDEDOS, F.; JOUVENET, N.; AMARA, A. Vaccine and Wild-Type Strains of Yellow Fever Virus Engage Distinct Entry Mechanisms and Differentially Stimulate Antiviral Immune Responses. **Mbio.,**

v.7, n. 1, 2016.

111. INGELBEEN, B.; WEREGEMERE, N.A.; NOEL, H.; TSHAPENDA, G.P.; MOSSOKO, M.; NSIO, J.; RONSSE, A.; AHUKA-MUNDEKE, S.; COHUET, S.; KEBELA, B.I. Urban yellow fever outbreak—Democratic Republic of the Congo, 2016: Towards more rapid case detection. **PLoS Negl Trop Dis.**, v.12, n.12, 2018.

112. QUARESMA, J.A.; PAGLIARI, C; MEDEIROS, D.B.; DUARTE, M.I.; VASCONCELOS, P.F. Immunity and immune response, pathology and pathologic changes: progress and challenges in the immunopathology of yellow fever. **Rev Med Virol**., 23, 5, p. 305-18, 2013.

113. LOPES, R.L.; PINTO, J.R.; SILVA JUNIOR, G.B.D.; SANTOS, A.K.T.; SOUZA, M.T.O.; DAHER, E.F. Kidney involvement in yellow fever: a review. **Rev Inst Med Trop**, 22, 61, 2019.

114. KALLAS, E.G.; D'ELIA ZANELLA, L.G.F.A.B.; MOREIRA, C.H.V.; BUCCHERI, R.; DINIZ, G.B.F.; CASTIÑEIRAS, A.C.P.; COSTA, P.R.; DIAS, J.Z.C.; MARMORATO, M.P.; SONG, A.T.W.; MAESTRI, A.; BORGES, I.C.; JOELSONS, D.; CERQUEIRA, N.B.; SANTIAGO E SOUZA, N.C.; MORALES CLARO, I.; SABINO, E.C.; LEVI, J.E.; AVELINO-SILVA, V.I.; HO, Y.L. Predictors of mortality in patients with yellow fever: an observational cohort study. **Lancet Infect Dis.**, 19, 7, p.750-758, 2019.

115. NEVES, Y.C.S.; CASTRO-LIMA, V.A.C.; SOLLA, D.J.F.; OGATA, V.S.M.; PEREIRA, F.L.; ARAUJO, J.M; NASTRI, A.C.S.; HO, Y.L.; CHAMMAS, M.C. Staging liver fibrosis after severe yellow fever with ultrasound elastography in Brazil: A six-month follow-up study. **PLoS Negl Trop Dis**., 20, 15, 7, 2021.

116. VASCONCELOS, P.F.C. Febre Amarela. **Revista da Sociedade Brasileira deMedicina Tropical**, v.36, n.2, p. 275-293, 2003.

117. CAMPOS, R.K.; WONG, B.; XIE, X.; LU, Y.F.; SHI, P.Y.; POMPON, J.; GARCIA-BLANCO, M.A.; BRADRICK, S.S. RPLP1 and RPLP2 are essential *Flavivirus* host factors that promote early viral protein accumulation. **J Virol**, 91, 2017.

118. LE SOMMER, C.; BARROWS, N.J.; BRADRICK, S.S.; PEARSON, J.L.; GARCIA-BLANCO, M.A. G protein-coupled receptor kinase 2 promotes flaviviridae entry and replication. **PLoS Negl Trop Dis**, 6, 9, 2012.

119. CHU, J.J.; NG, M.L. Interaction of West Nile Virus with $\alpha_v\beta_3$ Integrin MediatesVirus Entry into Cells. **The Journal of Biological Chemistry**, v. 279, n. 52, p. 54533–54541, 2004.

120. TASSANEETRITHEP, B.; BURGESS, T.H.; GRANELLI-PIPERNO, A.; TRUMPFHELLER, C.; FINKE, J.; SUN, W.; ELLER, M.A.; PATTANAPANYASAT, K.; SARASOMBATH, S.; BIRX, D.L.; STEINMAN,

R.M; SCHLESINGER, S.; MAROVICH, M.A. DC-SIGN (CD209) mediates dengue virus infection of human dendritic cells. **J Exp Med**., 197, 7, p. 823-9, 2003.

121. MILLER, J.L.; DE WET, B.J.M.; MARTINEZ-POMARES, L.; RADCLIFFE, C.M.; DWEK, R.A.; RUDD, P.M.; GORDON, S. Correction: The Mannose Receptor Mediates Dengue Virus Infection of Macrophages. **PLoS Pathog.** , 4, 3, 2008.

122. DAS, S.; LAXMINARAYANA, S.V.; CHANDRA, N.; RAVI, V.; DESAI, A. Heat shock protein 70 on neuro2a cells is a putative receptor for japanese encephalitis virus. **Virology**, 385, p. 47-57, 2009.

123. SAKOONWATANYOO, P.; BOONSANAY, V.; SMITH, D.R. Growth and production of the Dengue Virus in C6/36 Cells and Identification of a Laminin-Binding Protein as a Candidate Serotype 3 and 4 Receptor Protein. **Intervirology**, v.49, n.3, p. 161–172, 2006.

124. CHEN, S.T.; LIU, R.S.; WU, M.F.; LIN, Y.L.; CHEN, S.Y.; TAN, D.T.; CHOU, T.Y.; TSAI, I.S.; LI, L.; HSIEH, S.L. CLEC5A Regulates japanese encephalitis virus-induced neuroinflammation and lethality. **PLoS Pathog.**, v.8, n.4, 2012.

125. MEERTENS, L.; CARNEC, X.; LECOIN, M.P.; RAMDASI, R.; GUIVEL-BENHASSINE, F.; LEW, E.; LEMKE, G.; SCHWARTZ,O.; AMARA, A. The TIM and TAM Families of Phosphatidylserine Receptors Mediate Dengue Virus Entry. **Cell Host & Microbe,** v. 12, p. 544–557, 2012.

126. KAUFMANN B.; ROSSMANN, M.G. Molecular mechanisms involved in the early steps of flavivirus cell entry. **Microbes Infect.,** v.13, n.1, p. 1–9, 2011.

127. CAMPOS, J.L.S.; MONGKOLSAPAYA, J.; SCREATON, G.R. The immune response against flaviviruses. **Nature Immunology**, v. 19, p. 1189–1198, 2018.

128. RAMANATHAN, H.N.; ZHANG, S.; DOUAM, F.; MAR, K.B.; CHANG, J.; YANG, P.L.; SCHOGGINS, J.W.; PLOSS, A.; LINDENBACH, B.D. A Sensitive Yellow Fever Virus Entry Reporter Identifies Valosin-Containing Protein (VCP/p97) as an Essential Host Factor for Flavivirus Uncoating. **Mbio**, v.11, n.2, 2020.

129. GEROLD, G.; BRUENING, J.; WEIGEL, B.; PIETSCHMANN, T. Protein Interactions during the Flavivirus and Hepacivirus Life Cycle. **Mol Cell Proteomics**.,16, 4, 2017.

130. APTE-SENGUPTA, S.; SIROHI, D.; KUHN, R.J. Coupling of replication and assembly in flaviviruses. **Curr. Opin. Virol.**, 9, p. 134–142, 2014.

131. ELSHUBER, S.; ALLISON, S.L.; HEINZ, F.X.;, MANDL, C.W. Cleavage of protein prM is necessary for infection of BHK-21 cells by tick-borne encephalitis virus. **J Gen Virol.** 84, p. 183-191, 2003.

132. STADLER, K.; ALLISON, S.L.; SCHALICH, J.; HEINZ, F.X. Proteolytic activation of tick-borne encephalitis virus by furin. **J Virol.**, 71, 11, p. 8475-81, 1997.

133. KUHN, R.J.; ZHANG, W.; ROSSMANN, M.G.; PLETNEV, S.V.; CORVER, J.; LENCHES, E.; JONES, C.T.; MUKHOPADHYAY, S.; CHIPMAN, P.R.; STRAUSS, E.G.; BAKER, T.S.; STRAUSS, J.H. Structure of dengue virus: implications for flavivirus organization, maturation, and fusion. **Cell**., 108, 5, p.717-25, 2002.

134. SIROHI, D.; CHEN, Z.; SUN, L.; KLOSE, T.; PIERSON, T.C.; ROSSMANN, M.G.; KUHN, R.J. The 3.8 Å resolution cryo-EM structure of Zika virus. **Science.**, 352, 6284, p. 467-70, 2016.

135. CHERRIER, M.V.; KAUFMANN, B.; NYBAKKEN, G.E.; LOK, S.M.; WARREN, J.T.; CHEN, B.R.; NELSON, C.A.; KOSTYUCHENKO, V.A.; HOLDAWAY, H.A.; CHIPMAN, P.R.; KUHN, R.J.; DIAMOND, M.S.; ROSSMANN, M.G.; FREMONT, D.H. Structural basis for the preferential recognition of immature flaviviruses by a fusion-loop antibody. **The EMBO Journal**, 28, p. 3269-3276, 2009.

136. PLEVKA, P.; BATTISTI, A.J.; JUNJHON, J.; WINKLER, D.C.; HOLDAWAY, H.A.; KEELAPANG, P.; SITTISOMBUT, N.; KUHN, R.J.; STEVEN, A.C.; ROSSMANN, M.G. Maturation of flaviviruses starts from one or more icosahedrally independent nucleation centres. **European Molecular Biology Organization Reports**,v. 12, n. 6, 2011.

137. YU, I.M.; ZHANG, W.; HOLDAWAY, H.A.; LI, L.; KOSTYUCHENKO, V.A.; CHIPMAN, P.R.; KUHN, R.J.; ROSSMANN, M.G.; CHEN, J. Structure of the immature dengue virus at low pH primes proteolytic maturation. **Science.**, 319, 5871, p. 1834-7, 2008.

138. ZHANG, X.; ZHANG, Y.; JIA, R.; WANG, M.; YIN, Z.; CHENG, A. Structure and function of capsid protein in flavivirus infection and its applications in the development of vaccines and therapeutics. **Vet Res.,** 52, 1, 98, 2021.

139. REY, F.A.; STIASNY, K.; HEINZ, F.X. Flavivirus structural heterogeneity: implications for cell entry. **Current Opinion in Virology**, 24, p. 132–139, 2017.

140. ZHANG, Y.; CORVER, J.; CHIPMAN, P.R.; ZHANG, W.; PLETNEV, S.V.; SEDLAK, D.; BAKER, T.S.; STRAUSS, J.H.; KUHN, R.J.; ROSSMANN, M.G. Structures of immature flavivirus particles. **EMBO J**., 22, p.2604–2613, 2003.

141. ZHANG, S.; HE, Y.; WU, Z.; WANG, M.; JIA, R.; ZHU, D.; LIU, M.; ZHAO, X.; YANG, Q.; WU, Y.; ZHANG, S.; HUANG, J.; OU, X.; GAO, Q.;

SUN, D.; ZHANG, L.; YU, Y.; CHEN, S.; CHENG, A. Secretory pathways and multiple functions of nonstructural protein 1 in flavivirus infection. **Front Immunol.,** 14, 2023.

142. WEN, J.; SHRESTA, S. Antigenic cross-reactivity between Zika and dengue viruses: is it time to develop a universal vaccine? **Curr. Opin. Immunol**., 59, p. 1–8, 2019.

143. MODHIRAN, N.; WATTERSON, D.; BLUMENTHAL, A.; BAXTER, A.G.; YOUNG, P.R.; STACEY, K.J. Dengue virus NS1 protein activates immune cells via TLR4 but not TLR2 or TLR6. **Immunol. Cell Biol.,** 95, p. 491–495, 2017.

144. MODHIRAN, N.; WATTERSON, D; MULLER, D.A.; PANETTA, A.K.; SESTER, D.P.; LIU, L.; HUME, D.A.; STACEY, K.J.; YOUNG, P.R. Dengue virus NS1 protein activates cells via Toll-like receptor 4 and disrupts endothelial cell monolayer integrity. **Sci. Transl. Med.,** 7, 2015.

145. VAN DEN ELSEN, K.; QUEK, J.P.; LUO, D. Molecular Insights into the Flavivirus Replication Complex. **Viruses**, *13*, 956, 2021.

146. ZHANG, H.L.; YE, H.Q.; LIU, S.Q.; DENG, C.L.; LI, X.D.; SHI, P.Y.; ZHANG, B. West Nile Virus NS1 antagonizes Interferon Beta production by targeting RIG-I and MDA5. **J Virol**., 91, 18, 2017.

147. LU, X.; XIAO, H.; LI, S.; PANG, X.; SONG, J.; LIU, S.; CHENG, H.; LI, Y.; WANG, X.; HUANG, C.; GUO, T.; TER MEULEN, J.; DAFFIS, S.; YAN, J.; DAI, L.; RAO, Z.; KLENK, H.D.; QI, J.; SHI, Y.; GAO, G.F. Double lock of a human neutralizing and protective monoclonal antibody targeting the yellow fever virus envelope. **Cell Reports**, 26, p. 438–446, 2019.

148. CRILL, W.D.; CHANG, G.-J.J. Localization and characterization of Flavivirus envelope glycoprotein cross-reactive epitopes. **Journal of Virology,** 2004.

149. DAI, L.; SONG, J.; LU, X.; DENG, Y.Q.; MUSYOKI, A.M.; CHENG, H.; ZHANG, Y.; YUAN, Y.; SONG, H.; HAYWOOD, J.; XIAO, H.; YAN, J.; SHI, Y.; QIN, C.F.; QI, J.; GAO, G.F. Structures of the zika virus envelope protein and its complex with aflavivirus broadly protective antibody. **Cell Host & Microbe**, 9, p. 696–704, 2016.

150. VENKATACHALAM, R.; SUBRAMANIYAN, V. Homology and conservation of amino acids in E-protein sequences of dengue serotypes. **Asian Pacific J. Trop. Dis.,** 4, p. 573–577, 2014.

151. STIASNY, K; KIERMAYR, S.; HOLZMANN, H.; HEINZ, F.X. Cryptic properties of a cluster of dominant flavivirus cross-reactive antigenic sites. **Journal of Virology**, v. 80, n. 19, p. 9557–9568, 2006.

152. PRIYAMVADA, L.; QUICKE, K.M.; HUDSON, W.H.; ONLAMOON, N.; SEWATANON, J.; EDUPUGANTI, S.; PATTANAPANYASAT, K.; CHOKEPHAIBULKIT, K.; MULLIGAN, M.J.; WILSON, P.C.; AHMED, R.; SUTHAR, M.S.; WRAMMERT, J. Human antibody responses after dengue virus infection are highly cross-reactive to Zika virus. **Proc Natl Acad Sci USA**. v.113, n.28, p. 852-7857, 2016.

153. STETTLER, K.; BELTRAMELLO, M.; ESPINOSA, D.A.; GRAHAM, V.; CASSOTTA, A.; BIANCHI, S.; VANZETTA, F.; MINOLA, A.; JACONI, S.; MELE, F.; FOGLIERINI, M.; PEDOTTI, M.; SIMONELLI, L.; DOWALL, S.; ATKINSON, B.; PERCIVALLE, E.; SIMMONS, C.P.; VARANI, L.; BLUM, J.; BALDANTI, F.; CAMERONI, E.; HEWSON, R.; HARRIS, E.; LANZAVECCHIA, A.; SALLUSTO, F.; CORTI, D. Specificity, cross-reactivity, and function of antibodies elicited by zika virus infection. **Science,** 353, 6301, p. 823–826, 2016.

154. CHAKRABORTY, S. Computational analysis of perturbations in the post-fusion dengue virus envelope protein highlights known epitopes and conserved residues in the zika virus. **F1000Research**, 5, 1150, 2016.

155. LI, L.; LOK, S.M.; YU, I.M.; ZHANG, Y.; KUHN, R.J.; CHEN, J.; ROSSMANN, M.G. The flavivirus precursor membrane-envelope protein complex: structure and maturation. **Science,** 319, 5871, p.1830-4, 2008.

156. DOWD, K.A.; SIROHI, D.; SPEER, S.D.; VANBLARGAN, L.A.; CHEN, R.E.; MUKHERJEE, S.; WHITENER, B.M.; GOVERO, J.; ALESHNICK, M.; LARMAN, B.; SUKUPOLVI-PETTY, S.; SEVVANA, M.; MILLER, A.S.; KLOSE, T.; ZHENG, A.; KOENIG, S.; KIELIAN, M.; KUHN, R.J.; DIAMOND, M.S.; PIERSON, T.C. prM-reactive antibodies reveal a role for partially mature virions in dengue virus pathogenesis. **Proc Natl Acad Sci**., 120, 3, 2023.

157. SUI, L.; ZHAO, Y.; WANG, W.; CHI, H.; TIAN, T.; WU, P.; ZHANG, J.; ZHAO, Y.; WEI, Z.K.; HOU, Z.; ZHOU, G.; WANG, G.; WANG, Z.; LIU, Q. Flavivirus prM interacts with MDA5 and MAVS to inhibit RLR antiviral signaling. **Cell Biosci**, 13, 9, 2023.

158. KUHN, R.J.; DOWD, K.A.; BETH POST, C.; PIERSON, T.C. Shake, rattle, and roll: impact of the dynamics of flavivirus particles on their interactions with the host. **Virology,** 479–480, p. 508-517, 2015.

159. DOWD, K.A.; PIERSON, T.C. The many faces of a dynamics virion: implications of viral breathing on flavivirus biology and immunogenicity. **Annu Rev Virol**., 5, p. 185–207, 2018.

160. FIBRIANSAH, G., LIM, X.N.; LOK, S.M. Morphological Diversity and Dynamics of Dengue Virus Affecting Antigenicity. **Viruses.** 13, 2021.

161. GOO, L.; DOWD, K.A.; SMITH, A.R.; PELC, R.S.; DEMASO, C.R.; PIERSON, T.C. Zika virus is not uniquely stable at physiological temperatures compared to other flaviviruses. **MBio**., 7, 16, 2016.

162. LIM, X.N.; SHAN, C.; MARZINEK, J.K; DONG, H.; NG, T.S.; OOI, J.S.G.; FIBRIANSAH, G.; WANG, J.; VERMA, C.S.; BOND, P.J.; SHI, P.Y.; LOK, S.M. Molecular basis of dengue virus serotype 2 morphological switch from 29 degrees C to 37 degrees. **C. PLoS Pathog**., 15, 2019.

163. RATHORE ABHAY, P. S.; ST. JOHN ASHLEY, L. Cross-Reactive Immunity Among Flaviviruses. **Frontiers in Immunology**, 11, 2020.

164. CALISHER, C.H.; KARABATSOS, N.; DALRYMPLE, J.M.; SHOPE, R.E.; PORTERFIELD, J.S.; WESTAWAY, E.G.; BRANDT, W.E. Antigenic relationships between Flaviviruses as determined by cross-neutralization tests with polyclonal antisera. **J Gen Virol**., 70, p. 37–43, 1989.

165. ZOMPI, S.; MONTOYA, M.; POHL, M. O.; BALMASEDA, A.; HARRIS, E. Dominant cross-reactive B cell response during secondary acute dengue virus infection in humans. **PLoS Negl. Trop. Dis.,** 6, 2012.

166. PRIYAMVADA, L.; CHO, A.; ONLAMOON, N.; ZHENG, N.Y.; HUANG, M.; KOVALENKOV, Y.; CHOKEPHAIBULKIT, K.; ANGKASEKWINAI, N.; PATTANAPANYASAT, K.; AHMED, R.; WILSON, P.C.; WRAMMERT, J. B cell responses during secondary dengue virus infection are dominated by highly cross-reactive, memory-derived Plasmablasts. **J. Virol**., 90, p. 5574–5585, 2016.

167. HATTAKAM, SARARAT & NGONO, ANNIE & MCCAULEY, MELANIE & SHRESTA, SUJAN & YAMABHAI, MONTAROP. Repeated exposure to dengue virus elicits robust cross-neutralizing antibodies against Zika virus in residents of Northeastern Thailand. **Sci Rep**, 11, 9634, 2021.

168. ANDRADE, P.; NARVEKAR, P.; MONTOYA, M.; MICHLMAYR, D.; BALMASEDA, A.; COLOMA, J.; HARRIS, E. Primary and secondary dengue virus infections elicit similar memory b-cell responses, but breadth to other serotypes and cross-reactivity to zika virus is higher in secondary dengue. **J. Infect. Dis.**, 222, p. 590–600, 2020.

169. MALAFA, S.; MEDITS, I.; ABERLE, J.H.; ABERLE, S.W.; HASLWANTER, D.; TSOUCHNIKAS, G.; WÖLFEL, S.; HUBER, K.L.; PERCIVALLE, E.; CHERPILLOD, P.; THALER, M.; ROßBACHER, L.; KUNDI, M.; HEINZ, F.X.; STIASNY, K. Impact of flavivirus vaccine-induced immunity on primary Zika virus antibody response in humans. **PLoS Negl Trop Dis.**, v.14, n.2, p. 1-27, 2020.

170. KUM, D.B.; MISHRA, N.; BOUDEWIJNS, R.; GLADWYN-NG, I.; ALFANO, C.; MA, J.; SCHMID, M.A.; MARQUES, R.E.; SCHOLS, D.; KAPTEIN, S.; NGUYEN, L.; NEYTS, J.; DALLMEIER, K. A yellow fever-Zika chimeric virus vaccine candidate protects against Zika infection and congenital malformations in mice. **NPJ Vaccines**, v.3, n.56,2018.

171. OLIVEIRA, R.A.; DE OLIVEIRA-FILHO, E.F.; FERNANDES, A.I.; BRITO, C.A.; MARQUES, E.T.; TENÓRIO, M.C.; GIL, L.H. Previous dengue or Zika virus exposure can drive toinfection enhancement or neutralisation of other flaviviruses. **Mem Inst Oswaldo Cruz,** v.114, 1-7p., 2019.

172. HOU, B.; CHEN, H.; GAO, N.; AN, J. Cross-Reactive Immunity among Five Medically Important Mosquito-Borne Flaviviruses Related to Human Diseases. **Viruses**, 14, 1213, 2022.

173. SALGADO, B.B.; MAUÉS, F.C.J.; JORDÃO, M.; PEREIRA, R.L.; TOLEDO-TEIXEIRA, D.A.; PARISE, P.L.; GRANJA, F.; SOUZA, H.F.S.; YAMAMOTO, M.M.; CHIANG, J.O.; MARTINS, L.C.; BOSCARDIN, S.B.; LALWANI, J.D.B.; VASCONCELOS, P.F.C.; PROENÇA-MODENA, J.L.; LALWANI, P. Antibody cross-reactivity and evidence of susceptibility to emerging Flaviviruses in the dengue-endemic Brazilian Amazon. **Int J Infect Dis.**,129, p.142-151, 2023.

174. BRADT, V.; MALAFA, S.; VON BRAUN, A.; JARMER, J.; TSOUCHNIKAS, G.; MEDITS, I.; WANKE, K.; KARRER, U.; STIASNY, K.; HEINZ, F.X. Pre-existing yellow fever immunity impairs and modulates the antibody response to tick-borne encephalitis vaccination. **NPJ Vaccines**., 4, 38, 2019.

175. ZAMBRANA, J.V.; HASUND, C.M.; AOGO, R.A.; BOS, S.; ARGUELLO, S.; GONZALEZ, K.; COLLADO, D.; MIRANDA, T.; KUAN, G.; GORDON, A.; BALMASEDA, A.; KATZELNICK, L; HARRIS, E. Primary exposure to Zika virus increases risk of symptomatic dengue virus infection with serotypes 2, 3, and 4 but not serotype 1. **medRxiv**, 2023.

176. DEJNIRATTISAI, W.; SUPASA, P.; WONGWIWAT, W.; ROUVINSKI, A.; BARBA-SPAETH, G.; DUANGCHINDA, T.; SAKUNTABHAI, A.; CAO-LORMEAU, V.M.; MALASIT, P.; REY, F.A.; MONGKOLSAPAYA, J.; SCREATON, G.R. Dengue virus sero-cross-reactivity drives antibody- dependent enhancement of infection with zika virus. **Nature Immunology,** v. 17, n. 9,2016. 1102-1108p.

177. KATZELNICK, L.C.; GRESH, L. ; HALLORAN, M.E. ; MERCADO, J.C.; KUAN, G.; GORDON, A.; BALMASEDA, A.; HARRIS, E. Antibody-dependent enhancement of severe dengue disease in humans. **Science.** 358, p. 929-932, 2017.

178. AJMERIYA, S.; KUMAR, A.; KARMAKAR, S.; RANA, S.; SINGH, H. Neutralizing Antibodies and Antibody-Dependent Enhancement in COVID-19: A Perspective. **J Indian Inst Sci**., 102, 2, p. 671-687, 2022.

179. SCHLESINGER, J.J.; BRANDRISS, M.W. 17D Yellow Fever Virus Infection of$P388D_1$ Cells Mediated by Monoclonal Antibodies: Properties of the Macrophage Fc Receptor. **J. gen. Virol.**, 64, p. 1255-1262, 1983.

180. SCHLESINGER, J.J.; BRANDRISS, M.W. Antibody-mediated infection of macrophages and macrophage-like cell lines with 17D yellow fever virus. **Journal ofMedical Virology**, 8, p. 103-117, 1981.

181. BARRET, A.D.T; GOULD, E.A. Antibody-mediated Early Death *in vivo* after Infection with Yellow Fever Virus. **J. gen. Virol.**, 67, p.2539-2542, 1986.

182. PIERSON, T.C.; DIAMOND, M.S. A game of numbers: the stoichiometry of antibody-mediated neutralization of flavivirus infection. **Prog Mol Biol Transl Sci,** 129, p. 141-166, 2015.

183. BOURNAZOS, S.; GUPTA, A.; RAVETCH, J.V. The role of IgG Fc receptors in antibody-dependent enhancement. **Nat. Rev. Immunol.,** 20, p. 633–643, 2020.

184. ROEHRIG, J.T. Antigenic structure of flavivirus proteins. **Advances in VirusResearch**, v. 59, 2003.

185. VRATSKIKH, O.; STIASNY, K.; ZLATKOVIC, J.; TSOUCHNIKAS, G.; JARMER, J.; KARRER, U.; ROGGENDORF, M.;, ROGGENDORF, H.;, ALLWINN, R.; HEINZ, F.X. Dissection of antibody specificities induced by yellow fever vaccination. **PLoS Pathog**., 2013.

186. CRILL, W.D.; HUGHES, H.R.; DELOREY, M.J.; CHANG, G.J. Humoral Immune Responses of Dengue Fever Patients using epitope-Specific Serotype-2 Virus-Like Particle Antigens. **PLoS ONE**, v.4, n.4, 2009.

187. DENG, Y.Q.; DAI, J.X.; JI, G.H.; JIANG, T.; WANG, H.J.; YANG, H.O.; TAN, W.L.; LIU, R.; YU, M.; GE, B.X.; ZHU, Q.Y.; QIN, E.D.; GUO, Y.J.; QIN, C.F. A Broadly *Flavivirus* Cross-Neutralizing Monoclonal Antibody that Recognizes a Novel Epitope within the Fusion Loop of E Protein. **PLoS ONE**, 6, 1,2011.

188. DAFFIS, S.; KONTERMANN, R.E.; KORIMBOCUS, J.; ZELLER, H.; KLENK, H.D.; TER MEULEN, J. Antibody responses against wild-type yellow fever virus and the17D vaccine strain: Characterization with human monoclonal antibody fragments and neutralization escape variants. **Virology,** 2005.

189. LOBIGS, M.; DALGARNO, L.; SCHLESINGER, J.J.; WEIR, R.C. Location of a neutralization determinant in the E protein ofyellow fever virus (17d vaccine strain). **Virology**, v.161, p. 474-478, 1987.

190. SEVVANA M.; KUHN, R.J. Mapping the diverse structural landscape of the Flavivirus antibody repertoire. **Curr. Opin. Virol.,** 45, p. 51-64, 2020.

191. RYMAN, K.D.; LEDGER, T.N.; WEIR, R.C.; SCHLESINGER, J.J.; BARRETT, A.D. Yellow fever virus envelope protein has two discrete type-specific neutralizing epitopes. **Journal of General Virology**, 78, p. 1353–1356, 1997.

192. RYMAN, K.D.; LEDGER, T.N.; CAMPBELL, G.A.; WATOWICH, S.J.; BARRETT, A.D. Mutation in a 17D-204 vaccine substrain-specific envelope protein epitope alters the pathogenesis of yellow fever virus in mice. **Virology,** 244, p. 59-65, 1998.

193. MANDL, C.W.; GUIRAKHOO, F.; HOLZMANN, H.; HEINZ, F.X.; KUNZ, C. Antigenic structure of the flavivirus envelope protein E at the molecular level, using tick-borne encephalitis virus as a model. **Journal of Virology**, v.63, n. 2, p. 564-571, 1989.

194. ROEHRIG J.T; BOLIN, R.A.; KELLY, R.G. Monoclonal antibody mapping of the envelope glycoprotein of the Dengue 2 Virus, Jamaica. **Virology**, 246, p. 317-328, 1998.

195. CRILL, W.D.; ROEHRIG, J.T. Monoclonal antibodies that bind to domain III of dengue virus E glycoprotein are the most efficient blockers of virus adsorption to Vero cells. **J Virol.,** 75, p.7769–7773, 2001.

196. GROMOWSKI, G.D.; BARRETT, A.D. Characterization of an antigenic site that contains a dominant, type-specific neutralization determinant on the envelope protein domain III (ED3) of dengue 2 virus. **Virology,** 366, p.349–360, 2007.

197. ROBBIANI, D.F.; BOZZACCO, L.; KEEFFE, J.R; KHOURI, R.; OLSEN, P.C.; GAZUMYAN, A.; SCHAEFER-BABAJEW, D.; AVILA-RIOS, S.; NOGUEIRA, L.; PATEL, R. Recurrent potent human neutralizing antibodies to Zika virus in Brazil and Mexico. **Cell**, 169, p. 597-609, 2017.

198. DE ALWIS, R.; SMITH, S.A.; OLIVAREZ, N.P.; MESSER, W.B.; HUYNH, J.P.; WAHALA, W.M.; WHITE, L.J.; DIAMOND, M.S.; BARIC, R.S.; CROWE, J.E. JR.; DE SILVA, A.M. Identification of human neutralizing antibodies that bind to complex epitopes on dengue virions. **PNAS**, v. 109, n. 19, p. 7439–7444, 2012.

199. FIBRIANSAH, G.; TAN, J.L.; SMITH, S.A.; DE ALWIS, A.R.; NG, T.S.; KOSTYUCHENKO, V.A.; IBARRA, K.D.; WANG, J.; HARRIS, E.; DE SILVA, A.; CROWE, J.E.JR.; LOK, S.M. A potent anti-dengue human antibody preferentially recognizes the conformation of E protein monomers assembled on the virus surface.**EMBO Molecular Medicine**, v.6, n.3, 2014.

200. SANKHALA, R.S.; DUSSUPT, V.; DONOFRIO, G.; GROMOWSKI, G.D.; DE LA BARRERA, R.A.; LAROCCA, R.A.; MENDEZ-RIVERA, L.; LEE, A.; CHOE, M.; ZAKY, W.; MANTUS, G.; JENSEN, J.L.; CHEN, W.H.; GOHAIN, N.; BAI, H.; MCCRACKEN, M.K.; MASON, R.D.; LEGGAT, D.; SLIKE, B.M.; TRAN, U.; JIAN, N.; ABBINK, P.; PETERSON, R.; MENDES, E.A.; FREITAS DE OLIVEIRA FRANCA, R.; CALVET, G.A.; BISPO DE FILIPPIS, A.M.; MCDERMOTT, A.; ROEDERER, M.; HERNANDEZ, M.; ALBERTUS, A.; DAVIDSON, E.; DORANZ, B.J.; ROLLAND, M.; ROBB, M.L.; LYNCH, R.M.; BAROUCH, D.H.; JARMAN, R.G.; THOMAS, S.J.; MODJARRAD, K.; MICHAEL, N.L.; KREBS, S.J.; JOYCE, M.G. Zika-specific neutralizing antibodies targeting inter-dimer envelope epitopes. **Cell Rep**., 42, 8, 2023.

201. KAUFMANN, B.; VOGT, M.R.; GOUDSMIT, J.; HOLDAWAY, H.A.; AKSYUK, A.A.; CHIPMAN, P.R.; KUHN, R.J.; DIAMOND, M.S.; ROSSMANN, M.G. Neutralization of West Nile virus by cross-linking of its surface proteins with Fab fragments of the human monoclonal antibody CR4354. **PNAS**, v. 107, n. 44, p. 18950-18955, 2010.

202. QIU, X.; LEI, Y.; YANG, P.; GAO, Q.; WANG, N.; CAO, L.; YUAN, S.; HUANG, X.; DENG, Y.; MA, W.; DING, T.; ZHANG, F.; WU, X.; HU, J.; LIU, S.L.; QIN, C.; WANG, X.; XU, Z.; RAO, Z.. Structural basis for neutralization of Japanese encephalitis virus by two potent therapeutic antibodies. **Nat. Microbiol.**, 3, 3, p. 287–294, 2018.

203. HASAN, S.S.; MILLER, A.; SAPPARAPU, G.; FERNANDEZ, E.; KLOSE, T.; LONG, F.; FOKINE, A.; PORTA, J.C.; JIANG, W.; DIAMOND, M.S.; CROWE, J.E. JR.; KUHN, R.J.; ROSSMANN, M.G. A human antibody against zika virus crosslinks the E protein to prevent infection. **Nat. Commun**, 8, 1, p. 1–6, 2017.

204. BERNECK, B.S.; ROCKSTROH, A.; FERTEY, J.; GRUNWALD, T.; ULBERT, S. A. Recombinant Zika Virus Envelope Protein with Mutations in the Conserved Fusion Loop Leads to Reduced Antibody Cross-Reactivity upon Vaccination. **Vaccines**, 8, 603, 2020.

205. DEJNIRATTISAI W, JUMNAINSONG A, ONSIRISAKUL N, FITTON P, VASANAWATHANA S, LIMPITIKUL W, PUTTIKHUNT C, EDWARDS C, DUANGCHINDA T, SUPASA S, CHAWANSUNTATI K, MALASIT P, MONGKOLSAPAYA J, SCREATON G. Cross-reacting antibodies enhance dengue virus infection in humans. **Science,** 328, 5979, p.745-8, 2010.

206. MODHIRAN, N.; SONG, H.; LIU, L.; BLETCHLY, C.; BRILLAULT, L.; AMARILLA, A.A.; XU, X.; QI, J.; CHAI, Y.; CHEUNG, S.T.M.; TRAVES, R.; SETOH, Y.X.; BIBBY, S.; SCOTT, C.A.P.; FRENEY, M.E.; NEWTON, N.D.; KHROMYKH, A.A.; CHAPPELL, K.J.; MULLER, D.A.; STACEY, K.J.; LANDSBERG, M.J.; SHI, Y.; GAO, G.F.; YOUNG, P.R.; WATTERSON, D. A broadly protective antibody that targets the flavivirus NS1 protein. **Science**, 371, p. 190-194, 2021.

207. JAYATHILAKA, D.; GOMES, L.; JEEWANDARA, C.; JAYARATHNA, G.S.B.; HERATH, D.; PERERA, P.A.; FERNANDO, S.; WIJEWICKRAMA, A.; HARDMAN, C.S.; OGG, G.S.; MALAVIGE, G.N. Role of NS1 antibodies in the pathogenesis of acute secondary dengue infection. **Nat Commun.,** 9, 1, 5242, 2018.

208. VICTORA, G.D.; NUSSENZWEIG, M.C. Germinal Centers. **Annu Rev Immunol.**, 40, p.413-442, 2022.

209. GODOY-LOZANO, E.E.; TÉLLEZ-SOSA, J.; SÁNCHEZ-GONZÁLEZ, G.; SÁMANO-SÁNCHEZ, H.; AGUILAR-SALGADO, A.; SALINAS-RODRÍGUEZ, A.; CORTINA-CEBALLOS, B.; VIVANCO-CID, H.; HERNÁNDEZ-FLORES, K.; PFAFF, J.M.; KAHLE, K.M.; DORANZ, B.J.;

GÓMEZ-BARRETO, R.E.; VALDOVINOS-TORRES, H.; LÓPEZ-MARTÍNEZ, I.; RODRIGUEZ, M.H.; MARTÍNEZ-BARNETCHE, J. Lower IgG somatic Hypermutation rates during acute dengue virus infection is compatible with a germinal center-independent B cell response. **Genome Med.,** 8, 23, 2016.

210. SARKER, A.; DHAMA, N.; GUPTA RINKOO, D. Dengue virus neutralizing antibody: a review of targets, cross-reactivity, and antibody-dependent enhancement. **Frontiers in Immunology**, 14, 2023.

211. RUIZ, F.; FOREMAN, W.; LILLY, M.; BAHARANI, V.A.; DEPIERREUX , D.M.; CHOHAN, V.; TAYLOR, A.L.; GUENTHOER, J.; RALPH, D.; MATSEN, F.A.; CHU, H.Y.; BIENIASZ, P.D.; CÔTÉ, M.; STARR, T.N.; OVERBAUGH, J. Delineating the functional activity of antibodies with cross-reactivity to SARS-CoV-2, SARS-CoV-1 and related sarbecoviruses. **bioRxiv [Preprint],** 2024.

212. NIELSEN, S.C.A.; YANG, F.; JACKSON, K.J.L.; HOH, R.A.; RÖLTGEN, K.; JEAN, G.H.; STEVENS, B.A.; LEE, J.Y.; RUSTAGI, A.; ROGERS, A.J.; POWELL, A.E.; HUNTER, M.; NAJEEB, J.; OTRELO-CARDOSO, A.R.; YOST, K.E.; DANIEL, B.; NADEAU, K.C.; CHANG, H.Y.; SATPATHY, A.T.; JARDETZKY, T.S.; KIM, P.S.; WANG, T.T.; PINSKY, B.A.; BLISH, C.A.; BOYD, S.D. Human B cell clonal expansion and convergent antibody responses to SARS-CoV-2. **Cell Host Microbe,** 28, 5, p. 516–525, 2020.

213. PATEL, B.; LONGO, P.; MILEY, M. J.; MONTOYA, M.; HARRIS, E.; DE SILVA, A. M. Dissecting the human serum antibody response to secondary dengue virus infections. **PLoS Negl. Trop. Dis**., 11, 2017.

214. CHERNYSHEV, M.; SAKHARKAR, M.; CONNOR, R.I.; DUGAN, H.L.; SHEWARD, D.J.; RAPPAZZO, C.G.; STÅLMARCK, A.; FORSELL ,M.N.E.; WRIGHT, P.F.; CORCORAN, M.; MURRELL, B.; WALKER, L.M.; KARLSSON HEDESTAM, G.B. Vaccination of SARS-CoV-2-infected individuals expands a broad range of clonally diverse affinity-matured B cell lineages. **Nat Commun.**, 14, 1, 2249, 2023.

215. ESSWEIN, S.R.; GRISTICK, H.B.; JURADO, A.; PEACE, A.; KEEFFE, J.R.; LEE, Y.E.; VOLL, A.V.; SAEED, M.; NUSSENZWEIG, M.C.; RICE, C.M.; ROBBIANI, D.F.; MacDONALD, M.R.; BJORKMAN, P.J. Structural basis for Zika envelope domain III recognition by a germline version of a recurrent neutralizing antibody. **Proc Natl Acad Sci U S A,** 117, 18, p.9865-9875, 2020.

216. THAI, E.; MURUGAN, R.; BINTER, Š.; BURN ASCHNER, C.; PRIETO, K.; KASSARDJIAN, A.; OBRAZTSOVA, A.S.; KANG, R.W.; FLORES-GARCIA, Y.; MATHIS-TORRES, S.; LI, K.; HORN, G.Q.; HUNTWORK, R.H.C.; BOLSCHER, J.M.; DE BRUIJNI, M.H.C.; SAUERWEIN, R.; DENNISON, S.M.; TOMARAS, G.D.; ZAVALA, F.; KELLAM, P.; WARDEMANN, H.; JULIEN, J.P. Molecular determinants of cross-reactivity and potency by VH3-33 antibodies against the Plasmodium falciparum circumsporozoite protein. **Cell Rep.**, 42, 11, 13330, 2023.

217. AGUIAR, M.; STOLLENWERK, N.; HALSTEAD, SB. The risks behind Dengvaxia recommendation. **Lancet Infect Dis.**, 16, 8, p. 882-3, 2016.

218. FERGUSON, N.M.; RODRIGUEZ-BARRAQUER, I.; DORIGATTI, I.; MIER-Y-TERAN-ROMERO, L.; LAYDON, D.J.; CUMMINGS, D.A. Benefits and risks of the Sanofi-Pasteur dengue vaccine: modeling optimal deployment. **Science,** 353, p.1033–1036, 2016.

219. CHAUDHARY, N.; WESEMANN, D.R. Analyzing immunoglobulin repertories. **Frontiers in Immunology**, v.9, n.462, 2018.

220. KATZELNICK, L.C.; ZAMBRANA, J.V.; ELIZONDO, D.; COLLADO, D.; GARCIA, N.; ARGUELLO, S.; MERCADO, J.C.; MIRANDA, T.; AMPIE, O.; MERCADO, B.L.; NARVAEZ, C.; GRESH, L.; BINDER, R.A.; OJEDA, S.; SANCHEZ, N.; PLAZAOLA, M.; LATTA, K.; SCHILLER, A.; COLOMA, J.; CARRILLO, F.B.; NARVAEZ, F.; HALLORAN, M.E.; GORDON, A.; KUAN, G.; BALMASEDA, A.; HARRIS, E. Dengue and Zika virus infections in children elicit cross-reactive protective and enhancing antibodies that persist long term. **Sci Transl Med.**, 13, 614, 2021.

221. POND, W. L.; EHRENKRANZ, N. J.; DANAUSKAS, J. X.; CARTER, M. J. Heterotypic serologic responses after yellow fever vaccination; detection of persons with past St. Louis Encephalitis or Dengue. **J. Immunol.,** 98, 673, 1967.

222. SIMÕES, M.; DA SILVA, S.A.; LÚCIO, K.A.; DE OLIVEIRA VIEIRA, R.; SCHWARCZ, W.D.; DE LIMA, S.M.B.; CAMACHO, L.A.B. Standardization, validation, and comparative evaluation of a faster and high-performance test for quantification of yellow fever neutralizing antibodies. **J Immunol Methods**, 522, 113568, 2023.

223. DENANI, C.B.; VIEIRA, R.O.; SETATINO, B.P.; LINHARES, J.H.R.; AZEVEDO, A.S.; SCHWARCZ, W.D.; LIMA, S.M.B. Improvement in Throughput and Accuracy of Neutralization Assay Results by the Automation of Image Acquisition and Analysis. **Biomed J Sci & Tech Res,** 25, 5, 2020.

224. ABREU, F.V.S.; FERREIRA-DE-BRITO, A.; AZEVEDO, A.S.; LINHARES, J.H.R.; DE OLIVEIRA SANTOS, V.; HIME MIRANDA, E.; NEVES, M.S.A.S.; YOUSFI, L.; RIBEIRO, I.P.; SANTOS, A.A.C.D.; DOS SANTOS, E.; SANTOS, T.P.D.; TEIXEIRA, D.S.; GOMES, M.Q.; FERNANDES, C.B.; SILVA, A.M.V.D.; LIMA, M.D.R.Q.; PAUPY, C.; ROMANO, A.P.M.; ANO BOM, A.P.D.; OLIVEIRA-PINTO, L.M.; MOUTAILLER, S.; MOTTA, M.A.; CASTRO, M.G.; BONALDO, M.C.; MARIA BARBOSA DE LIMA, S.; LOURENÇO-DE-OLIVEIRA, R. Survey on Non-Human Primates and Mosquitoes Does not Provide Evidences of Spillover/Spillback between the Urban and Sylvatic Cycles of Yellow Fever and Zika Viruses Following Severe Outbreaks in Southeast Brazil. **Viruses**, 12, 4, 364, 2020.

225. HEIDEN, J.A.V.; YAARI, G.; UDUMAN, M.; STERN, J.N.H.; O'CONNOR, K.C.; HAFLER, D.A.; VIGNEAULT, F.; KLEINSTEIN, S.H.

pRESTO: a toolkit for processing high-throughput sequencing raw reads of lymphocyte receptor repertoires, **Bioinformatics,** 30, 13, p. 1930–1932, 2014.

226. GUPTA, N.T.; HEIDEN, J.A.V.; UDUMAN, M.; GADALA-MARIA, D.; YAARI, G.; KLEINSTEIN, S.H. Change-O: a toolkit for analyzing large-scale B cell immunoglobulin repertoire sequencing data, **Bioinformatics,** 31, 20, p. 3356–3358, 2015.

227. COCK, P. J. A.; ANTAO, T.; CHANG, J.T.; CHAPMAN, B.A.; COX, C.J.; DALKE, A.; FRIEDBERG, I.; HAMELRYCK, T.; KAUFF, F.; WILCZYNSKI, B.; HOON, M.J.L. Biopython: freely available Python tools for computational molecular biology and bioinformatics, **Bioinformatics,** 25, 11, p. 1422–1423, 2009.

228. YE, J.; MA, N.; MADDEN, T.L.; OSTELL, J.M. IgBLAST: an immunoglobulin variable domain sequence analysis tool. **Nucleic Acids Res.**, p. 34-40, 2013.

229. LEFRANC, MP. IMGT, the International ImMunoGeneTics Information System. **Cold Spring Harb Protoc.,** 6, p. 595-603, 2011.

230. HEIDEN, J.A.V., MARQUEZ S.; MARTHANDAN N.; BUKHARI, S.A.C.; BUSSE, C.E.; CORRIE, B.; HERSHBERG, U.; KLEINSTEIN, S.H.; MATSEN, I.V.F.A.; DUNCAN, R.K.; ROSENFELD, A.M.; SCHRAMM, C.A.; THE AIRR COMMUNITY , SCOTT, C.; LASERSON, U.R.I. AIRR Community Standardized Representations for Annotated Immune Repertoires. **Frontiers in Immunology**, 9, 2018.

231. GERVÁSIO, J.; FERREIRA, A.; FELICORI, L.F. Yclon: Ultrafast clustering of B cell lineages from high-throughput immunoglobulin repertoire sequencing data. **J Immunol Methods**, 523, 113576, 2023.

232. McCUNE, B.; GRACE, J.B.; URBAN, D.L. Analysis of Ecological Communities. **MjM Software Design**. 2002.

233. DUNBAR, J.; DEANE, C.M. ANARCI: antigen receptor numbering and receptor classification. **Bioinformatics**, 32, 2, p. 298-300, 2016.

234. ABANADES, B.; WONG, W.K.; BOYLES, F.; GEORGES, G.; BUJOTZEK, A.; DEANE, C.M. ImmuneBuilder: Deep-Learning models for predicting the structures of immune proteins. **Commun Biol.**, 6, 1, p. 575, 2023.

235. SPOENDLIN, F.C.; ABANADES, B.; RAYBOULD, M. I. J.; WONG, W. K.; GEORGES, G.; DEANE, C. M. Improved computational epitope profiling using structural models identifies a broader diversity of antibodies that bind the same epitope. **Frontiers in Molecular Biosciences**, 10, 2023.

236. CAMPI-AZEVEDO, A.C.; REIS, L.R.; PERUHYPE-MAGALHÃES, V.; COELHO-DOS-REIS, J.G.; ANTONELLI, L.R.; FONSECA, C.T.; COSTA-PEREIRA, C.; SOUZA-FAGUNDES, E.M.; DA COSTA-ROCHA, I.A.;

MAMBRINI, J.V.M.; LEMOS, J.A.C.; RIBEIRO, J.G.L.; CALDAS, I.R.; CAMACHO, L.A.B.; MAIA, M.L.S.; DE NORONHA, T.G.; DE LIMA, S.M.B.; SIMÕES, M.; FREIRE, M.D.S.; MARTINS, R.M.; HOMMA, A.; TAUIL, P.L.; VASCONCELOS, P.F.C.; ROMANO, A.P.M.; DOMINGUES, C.M.; TEIXEIRA-CARVALHO, A.; MARTINS-FILHO, O.A. Short-Lived Immunity After 17DD Yellow Fever Single Dose Indicates That Booster Vaccination May Be Required to Guarantee Protective Immunity in Children. **Front Immunol.**, 10, 2192, 2019.

237. KOHLER, S.; BETHKE, N.; BÖTHE, M.; SOMMERICK, S.; FRENTSCH, M.; ROMAGNANI, C.; NIEDRIG, M.; THIEL, A. The early cellular signatures of protective immunity induced by live viral vaccination. **Eur. J. Immunol**., 42, p. 2363–2373, 2012.

238. BASSI, M.R.; KONGSGAARD, M.; STEFFENSEN, M. A.; FENGER, C.; RASMUSSEN, M.; SKJØDT, K.; FINSEN, B.; STRYHN, A.; BUUS, S.; CHRISTENSEN, J.P.; THOMSEN, A.R. CD8+ T Cells complement antibodies in protecting against yellow fever virus. **J Immunol**, 194, p. 1141-1153, 2015.

239. KONGSGAARD, M.; BASSI, M.R.; RASMUSSEN, M.; SKJØDT, K.; THYBO, S.; GABRIEL, M.; HANSEN, M.B.; CHRISTENSEN, J.P.; THOMSEN, A.R.; BUUS, S.; STRYHN, A. Adaptive immune responses to booster vaccination against yellow fever virus are much reduced compared to those after primary vaccination. **Sci Rep.**, 7, 662, 2017.

240. MUYANJA, E.; SSEMAGANDA, A.; NGAUV, P.; CUBAS, R.; PERRIN, H.; SRINIVASAN, D.; CANDERAN, G.; LAWSON, B.; KOPYCINSKI, J.; GRAHAM, A.S.; ROWE, D.K.; SMITH, M.J.; ISERN, S.; MICHAEL, S.; SILVESTRI, G.; VANDERFORD, T.H.; CASTRO, E.; PANTALEO, G.; SINGER, J.; GILLMOUR, J.; KIWANUKA, N.; NANVUBYA, A.; SCHMIDT, C.; BIRUNGI, J.; COX, J.; HADDAD, E.K.; KALEEBU, P.; FAST, P.; SEKALY, R.P.; TRAUTMANN, L.; GAUCHER, D. Immune activation alters cellular and humoral responses to yellow fever 17D vaccine. **J Clin Invest**, 124, 7, p. 3147-3158, 2014.

241. LI, Y.; MERBAH, M.; WOLLEN-ROBERTS, S.; BECKMAN, B.; MDLULI, T.; CURTIS, D.J.; CURRIER, J.R.; MENDEZ-RIVERA, L.; DUSSUPT, V.; KREBS, S.J.; DE LA BARRERA, R.; MICHAEL, N.L.; PAQUIN-PROULX, D.; ELLER, M.A.; KOREN, M.A.; MODJARRAD, K.; ROLLAND, M. Priming with Japanese encephalitis virus or yellow fever virus vaccination led to the recognition of multiple flaviviruses without boosting antibody responses induced by an inactivated Zika virus vaccine. **EBioMedicine**, 97, 104815, 2023.

242. DOMINGO, C.; FRAISSINET, J.; ANSAH, P.O.; KELLY, C.; BHAT, N.; SOW, S.O.; MEJÍA, J.E. Long-term immunity against yellow fever in children vaccinated during infancy: a longitudinal cohort study. **The Lancet Infectious Diseases**, 19, 12, p.1363-1370, 2019.

243. APPANNA, R.; KG, S.; XU, M.H.; TOH, Y.X.; VELUMANI, S.; CARBAJO, D.; LEE, C. Y.; ZUEST, R.; BALAKRISHNAN, T.; XU, W.; LEE, B.; POIDINGER, M.; ZOLEZZI, F.; LEO, Y.S.; THEIN, T.L.; WANG, C-I.; FINK,

K. Plasmablasts During Acute Dengue Infection Represent a Small Subset of a Broader Virus-specific Memory B Cell Pool, **EBioMedicine**, 12, p. 178-188, 2016.

244. STONE, M.; BAKKOUR, S.; LANTERI, M.C.; BRAMBILLA, D.; SIMMONS, G.; BRUHN, R.; KAIDAROVA, Z.; LEE, T.H.; ORLANDO ALSINA, J.; WILLIAMSON, P.C.; GALEL, S.A.; PATE, L.L.; LINNEN, J.M.; KLEINMAN, S.; BUSCH, M.P.; NHLBI RECIPIENT EPIDEMIOLOGY DONOR EVALUATION STUDY REDS-III PROGRAM. Zika virus RNA and IgM persistence in blood compartments and body fluids: a prospective observational study. **Lancet Infect. Dis.**, 20, p. 1446–1456, 2020.

245. GRIFFIN, I.; MARTIN, S.W.; FISCHER, M.; CHAMBERS, T.V.; KOSOY, O.; FALISE, A.; PO-NOMAREVA, O.; GILLIS, L.D.; BLACKMORE, C.; JEAN, R. Zika virus IgM detection and neutralizing antibody profiles 12–19 months after illness onset. **Emerg. Infect. Dis**., 25, 299–303, 2019.

246. WAICKMAN, A.T.; GROMOWSKI, G.D.; RUTVISUTTINUNT, W.; LI, T.; SIEGFRIED, H.; VICTOR, K.; KUKLIS, C.; GOMOOTSUKAVADEE, M.; MCCRACKEN, M.K.; GABRIEL, B.; MATHEW, A.; GRINYO, I. E. A.; FOUCH, M.E.; LIANG, J.; FERNANDEZ, S.; DAVIDSON, E.; DORANZ, B.J.; SRIKIATKHACHORN, A.; ENDY, T.; THOMAS, S.J.; ELLISON, D.; ROTHMAN, A.L.; JARMAN, R.G.; CURRIER, J.R.; FRIBERG, H.. Transcriptional and Clonal Characterization of B Cell Plasmablast Diversity Following Primary and Secondary Natural DENV Infection. **EBioMedicine**, 54, 2020.

247. WAICKMAN, A.T.; LU, J.Q.; FANG, H.; WALDRAN, M.J.; GEBO, C.; CURRIER, J.R.; WARE, L.; VAN WESENBEECK, L.; VERPOORTEN, N.; LENZ, O.; TAMBUYZER, L.; HERRERA-TARACENA, G.; VAN LOOCK, M.; ENDY, T.P.; THOMAS, S.J. Evolution of inflammation and immunity in a dengue virus 1 human infection model. **Sci. Transl. Med.,** 14, 2022.

248. WEGMAN, A.D.; WALDRAN, M.J.; BAHR, L.E.; LU, J.Q.; BAXTER, K.E.; THOMAS, S.J.; WAICKMAN, A.T. DENV-specific IgA contributes protective and non-pathologic function during antibody-dependent enhancement of DENV infection. **PLoS Pathog**.,19, 8, 2023.

249. WEGMAN, A.D.; FANG, H.; ROTHMAN, A.L.; THOMAS, S.J.; ENDY, T.P.; MCCRACKEN, M.K.; CURRIER, J.R.; FRIBERG, H.; GROMOWSKI, G.D.; WAICKMAN, A.T. Monomeric IgA Antagonizes IgG-Mediated Enhancement of DENV Infection. **Front Immunol**.,12, 2021.

250. LUPPE, M.J.; VERRO, A.T.; BARBOSA, A.S.; NOGUEIRA, M.L.; UNDURRAGA, E.A.; DA SILVA, N.S. Yellow fever (YF) vaccination does not increase dengue severity: A retrospective study based on 11,448 dengue notifications in a YF and dengue endemic region. **Travel. Med. Infect. Dis**., 30, p. 25–31, 2019.

251. REIS, L.R.; DA COSTA-ROCHA, I.A.; CAMPI-AZEVEDO, A.C.; PERUHYPE-MAGALHÃES, V.; COELHO-DOS-REIS, J.G.; COSTA-PEREIRA, C.; OTTA, D.A.;

FREIRE, L.C.; DE LIMA, S.M.B.; AZEVEDO, A.S.; SCHWARCZ, W.D.; BOM, A.P.D.A.; DA SILVA, A.M.V.; DE SOUZA, A.F.; DE CASTRO, T.M.; FERROCO, C.L.V.; DE FILIPPIS, A.M.B.; NOGUEIRA, F.B.; HOMMA, A.; DOMINGUES, C.M.; SOUSA, E.S.S.; CAMACHO, L.A.B.; MAIA, M.L.S.; TEIXEIRA-CARVALHO, A.; MARTINS-FILHO, O.A. Exploratory study of humoral and cellular immunity to 17DD Yellow Fever vaccination in children and adults residents of areas without circulation of Yellow Fever Virus, **Vaccine,** 40, 5, p. 798-810, 2022.

252. PINCUS, S.; MASON, P.W.; KONISHI, E.; FONSECA, B.A.; SHOPE, R.E.; RICE, C.M.; PAOLETTI, E. Recombinant vaccinia virus producing the prM and E proteins of yellow fever virus protects mice from lethal yellow fever encephalitis. **Virology**, 187, p. 290–297, 1992.

253. SRINIVASAPPA, J.; SAEGUSA, J.; PRABHAKAR, B.S.; GENTRY, M.K.; BUCHMEIER, M.J.; WIKTOR, T.J.; KOPROWSKI, H.; OLDSTONE, M.B.; NOTKINS, A.L. Molecular mimicry: frequency of reactivity of monoclonal antiviral antibodies with normal tissues. **J Virol.**, 57, 1, p. 397-401, 1986.

254. MEGREMIS, S.; WALKER, T.D.J.; HE, X.; OLLIER, W.E.R.; CHINOY, H.; HAMPSON, L.; HAMPSON, I.; LAMB, J.A. Antibodies against immunogenic epitopes with high sequence identity to SARS-CoV-2 in patients with autoimmune dermatomyositis. **Ann Rheum Dis**., 79, p. 1383-1386, 2020.

255. GUO, C.; FENG, Q.; XIE, X.; LI, Y.; HU, H.; HU, J.; FANG, S.; SHANG, L. Cross-reaction mediated by distinct key amino acid combinations in the complementary-determining region (CDR) of a monoclonal antibody. **J Med Virol**., 96, 29430, 2024.

256. SHARMA, A.; ZHANG, X.; DEJNIRATTISAI, W.; DAI, X.; GONG, D.; WONGWIWAT, W.; DUQUERROY, S.; ROUVINSKI, A.; VANEY, M.C.; GUARDADO-CALVO, P.; HAOUZ, A.; ENGLAND, P.; SUN, R.; ZHOU, Z.H.; MONGKOLSAPAYA, J.; SCREATON, G.R.; REY, F.A. The epitope arrangement on flavivirus particles contributes to Mab C10's extraordinary neutralization breadth across Zika and dengue viruses. **Cell,** 184, p. 6052-6066, 2021.

257. WRIGHT, P.E.; DYSON, H.J. Intrinsically unstructured proteins: re-assessing the protein structure-function paradigm. **Journal of Molecular Biology**, 293, p.321–331, 1999.

258. PONS, J.; STRATTON, J.R.; KIRSCH, J.F. How do two unrelated antibodies, hyhel-10 and f9. 13.7, recognize the same epitope of hen egg-white lysozyme? **Protein Sci.**, 11, p.2308–15, 2002.

259. SALJE, H.; CUMMINGS, D.A.T.; RODRIGUEZ-BARRAQUER, I.; KATZELNICK, L.C.; LESSLER, J.; KLUNGTHONG, C.; THAISOMBOONSUK, B.; NISALAK, A.; WEG, A.; ELLISON, D.; MACAREO, L.; YOON, I.K.; JARMAN, R.; THOMAS, S.; ROTHMAN, A.L.; ENDY, T.; CAUCHEMEZ, S. Reconstruction of antibody dynamics and infection histories to evaluate dengue risk. **Nature,** 557, 7707, p. 719–723, 2018.

260. SLON CAMPOS, J.L.; MARCHESE, S.; RANA, J.; MOSSENTA, M.; POGGIANELLA, M.; BESTAGNO, M.; BURRONE, O.R. Temperature-dependent

folding allows stable dimerization of secretory and virus-associated E proteins of Dengue and Zika viruses in mammalian cells. **Sci Rep.**, 7, 1, 966, 2017.

261. PHAN T.T.N.; HVASTA, M.G.; KUDLACEK, S.T.; THIONO, D.J.; TRIPATHY, A.; NICELY, N.I.; DE SILVA, A.M.; KUHLMAN, B. A conserved set of mutations for stabilizing soluble envelope protein dimers from dengue and Zika viruses to advance the development of subunit vaccines. **J Biol Chem.**, 298, 7, 102079, 2022.

262. GOULD, L.H.S.U.I. J.; FOELLMER, H.; OLIPHANT, T.; WANG, T.; LEDIZET, M.; MURAKAMI, A.; NOONAN, K.; LAMBETH, C.; KAR, K.; ANDERSON, J.F.; DE SILVA, A.M.; DIAMOND, MSKOSKI, R.A.; MARASCO, W.A.; FIKRIG, E. Protective and Therapeutic Capacity of Human Single-Chain Fv-Fc Fusion Proteins against West Nile Virus. **J Virol,** 79, 2005.

263. ELLEFSON, J.W.; GOLLIHAR, J.; SHROFF, R.; SHIVRAM, H.; IYER, V.R.; ELLINGTON, A.D. Synthetic evolutionary origin of a proofreading reverse transcriptase. **Science**, 352, p. 1590–1593, 2016.

264. ZHANG, J.; KOBERT, K.; FLOURI, T.; STAMATAKIS, A. PEAR: a fast and accurate Illumina Paired-End reAd mergeR. **Bioinforma. Oxf. Engl.,** 30, p.614–620, 2014.

265. BOLOTIN, D. A.; POSLAVSKY, S.; MITROPHANOV, I.; SHUGAY, M.; MAMEDOV, I. Z.; PUTINTSEVA, E. V.; CHUDAKOV, D. M. MiXCR: Software for comprehensive adaptive immunity profiling. **Nat. Methods,** 12, p. 380–381, 2015.

266. BOLGER, A. M.; LOHSE, M.; USADEL, B. Trimmomatic: A flexible trimmer for Illumina sequence data. **Bioinformatics**, 30, p. 2114–2120, 2014.

267. EDGAR, R. C. Search and clustering orders of magnitude faster than BLAST. **Bioinforma. Oxf. Engl**., 26, p. 2460–2461, 2010.

268. VOSS, W.N.; HOU, Y.J.; JOHNSON, N.V.; DELIDAKIS, G.; KIM, J.E.; JAVANMARDI, K.; HORTON, A.P.; BARTZOKA, F.; PARESI, C.J.; TANNO, Y.; CHOU, C.W.; ABBASI, S.A.; PICKENS, W.; GEORGE, K.; BOUTZ, D.R.; TOWERS, D.M.; MCDANIEL, J.R.; BILLICK, D.; GOIKE, J.; ROWE, L.; BATRA, D.; POHL, J.; LEE, J.; GANGAPPA, S.; SAMBHARA, S.; GADUSH, M.; WANG, N.; PERSON, M.D.; IVERSON, B.L.; GOLLIHAR, J.D.; DYE, J.M.; HERBERT, A.S.; FINKELSTEIN IJ, BARIC, R.S.; MCLELLAN, J.S.; GEORGIOU, G.; LAVINDER, J.J.; IPPOLITO, G.C. Prevalent, protective, and convergent IgG recognition of SARS-CoV-2 non-RBD spike epitopes. **Science,** 372, p. 1108–1112, 2021.

269. WU, X.; ZHOU, T.; ZHU, J.; ZHANG, B.; GEORGIEV, I.; WANG, C.; CHEN, X.; LONGO, N.S.; LOUDER, M.; MCKEE, K.; O'DELL, S.; PERFETTO, S.; SCHMIDT, S.D.; SHI, W.; WU, L.; YANG, Y.; YANG, Z.Y.; YANG, Z.; ZHANG, Z.; BONSIGNORI, M.; CRUMP, J.A.; KAPIGA, S.H.; SAM, N.E.; HAYNES, B.F.; SIMEK, M.; BURTON, D.R.; KOFF, W.C.; DORIA-ROSE, N.A.; CONNORS, M.; NISC COMPARATIVE SEQUENCING PROGRAM; MULLIKIN, J.C.; NABEL, G.J.; ROEDERER, M.; SHAPIRO, L.;

KWONG, P.D.; MASCOLA, JR. Focused evolution of HIV-1 neutralizing antibodies revealed by structures and deep sequencing. **Science**, 333, p. 1593–1602, 2011.

270. DURHAM, N.D.; AGRAWAL, A.; WALTARI, E.; CROOTE, D.; ZANINI, F.; FOUCH, M.; DAVIDSON, E.; SMITH, O.; CARABAJAL, E.; PAK, J.E.; DORANZ, B.J.; ROBINSON, M.; SANZ, A.M.; ALBORNOZ, L.L.; ROSSO, F.; EINAV, S.; QUAKE, S.R.; MCCUTCHEON, K.M.; GOO, L. Broadly neutralizing human antibodies against dengue virus identified by single B cell Transcriptomics. **Elife**, 8, 52384, 2019.

271. FAHAD, A.S.; TIMM, M.R.; MADAN, B.; BURGOMASTER, K.E.; DOWD, K.A.; NORMANDIN, E.; GUTIERREZ-GONZALEZ, M.F.; PENNINGTON, J.M.; DE SOUZA, M.O.; HENRY, A.R.; LABOUNE, F.; WANG, L.; AMBROZAK, D.R.; GORDON, I.J.; DOUEK, D.C.; LEDGERWOOD, J.E.; GRAHAM, B.S.; CASTILHO, L.R.; PIERSON, T.C.; MASCOLA, J.R.; DEKOSKY, B.J. Functional Profiling of Antibody Immune Repertoires in Convalescent Zika Virus Disease Patients. **Front. Immunol.,** 12, 615102, 2021.

272. BRASIL. Ministério da Saúde. **Banco de dados do Sistema Único de Saúde - DATASUS**. [2021]. Available in: https://datasus.saude.gov.br/acesso-a-informacao/doencas-e-agravos-de-notificacao-de-2007-em-diante-sinan/ Accessed in 31st May 2024.

273. LEE, J.; BOUTZ, D.R.; CHROMIKOVA, V.; JOYCE, M.G.; VOLLMERS, C.; LEUNG, K.; HORTON, A.P.; DEKOSKY, B.J.; LEE, C.H.; LAVINDER, J.J.; MURRIN, E.M.; CHRYSOSTOMOU, C.; HOI, K.H.; TSYBOVSKY, Y.; THOMAS, P.V.; DRUZ, A.; ZHANG, B.; ZHANG, Y.; WANG, L.; KONG, W.P.; PARK, D.; POPOVA, L.I.; DEKKER, C.L.; DAVIS, M.M.; CARTER, C.E.; ROSS, T.M.; ELLINGTON, A.D.; WILSON, P.C.; MARCOTTE, E.M.; MASCOLA, J.R.; IPPOLITO, G.C.; KRAMMER, F.; QUAKE, S.R.; KWONG, P.D.; GEORGIOU, G. Molecular-level analysis of the serum antibody repertoire in young adults before and after seasonal influenza vaccination. **Nat Med.,** 22, 12, p. 1456-1464, 2016.

SUPPLEMENTAL INFORMATION

EPIDEMIOLOGIC INQUIRY

IDENTIFICATION

Donor's Number:_____ (to be completed by the research team).

Age:_____ Gender: ( )Male ( )Female ( )Ignored

CLINICAL HISTORY

1) Have you ever been vaccinated against YFV?
   ( )Yes ( )No ( )Unknown
   If so, when did you get your last YFV vaccine shot?
   ___/___/___ ( )Unknown
2) Have you ever traveled to or lived in a country that has experienced a Flavivirus epidemic, such as countries in Africa, South America or Asia?
   ( )Yes ( )No ( )Unknown
3) Have you ever been diagnosed with Dengue Fever, Zika or Yellow Fever?
   ( )No ( )Dengue ( )Yellow Fever ( )Zika ( )Unknown
   If so, please specify when you were diagnosed:
   ___/___/___ ( )Unknown
4) If you have been exposed to Dengue, please inform the serotype:
   ( )DENV1 ( )DENV2 ( )DENV3 ( )DENV4 ( )Unknown
5) When did you get your last COVID-19 vaccine shot?
   ___/___/___ ( ) I have not been vaccinated.

Date:___/___/___

Signature:___/___/___

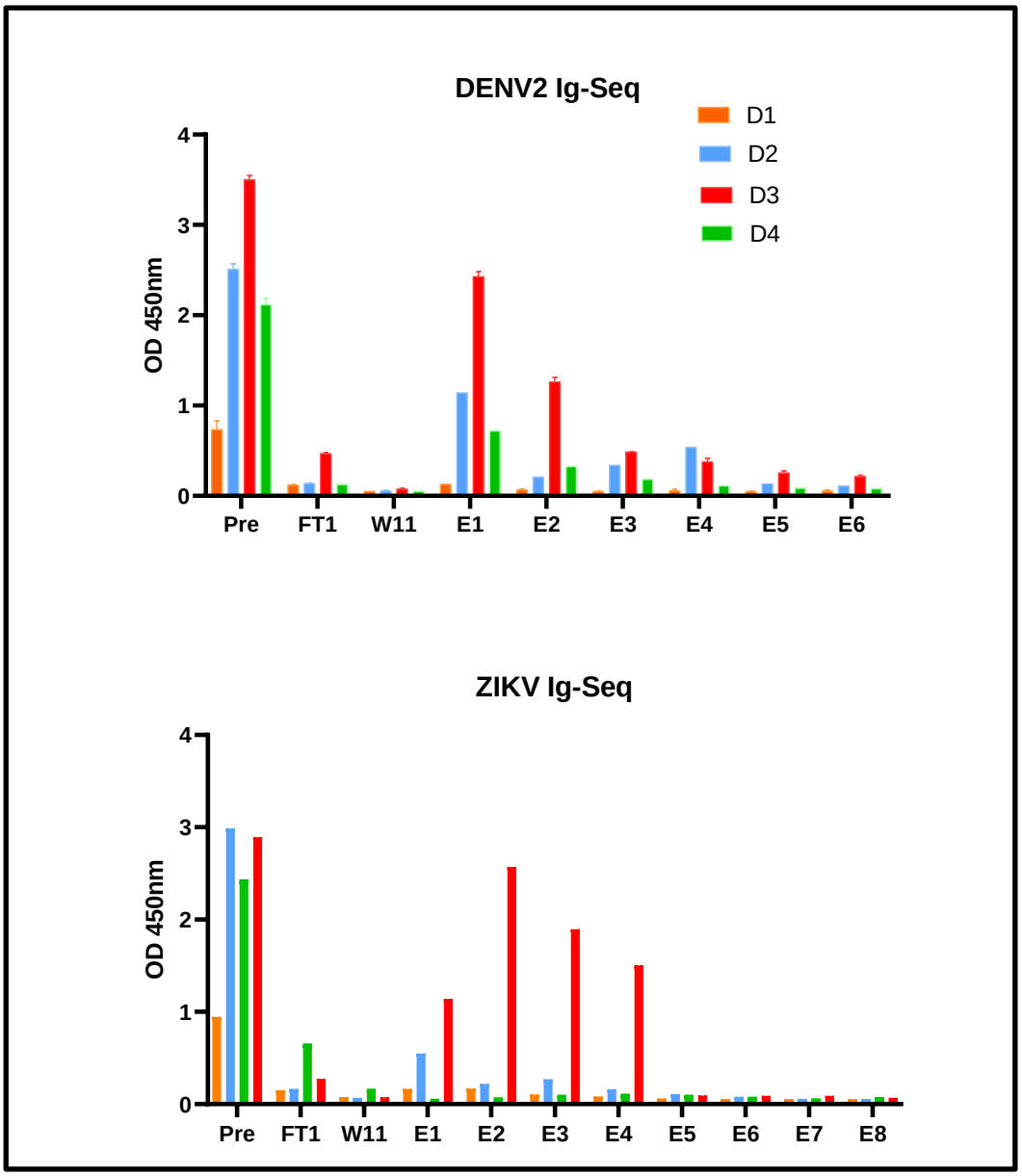

Figure S.1. DENV2 and ZIKV E-dimer ELISA performed after the IgG pull down. Pre represents the sample before affinity purification using DENV2 or ZIKV E-Dimer antigen coupled into NHS resin. FT1- flowthrough, W11- wash, E1-E6 - Elutions.